INDUCING EPITHELIAL MORPHOGENESIS IN HUMAN SALIVARY ACINAR-LIKE CELLS CULTURED IN 3D HYALURONIC ACID, LAMININ-MODIFIED HYDROGELS

by

Kevin Cannon

A thesis submitted to the Faculty of the University of Delaware in partial fulfillment of the requirements for the degree of Master of Science in Biological Sciences

Spring 2015

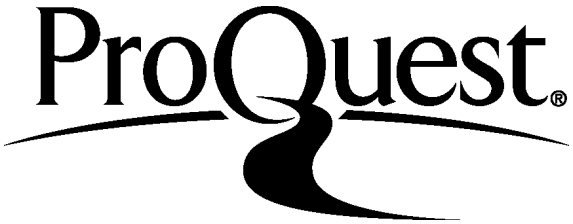

INDUCING EPITHELIAL MORPHOGENESIS IN HUMAN SALIVARY ACINAR-LIKE CELLS CULTURED IN 3D HYALURONIC ACID, LAMININ-MODIFIED HYDROGELS

by

Kevin Cannon

Approved: _____
Randall L. Duncan, Ph.D.
Professor in charge of thesis on behalf of the Advisory Committee

Approved: _____
Robert L. Witt, M.D.
Professor in charge of thesis on behalf of the Advisory Committee

Approved: _____
Robin Morgan, Ph.D.
Chair of the Department of Biological Sciences

Approved: _____
George H. Watson, Ph.D.
Dean of the College of Arts and Sciences

Approved: _____
James G. Richards, Ph.D.
Vice Provost for Graduate and Professional Education

ACKNOWLEDGMENTS

To my family, Mom, Dad, and Chris. During these years I found myself struggling just to get around the wind, but you were always there for me. Thank you for being there, thank you for loving me. To Archana Siddam, my second mother. Thank you and LJ for taking me into your home and making me tea when I was troubled and when I wasn't. You truly are a lovely person.

Swati, I don't know where to begin. There are simply too many things to remember. You taught me how to do science without bias. You took the time to learn who I was, when others had no room in frame. You urged me to stay in the sun, instead of in the rain. You listened to my ideas, my heartbreak, my aspirations, and my loneliness. You were there for my successes, failures, and the grey areas in between. You've had an immeasurable influence on my life and career. I find myself incredibly sad thinking about saying goodbye to you. I will miss you.

To Dan, I doubt that I'll meet anyone like you ever again. I hope you become a life-long friend. As my roommate and labmate throughout these years, we've been through some heavy things. Thank you for making me think about things I never thought I would think about. I wish I could remember all of the conversations we've had over the years; some were good, some sad, and most were atrocious. Blame it on the Platinums. Whatever it is that you decide to do with your life, I wish you the best. I will miss you. Always remember to laugh when life becomes futile.

To the beautiful Megan Dumas, you are the smartest, most genuine person I've ever met. Before you, I'd never met someone so eccentric, curious, intelligent, and so full of life. I have so much confidence in you as a person and a scientist. I think about you everyday. Megan, you are the bluebird in my heart. Thank you for everything.

TABLE OF CONTENTS

LIST OF ABBREVIATIONS

ANS: Autonomic Nervous System

ATP: Adenosine Triphosphate

Ach: Acetylcholine

BMP: Bone Morphogenic Protein

BrM: Branching Morphogenesis

Btl: Breathless

Bnl:Branchless

cAMP: Cyclic Adenosine Monophosphate

CCh: Carbachol

Cl^-: Chloride anion

ECM: Extracellular Matrix

EDA: Ectodysplasian A

EDAR: Ectodysplasia A Receptor

EGF: Epidermal Growth Factor

EGFR: Epidermal Growth Factor Receptor

FAK: Focal Adhesion Kinase

FGF: Fibroblast Growth Factor

FGFR: Fibroblast Growth Factor Receptor

GAG: Glycosaminoglycan

GDNF: Glial cell-Derived Neurotropic Factor

GPCR: G-Protein Coupled Receptor

GPI: Glyosyl

HA: Hyaluronic Acid

HAS: Hyaluronic Acid Synthase

HB-EGF: Heparan Binding Epidermal Growth Factor

HCO_3^-: Bicarbonate

hSACs: Human Salivary Acinar-like Cells

HS: Heparan Sulfate

HSPG: Heparan Sulfate Proteoglycan

ISN: Inferior Salivatory Nucleus

IP3: Inositol Triphosphate

IRB: Institutional Review Board

K5/8/14/19: Cytokeratins

M1/M3: Muscarinic Receptor 1/3

Na^+: Sodium cation

$Na^+/K^+/2Cl^-$ co-transporter: Sodium, potassium, chloride co-transporter

K^+: Potassium cation

MMP: Matrix Metalloproteinase

NC1: Non-collagenous domain 1

NRTN: Neuturin

PDMS: Poly Dimethyl Sulfoxide

PEGDA: Poly Ethylene Glycol DiAcrylate

PLGA: Poly Lactic-Glycolic Acid

PKA: Protein Kinase A

PKC: Protein Kinase C

PG: Parotid Gland

PSG: Parasympathetic Ganglion

ROCK: Rho-kinase

SCF: Stem Cell Factor

SCG: Superior Cervical Ganglion

SG: Sympathetic Ganglion

SLG: Sublingual Gland

SMG: Submandibular Gland

TEB: Terminal End Bud

TGF: Transforming Growth Factor

TNF: tumor Necrosis Factor

VIP: Vasoactive Intestinal Peptide

LIST OF FIGURES

ABSTRACT

Radiation therapy used to treat head and neck cancers results in salivary gland hypofunction and xerostomia. Salivary gland dysfunction is concurrent with a steady decline in oral health. The creation of a bioengineered salivary gland would provide a potential long term treatment option for those suffering from xerostomia, or dry mouth. The goal of this project was to create an extracellular matrix (ECM): hyaluronic acid (HA)-based hydrogel culture system to promote the survival, growth, and morphogenesis of human salivary acinar-like cells (hSACs) into higher-ordered, branched structures. Ultimately, we aim to create hSAC structures capable of secreting fluid and salivary-specific proteins in a vectorial fashion to be used for engineering a fully functional artificial salivary gland to be implanted into patients suffering from xerostomia.

Human salivary tissue was obtained from patients undergoing head and neck surgery under the approval of the Institutional Review Board (IRB) at Christiana Care Health Systems (CCHS) and the University of Delaware (UD). hSACs were identified in tissue explant culture. Gene expression and protein level analysis showed that hSACs express a variety of stem/progenitor cell markers in both two- and three-dimensional culture systems.

Here we report the effects of fibroblast growth factors, FGF7 and FGF10 on human salivary gland acinar-like cells (hSACs) grown in three-dimensional hyaluronic acid:laminin hydrogels. hSAC spheroids encapsulated in our culture system self-assemble into spheroid structures after seven days. Stimulation with FGFR2b ligands, FGF7 or FGF10 showed sustained hSAC proliferation and specific modes of morphogenesis. FGF7 treatment promoted the formation of epithelial cleft-like and lobule-like structures, whereas the addition of FGF10 to hSAC structures induced duct-like elongations. We found that hSACs treated with FGF7 and FGF10 increase fibronectin protein levels and deposition within the hydrogel network; however, FGF7 but not FGF10 increased protein levels of fibronectin-binding α_5-integrin. FGF10 treatment followed by FGF7 addition resulted in more complex

morphogenesis than either ligand alone. Interestingly, simultaneous stimulation with FGF7 and FGF10 had a minimal effect on overall hSAC morphogenesis. Sustained culture of hSAC structures treated with FGF10-heparin followed by FGF7 began to form lumens. To assess the capability of hSAC differentiation, acinar cell biomarker α-amylase protein expression was investigated. We observed amylase staining in hSAC structures undergoing morphogenesis. Interestingly, hSACs treated with EGFR ligand, HB-EGF, following sequential addition of FGF10 and FGF7 express ductal marker, cytokeratin 19 (CK19).

In summary, FGFR2b ligands FGF7 and FGF10 are capable of inducing morphogenesis of primary salivary gland cells into structures reminiscent of native salivary gland architectures, which can be used to restore glandular function in tissue engineering applications.

Chapter 1

GENERAL INTRODUCTION

1.1 Effects of Head and Neck Cancer Treatment on the Salivary Glands

1.1.1 Cancers of the Head and Neck

Cancers affecting the head and neck are responsible for 3-5% of all malignancies in the United States[1]. They encompass a heterogeneous class of aggressive cancer types including laryngeal and hypopharyngeal, nasal cavity and paranasal sinus, nasopharyngeal, oral and oropharyngeal, and salivary gland cancers. Several treatment options exist for those diagnosed with head and neck cancers including surgery, chemotherapy, radiation therapy, chemoradiation therapy, and immunotherapy[13].

1.1.2 Effects of Radiation Treatment on Salivary Gland Structure and Function

Most head and neck cancers are treated by surgically removing the cancerous tissue; however, if surgery is not a viable option, chemoradiation therapy is the primary treatment used to eradicate malignant tumors. Despite current attempts to localize ionizing beam radiation to the target tissue and minimize scatter to surrounding tissues, technologies including intensity modulated radiation therapy, proton and fast neutron beam therapies, cyberknife, and image guided radiotherapy have proven unsuccessful in preventing salivary gland damage following treatment[33]. As the salivary glands fall within the primary radiation zone for most head and neck cancers, they are subject to radiation-induced damage and dysfunction.

Atrophy and subsequent necrosis of secretory acini within the acino-tubular network of the salivary glands almost always results following radiation therapy. Immunohistochemical studies of irradiated salivary gland tissue sections show

the persistence of ductal structures with a concurrent loss of acini by apoptosis. It is currently unknown why ionizing beam radiation selectively induces acinar cell death, however, it has been suggested that the abundance of transition metal ion cofactors including copper, zinc, magnesium, and iron harbored within the zymogen granules of secretory acinar cells is responsible for their selective destruction. Metal cofactors are capable of generating free radicals following radiation therapy; thereby damaging acinar cell DNA and inducing programmed cell death. However, this model has not been confirmed and requires further investigation.

Other conjecture regarding radiation-induced loss of secretory acini suggests that damage to surrounding tissues required to maintain salivary gland homeostasis is responsible for salivary gland hypofunction. *Ex vivo* cultures of intact fetal submandibular gland (SMG) epithelium, mesenchyme, and parasympathetic ganglion irradiated with 5 Gy show increased apoptosis within mesenchymal and neuronal cell populations, accompanied by reduced epithelial branching morphogenesis[2]. Additionally, parasympathectomy within the SMGs of adult mice resulted in an overall decrease in gland size[34]. These results suggest that several tissue compartments within the salivary gland are responsible for maintaining and regulating structure and function from development and throughout adulthood.

Within the irradiated salivary bed, acinar cell loss is accompanied by an increase in surrounding fibrotic tissue, adipocyte accumulation, and lymphocytic invasion, completely disrupting native salivary gland structure and function. Dysfunctional salivary glands typically result in xerostomia, or dry mouth[3]. The loss of saliva within the oral cavity leads to several harmful oropharyngeal maladies including dental caries, dysphagia, difficulty in speech and mastication, and increased susceptibility to invasion by microorganisms[3,-5]

1.2 Salivary Gland Restoration Through Tissue Engineering

1.2.1 Current Treatments for Xerostomia and Tissue Engineering as a Practical Alternative

There is no cure for xerostomia. Current treatments are unsatisfactory and fail to answer the clinical need to improve the quality of life in those suffering from dry mouth. These approaches either seek to induce endogenous salivary flow or to directly replacing salivary fluid; however, their effects are short term and do not aim to repair damaged tissues[6,7]. Over the counter oral sialagogues including cholinomimetics attempt to stimulate basolateral M1/M3 muscarinic receptors on secretory acini, however this approach is futile, considering acinar lobules necrose following radiation therapy. Artificial saliva has also been suggested as a possible treatment for xerostomia; however, it has a short half-life and exhibits varying degrees of efficacy from patient to patient. The shortcomings of present day treatments for xerostomia could be circumvented through the creation of an artificially engineered salivary gland. Generation of implantable, bioengineered, three dimensional salivary gland neotissue will fulfill the clinical need to provide effective, long term restoration of native salivary gland function to restore the quality of life in patients suffering from dry mouth. Tissue engineering applications have shown great promise in recapitulating gland/organ function that has otherwise been lost. Recent breakthroughs within the field include the successful creation and implantation of a fully functional artificial bladder and trachea into human patients, respectively[8-11].

1.2.2 Guiding Principles of Tissue Engineering

Tissue engineering requires a multidisciplinary approach, relying on a comprehensive understanding of cell and developmental biology, physiology, and materials science and engineering to provide the most effective means to restore native gland/organ function. The major paradigm followed by most tissue engineers is the cell-cue(s)-scaffold model. Recent advances in stem cell biology, growth factor and

extracellular matrix (ECM) signaling have helped tissue engineers design the best method to restore gland function[7,10-14]. It is essential that tissue engineers select the correct cell type(s) required to form the foundation of three-dimensional, functional neotissues; the correct signaling factors to drive morphogenic events to generate the higher ordered morphologies observed in native tissues; and the use of correct ECM proteins/peptides to impart the topological, physical, and biochemical signals required to promote morphogenesis, differentiation, and structural support.

1.2.3 Hydrogels in Tissue Engineering Applications

Common methods for cell culture are reliant on two-dimensional substrates *in vitro*; however, these systems do not represent any physiological system observed *in vivo*. Polarized cell-cell and cell-matrix interactions in two-dimensional culture are aberrant when compared to those seen in intact tissue structures. Additionally, cells cultured in two-dimensions are flat and fail to grow in all three planes, making the generation of three dimensional architectures a formidable challenge in tissue engineering applications.

Hydrogels are water-absorbing networks of cross-linked polymers that maintain a characteristic 3D structure[15]. Hydrogels were the first materials designed for implantation into human patients when Wichterle and colleagues investigated the potential of poly(2-hydroxyethyl methacrylate)-based hydrogels to be used as contact lenses in 1960[16]. However, as the methods for traditional hydrogel synthesis were limited with respect to controlling chemical modifications and the presence harmful side reactions, hydrogel-based translational applications saw little promise. With the last decade, the advent of controlled chemical modification without harmful side reactions has allowed the creation of novel hydrogel designs seeking to recapitulate native cellular microenvironments that can be used in human patients. Hydrogels used in tissue engineering applications commonly use combinations of both natural and synthetic polymers within their hydrogel systems including poly-ethylene glycol, poly-glycolic acid, poly-lactic acid, hyaluronic acid, collagens, and peptide-based hydrogels.

1.2.4 Hyaluronic Acid-Based Hydrogels

Hyaluronic acid (HA) natural biological macromolecule that functions in withstanding compressive forces in dynamic tissues, regulating ECM hydrodynamics to maintain tissue organization, and facilitating egg fertilization during ovarian follicle maturation[17]. In addition to its innate bioactivity, HA is both biodegradable and non-immunogenic, making HA-based hydrogels an attractive building block in tissue engineering applications. However, native HA turnover is rapid, with a half-life of only 2-3 days in most tissue types[18]. Additionally, the mechanical properties of endogenous HA are not robust enough to support prolonged cell growth and assembly into tissue microstructures required of tissue engineering applications[19]. Despite these shortcomings, the carboxylic acid and hydroxyl functional groups within the HA backbone provide reactive handles for controlled chemical modification and covalent crosslinking to allow for the facile modification of mechanical properties and flexibility in fine-tuning a means of scaffold degradation (Figure 1.1)[20,21]. Chemical modifications of pendant functional groups along the backbone create enormous variety within hydrazide-, aldehyde-, (meth)acrylate-, and thiol-functionalized HA polymers, which can participate in various crosslinking schemes to form covalently crosslinked hydrogel networks with a defined set of physicochemical properties to best mimic the glandular microenvironment of interest[19].

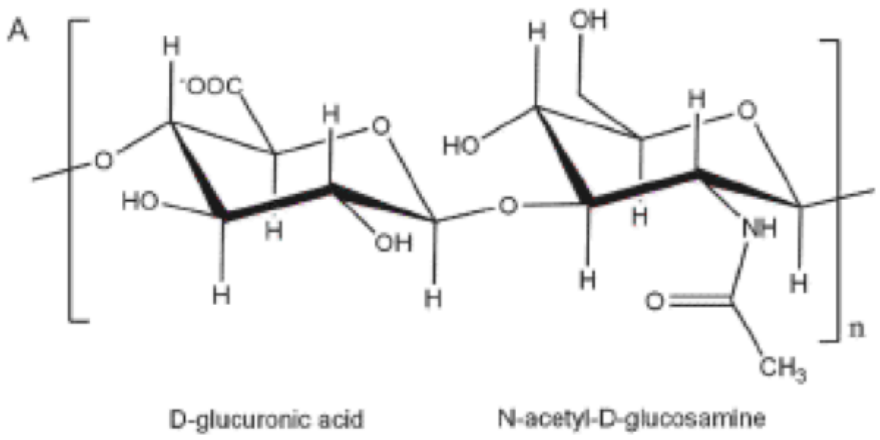

Figure 1.1 Chemical structure of hyaluronic acid. The carboxylic acid and hydroxyl moieties are the principle sites of controlled chemical modification

1.2.5 Biology of Hyaluronic Acid

Hyaluronic acid (HA) is a linear, non-sulfated glycosaminoglycan ubiquitously expressed within the extracellular matrix of many connective, epithelial, and neuronal tissue types. Repeating D-glucuronic acid and N-acetyl-D-glucosamine sugars linked via alternating 1,4- 1,3 glycosidic linkages constitute the HA chain. HA biosynthesis begins on the cytosolic leaflet of plasma membrane with hyaluronic acid synthase (HAS) extending the reducing end of the HA polymer while an internal pore within HAS promotes the translocation of HA into the extracellular space[19].

To date, three HAS isoforms have been identified, with each isoform exhibiting differential HA polymerization kinetics, generating HA polymers that vary in molecular weight, suggesting fine-tuned regulation of HA-mediated cell-, and tissue responses[22]. Extracellular HA binds cell surface receptors CD44 and RHAMM to propagate downstream signaling events that regulate cell adhesion, migration, survival, and proliferation[23,24]. Further complexity in HA signaling is conferred following chain catabolism, as various thresholds in HA fragment size can determine the range and extent of signaling responses.

1.2.6 Biochemical and Biophysical Properties of Hyaluronic Acid

Variability in the total number of disaccharide repeats leads to HA chain lengths that range from 250 to 25,000 monosaccharides per polymer with molecular weights spanning 10^4 to 10^7 Da. In neutral aqueous solution, electrostatic repulsion of juxtaposed carboxylic acid moieties and hydrogen bonding interactions with surrounding water molecules shape HA polymers to assume an extended random coil configuration[19]. Within the HA polymer, carboxylic acid and hydroxyl functional groups and the anomeric carbon on the neighboring sugar assume configurations, promoting the polar functional groups to adopt sterically favorable equatorial conformations[18]. Water uptake within the HA network allows swelling such that its volume of the can expand up to 1000 times its initial volume. Unlike other GAGs, hyaluronic acid does not contain any sulfate groups, and is the only GAG that is not

directly covalently linked to core protein domains on heparan sulfate proteoglycans (HSPGs).

If the HA concentration is increased above a certain threshold, HA chains intertwine and form entangled networks that are capable of elastic deformation and viscous flow in response to external forces. At higher concentrations HA chains form entangled molecular networks with viscoelastic properties. Such networks however, are not fruitful for artificial scaffold production as these networks display undesirable mechanical properties and turnover rates. Chemically modifying functional groups containing reactive handles is a common method to exploit desired modes of chemical crosslinking to impart the desired mechanical characteristics for a given hydrogel system.

1.2.7 Salivary Gland Tissue Engineering

Previous works from other labs have implored both basic and applied science strategies to investigate the most effective means to generate a fully functional artificial salivary gland. Investigators have used *ex vivo* culture of fetal submandibular glands from mice to study salivary gland development, immortalized salivary gland cell lines to analyze physical and biochemical parameters that contribute to salivary gland cell assembly and physiology, and primary cell lines to better understand the behavior of human-derived cell lines. Baker and colleagues have used the Par-C10 immortalized rat parotid cell line as a model to study tight junction formation and fluid/protein secretion. Par-C10 cells cultured on growth factor reduced Matrigel self-assemble into acinar-like spheres that range from 30 to 60 microns in diameter after two days in culture. Par-C10 cells comprising the acinar-like spheres show apically localized zonula occludens-1 (ZO-1), occludin, and claudin-3 around forming lumens, suggesting that these structures are beginning to differentiate towards the acinar-cell lineage[25].

Nelson et. al., generated curved hemisphere molds made from polydimethylsiloxane (PDMS) lined with electrospun poly-lactic-co-glycolic acid nanofibers to mimic the *in vivo* basement membrane structure surrounding acini lobules.

Both Par-C10 and ductal SIMS immortalized cell lines showed elevated occludin protein levels and apical localization, as well as increased *Apq5* expression following an increase in scaffold curvature[24]. These results suggest that tight junction formation and differentiation may be in part, dependent on basement membrane curvature.

Parotid gland cells isolated from *Rhesus* monkeys were able to form polarized epithelia with basal localization of Na/K/ATPase, as well as ZO-1 and claudin-1 localization to apico-lateral membrane microdomains. Additionally, Rhesus parotid gland cells transduced with adenoviral vectors expressed *Apq5* and were capable of mediating vectorial fluid flow[26]. Other labs seeking to generate artificial salivary glands are investigating the potential of implanting salivary stem/progenitor cells at sites of damaged tissue. In an elegant study, Ogawa and colleagues were able to regenerate fully functional parotid, submandibular, and sublingual major salivary glands through orthotopic transplantation of salivary gland germ into adult mice[27]. Despite the clinical implausibility in this approach, this work provides a proof-of-concept for the creation and implantation of fully functional salivary glands to be transplanted into patients suffering from xerostomia.

Previous work from our lab has shown the successful isolation and culture of primary salivary gland cells. These cells exhibit morphologies similar to acinar cells and express acinar-cell specific enzyme -amylase in two-dimensional culture[13]. When these cells are grown in three-dimensional hyaluronic acid-based hydrogels they self-assemble into spheroids, form lumens after prolonged culture, and show fluid and protein secretory responses to sympathetic and parasympathetic neuronal agonists isoproterenol and acetylcholine, respectively[28]. Gene expression analysis of our human salivary acinar-like cells (hSACs) revealed that these cells express a variety of stem/progenitor markers including c-Kit, musashi, keratin 5, and keratin 14, suggesting that they have the potential to undergo morphogenesis and differentiation into acinar, ductal, and myoepithelial cell types within the mature salivary gland (Pradhan-Bhatt and Hoffman unpublished).

1.2.8 Generation of an Artificial Salivary Gland

The generation of a bioengineered artificial salivary gland would fulfill the clinical need to provide the potential of long-term treatment, and possibly cure those suffering from xerostomia. Our overall methodology begins with the IRB-approved procurement of patient tissue prior to radiation therapy. The patient's autologous salivary gland cells are harvested, cultured, and expanded *in vitro.* The patient's native salivary gland cells are then encapsulated in a three-dimensional hyaluronic acid-based hydrogel scaffold. Within the biomimetic scaffold, salivary gland cells are then stimulated with the appropriate growth factor and extracellular matrix cues to drive cell assembly and morphogenesis into higher ordered, functional structures observed in native salivary tissue. We plan to implant functional neotissues into the salivary bed following radiation treatment (Figure 1.2)

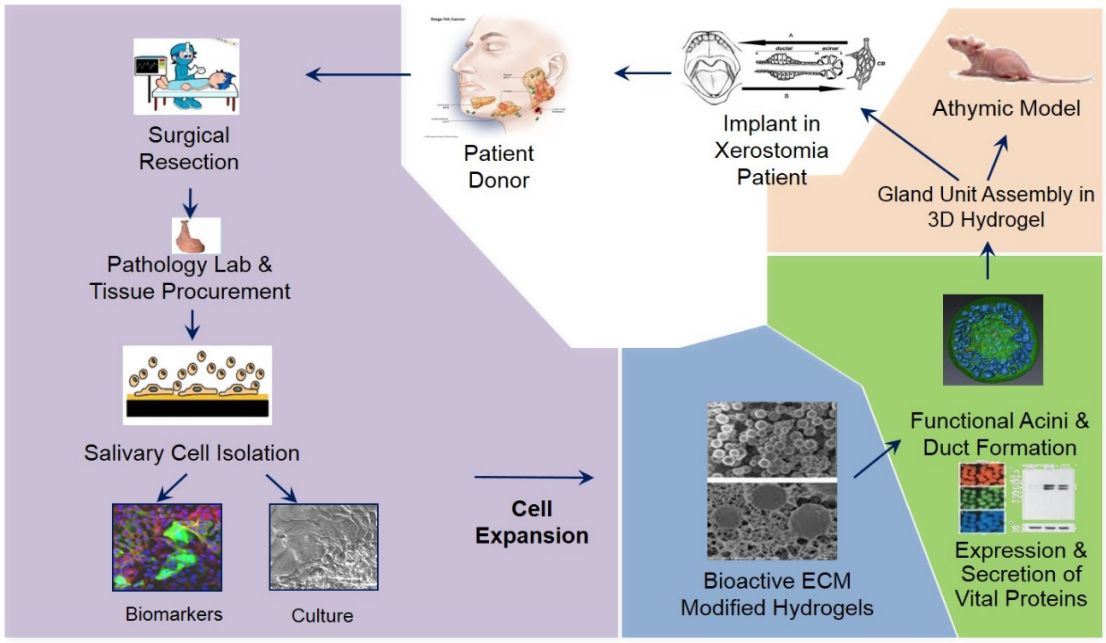

Figure 1.2 Methodology for the generation and implantation of an artificial salivary gland into patients suffering from xerostomia. Image courtesy of Swati Pradhan-Bhatt.

1.3 The Salivary Glands

1.3.1 Salivary Gland Anatomy

The salivary glands are a complex physiological system that function to maintain oral homeostasis and catalyze digestive processes essential for metabolism. In humans and rodents (rats and mice), the salivary glands locate to the upper aerodigestive tract and are partitioned into major and minor exocrine glands. The major glands, parotid, submandibular, and sublingual are paired and contribute to 95% of the salivary output within the oral cavity[1] (Figure 1.2). Six hundred to one thousand minor glands line the oral mucosa, further contributing to salivary secretions within mouth.

The largest of the salivary glands is the parotid (PG); weighing approximately 15-30g, the parotid locates within the preauricular region and along the posterior surface of the mandible covered by fascia and the parotid capsule[29]. Superior, anterior, and posterior to the parotid is the zygomatic arch, masseter, and the sternocleidomastoid, respectively. The parotid is often separated into superficial and deep lobes, located laterally and medially to the facial nerve, respectively. The major duct of the parotid, the Stenson's duct, forms from a collection of tubular ductal networks originating from both superficial and deep lobes. The Stenson's duct leaves the anterior border and travels parallel to the masseter muscle, turning to extend into the buccinator muscle where it enters the oral cavity opposite the second upper molar tooth. Located beneath the ramus of the mandible is the submandibular gland (SMG), exhibiting a horse-shoe morphology weighing approximately 7-16g

Most of the submandibular gland lies posterolateral to the mylohyoid muscle within the submandibular triangle surrounded by the mandible and the anterior and posterior bellies of the digastric muscle, where it is encapsulated by the deep middle layer of the deep cervical fascia[3].

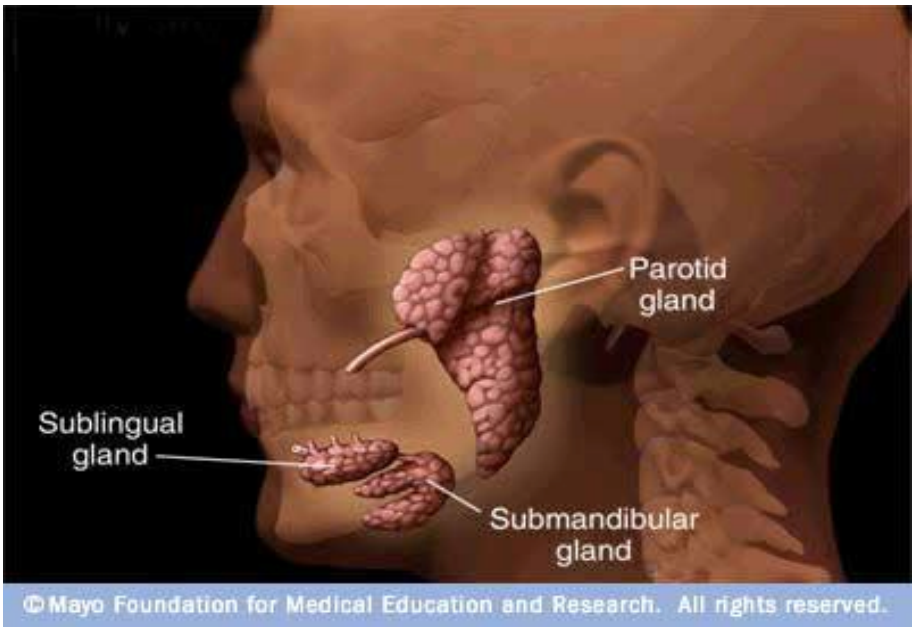

Figure 1.3 Anatomy of the major salivary glands. The major (pictured) and minor (not pictured) salivary glands locate to the upper aerodigestive tract. The major function of the salivary glands is to produce saliva.

The major duct of the submandibular gland, Wharton's duct is roughly 4-5 cm in length and empties salivary fluid in the floor of the mouth behind the lower incisor tooth.

The smallest of the major salivary glands is the sublingual gland (SLG), weighing from 2-4g. The SLG lies within the plane of the submucosa within the anterior floor of the mouth covered superiorly by oral mucosa instead of a capsule. Fluid from the SLG enters the oral cavity either through the ducts of Rivinis where saliva is emptied directly into the floor of the mouth or through the major duct of the SLG, the Bartholin's duct, from which it will connect to the Wharton's duct of the SMG[30].

600-1000 minor salivary glands line the oropharyngeal cavity, contributing only 5% to the total saliva content[31]. Ranging from 1-5mm in size, the minor salivary glands do not contain a heavily branched collecting ductal network. Instead, each minor salivary gland has branched salivary acini with one collecting duct, and localize to the lips, buccal mucosa, tongue, and palate.

1.3.2 Salivary Gland Innervation

From Pavlov's seminal studies, salivary gland function has long been affiliated with neuronal input and the ablation of salivary-nerve crosstalk causes salivary gland atrophy with subsequent cessation of salivary secretions. The sympathetic and parasympathetic branches of the autonomic nervous system innervate the major salivary glands. Removal of either branch of the ANS in mice has been shown to lead to defects in organogenesis during development, and salivary gland atrophy and dysfunction during adulthood, highlighting the essential role for innervation in regulating gland development, homeostasis, and function[32,33].

Parasympathetic innervation of the parotid gland occurs through cranial nerve IX, with preganglionic axons emanating from the inferior salivatory nucleus (ISN) within the medulla of the brainstem, ultimately synapsing at the otic ganglion. Postganglionic axons travel from the otic ganglion along cranial nerve V to innervate the parotid, providing the parasympathetic innervation required for fluid secretions.

Innervation by the sympathetic branch of the ANS begins originates within the upper thoracic regions of the spinal cord when preganglionic fibers synapse with the superior cervical ganglion. Postganglionic fibers extend to the carotid plexus and synaptogenesis between sympathetic fibers and the PG occurs following axon outgrowth from the carotid plexus (Figure 1.4).

Parasympathetic axons emanating from cranial nerve VII within the superior salivary nucleus travel through the chorda tympani nerve where they will converge with the lingual nerve. Preganglionic axons will then synapse at the submandibular ganglion, allowing the short postganglionic axons from the submandibular ganglion to synapse with the submandibular and sublingual glands. Preganglionic sympathetic fibers originating from the thoracic ganglion ascend up through the spinal cord to synapse at the superior cervical ganglion (SCG). Postganglionic sympathetic fibers from the SCG travel down the carotid plexus and facial artery to target the SMG and SLG.

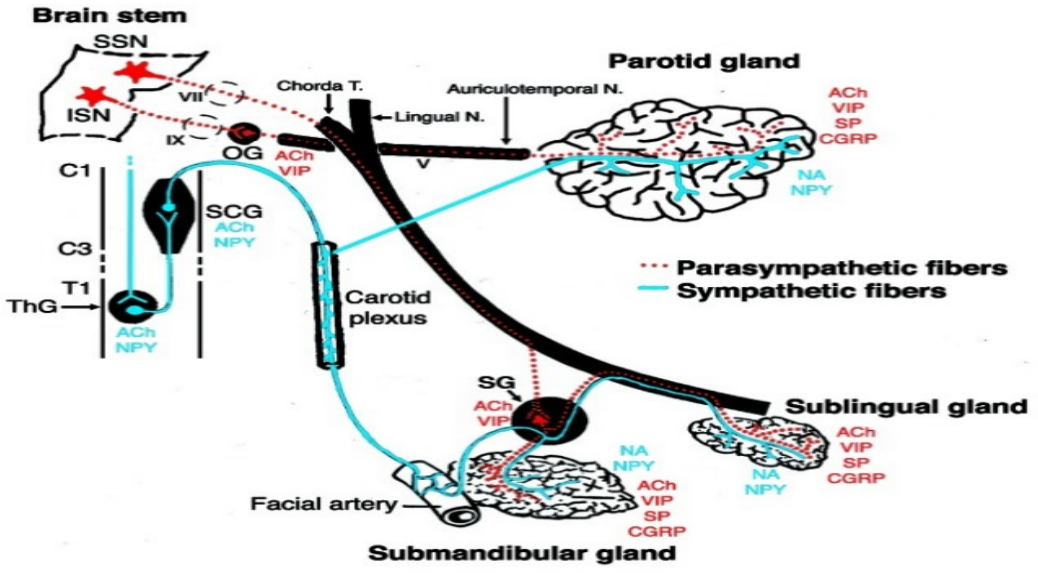

Figure 1.4 Innervation by the parasympathetic and sympathetic branches of the autonomic nervous system and their respective neurotransmitters. Legend: ISN (inferior salivatory nucleus); SSN (superior salivatory nucleus); OG (otic ganglion); C1-C3 (cervical vertebrata); T1 (thoracic vertebrata); ThG (thoracic ganglion); SCG (superior cervical ganglion); SG (submandibular ganglion); Ach (acetylcholine); VIP (vasoactive intestinal peptide); SP(substance P); CGRP(calcitonin gene related peptide); NA (noradrenaline); NPY (neuropeptide Y)

1.4 Salivary Gland Structure, Function, and Molecular Mechanism of Fluid and Protein Secretion

1.4.1 Salivary Gland Structure

Major and minor salivary glands are contiguous networks with highly branched, acinotubular morphologies (Figure 1.5). Mature salivary glands are comprised of three major epithelial cell types; acinar cells assemble into functional acini to provide proteinaceous and/or mucin rich secretions required to maintain oral homeostasis; ductal cells form a collection system of tubular extensions to capture, modify the ionic composition, and provide a conduit for the acini-derived saliva into the oral cavity; myoepithelial cells are seen at the boundary between salivary epithelia derived basement membrane and the surrounding stroma where they are suggested to expel primary saliva from the acini through actomyosin-mediated contraction.

Studies using mouse submandibular gland (SMG) ex vivo culture and genetic lineage tracing analysis suggest the presence of stem/progenitor cell population(s) within salivary gland endbud and ductal structures[34-37]. The stem/progenitor cell- nature of these cells within the salivary gland are currently being investigated, however, at the very least, these cell populations are suggested to have the potential to differentiate into all three mature salivary cell-lineages. Interestingly, it is currently unknown if the existence of progenitor populations is specific to the submandibular gland, or whether they exist in other salivary glands. It is also unclear if these populations function *in vivo* as they do *in vivo*. Such studies are currently being investigated.

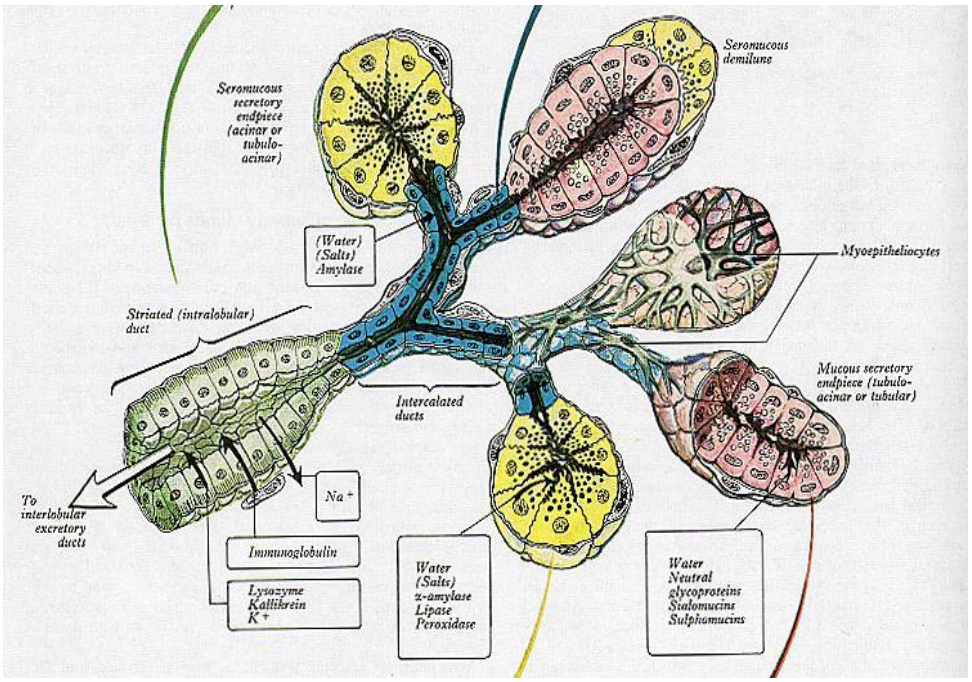

Figure 1.5 Fundamental salivary gland architecture. Both the major and minor salivary glands assume the same acinar-tubular branched structures. Saliva and salivary proteins are secreted into the acini lumens where they are carried into the oral cavity by a highly contiguous ductal network.

1.4.2 Salivary Gland Function

The major function of the salivary gland is to produce saliva. Although saliva is comprised of mostly water (99%) with the remaining 1% consisting of enzymes, glycoproteins and ions, its functions are comprehensive and essential for maintaining oral homeostasis[11]. In addition to digestive enzymes including the major salivary enzyme α-amylase, saliva also contains calcium and phosphate mineral deposits to prevent tooth decay, lysozyme, ribonuclease, proline rich proteins, histatins, and secretory light chain immunoglobulin A to further degrade any remaining particulate materials and to provide a protective layer for the underlying mucosal membranes for defense against harmful bacterial and mycotic microorganisms.

Saliva is characterized as being a non-Newtonian fluid, meaning that its viscosity or resistance to flow is a function of external shearing forces[38]. In the case of saliva, viscosity decreases with increasing shear. This is important for saliva function during mastication. Mechanical stimulation increases local shear forces within the oral cavity allowing saliva to effectively spread along the oral surface allowing it to lubricate the entire oral cavity and allow digestive enzymes within saliva to break down food particles. In the absence of shear, saliva viscosity increases, allowing retention of salivary fluid within the oral cavity.

1.4.3 Fluid and Protein Secretion

Over the course of a single day, the average adult generates two to four pints of saliva[39]. The salivary glands are densely innervated by the sympathetic and parasympathetic branches of the autonomic nervous system (ANS), which are important for regulating salivary flow. Saliva secretion is a continuous process that is mediated by the concerted actions of the two branches of the ANS. In the absence of mechanical and sensory stimulation, defined as resting flow, the average adult produces 0.5 milliliters of saliva every sixty seconds. This resting flow is mediated by low level-ANS stimulation through the orbitofrontal cortex and amygdala of the brain, which operate through the salivary nuclei within the brain stem[33]. Upon mechanical or sensory

stimulation, salivary flow is upregulated with the parotid gland being most responsive, providing 60% of the saliva within the oral cavity upon stimulation[30].

Axons of the parasympathetic ganglion stimulate high salivary flow with low protein content, whereas fibers emanating from the sympathetic ganglion are not responsible for salivary flow, but contribute to the protein content within saliva by regulating exocytosis of salivary specific enzymes including α-amylase. Acetylcholine released by parasymathetic fibers results in the stimulation of muscarinic receptors, M1 and M3, located on the basal surface of acinar cells comprising the acini lobule[3]. M1 and M3 muscarinic receptors are contained within the class of G_q-coupled GPCRs wherein ligand-binding events result in the phospholipase-dependent cleavage of phosphatidylinositol (3,4,5) triphosphate into freely diffusible inositol triphosphate (IP3) and membrane tethered diacylglycerol. Cytosolic calcium concentrations increase following IP3-mediated binding to ligand-gated calcium channels embedded within the membranes of endoplasmic reticulum[40,41].

Before the parasympathetic neurotransmitter acetylcholine can exert its effects on fluid flow, the acinar cells comprising the lobular acini must coordinate several ion transfer reactions to alter the local electrochemical potential. First, the Na/K ATPase maintains low intracellular sodium concentrations and high intracellular potassium concentrations by expelling three sodium atoms into the extracellular space while importing two potassium ions into the cell at the energetic expenditure of an adenosine triphosphate (ATP) molecule. Additionally, the ATP-requiring NaK2Cl co-transporter coordinates the entry of one sodium, one potassium, and two chlorine ions into the cytosol. The combined actions of these two active transporters leads to an intracellular accumulation of negatively charged chlorine ions and a high extracellular sodium concentration, thereby pushing the chloride ion concentration above its electrochemical equilibrium,. Rises in cytosolic calcium facilitated by acetylcholine release from parasympathetic axons open calcium-gated potassium and chloride channels located on the basal and apical membranes, respectively. Chlorine flows out into the acini lumens followed by a flow of sodium ions from the interstitial space through charge-sensitive

cell-cell junctions to maintain electroneutrality (Figure 1.6). Given that sodium is osmotically active, water from the blood will transverse the interstitial space into the lumen through transcellular or paracellular transport mechanisms, resulting in salivary fluid accumulation within the lobular lumens of acini[25,32,40,41].

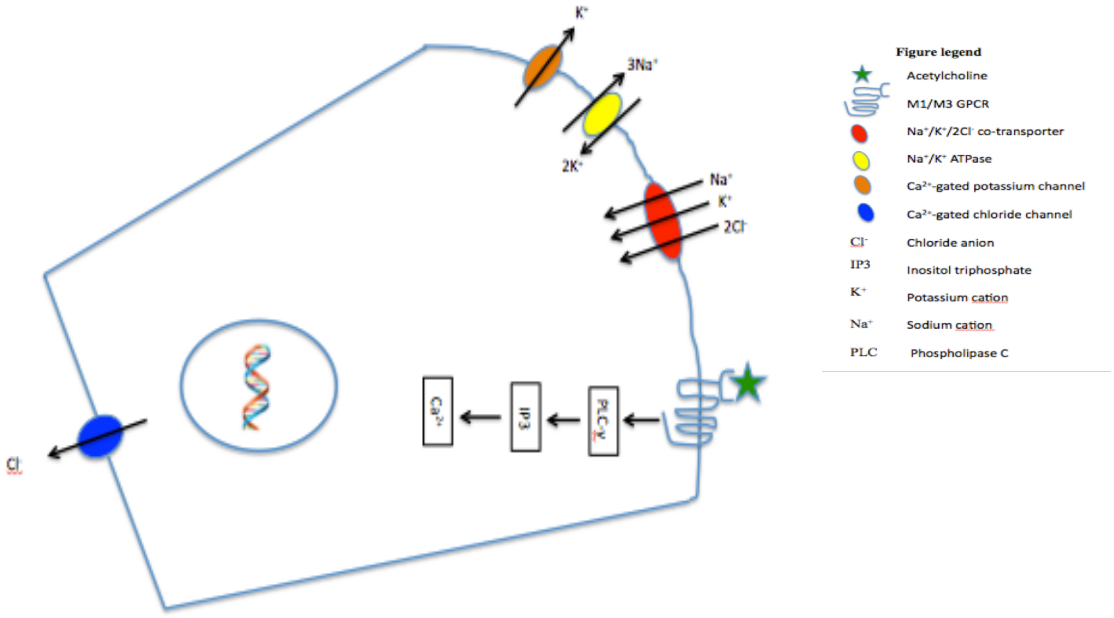

Figure 1.6 Salivary acinar cell fluid secretion See text for molecular mechanism behind fluid secretion.

Neural input from sympathetic fibres exerts its functions on salivary protein content via noradrenaline binding to acinar -, and to a lesser extent -adrenergic receptors. α/β-adrenergic receptors belong to the G_s-GPCR family of transmembrane receptors, wherein ligand:receptor interactions lead to elevated levels of intracellular cyclic adenosine monophosphate (cAMP) and downstream activation of protein kinase A (PKA)[32].

Salivary proteins exhibit directional exocytosis; protein synthesis occurs in a co-translational fashion, followed by vesicular delivery to the Golgi, and subsequent packaging into zymogen granules for delivery and cAMP/PKA-dependent accumulation docking at the cytosolic leaflet of the plasma membrane. Following rises in cytosolic calcium, via parasympathetic acetylcholine release, sympathetic substance P or noradrenaline release, binding M1/M3, substance P peptidergic, and adrenergic receptors, respectively, zymogen granules fuse with the plasma membrane and are subsequently exocytosed into the lumen of acini structures[40,42]

Chemical modification of the primary saliva occurs as a result of multiple ion channels working in a synergistic fashion. The Na^+/K^+ ATPase embedded in the basolateral membrane pumps 3 sodium ions out into the interstitium and 2 potassium ions into the cell at the expense of cytoplasmic ATP. Potassium, at a high intracellular concentration can then leave the cell through two pathways: The first is through a potassium channel located on the basolateral side of the membrane. The second is through the K^+/H^+ exchanger, located on the apical side of the membrane. When potassium leaves the cell via the K^+/H^+ exchanger, H^+ flow into the cell and can subsequently leave the cell through the Na^+/H^+ exchanger located on the basolateral side of the membrane. The net result of the Na^+/K^+ ATPase coupled with individual potassium channels, potassium/proton and sodium/proton exchangers, is a low concentration of sodium inside the cell. This is essential as the sodium in the primary saliva can readily be absorbed by the ductal cell through the Na^+ channel or by the Na^+/H^+ exchanger. As the ductal cell absorbs sodium, chloride from the ductal lumen

enters the ductal cell to maintain electroneutrality. Chloride enters through one of two pathways; a chloride channel or a bicarbonate/chloride exchanger, both located on the apical side of the membrane. In sum, sodium chloride is absorbed by the ductal cell via the Cl^-/HCO_3^- exchanger in concert with bicarbonate secretion (Figure 1.7).

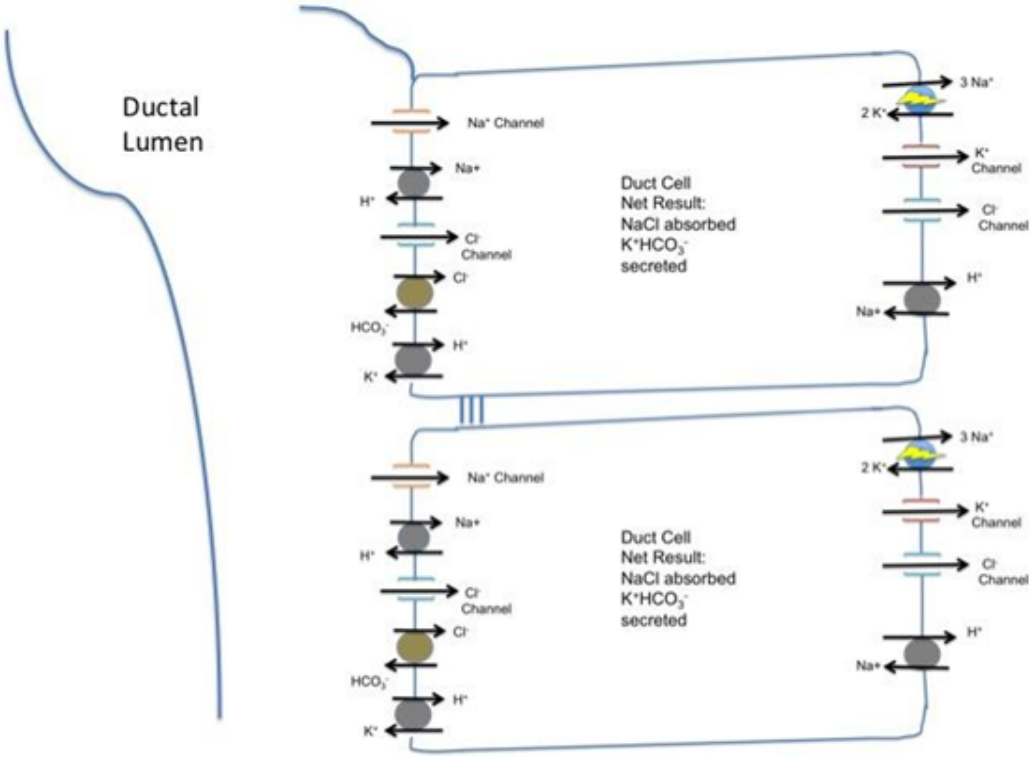

Figure 1.7 Mechanism for ductal cell ion exchange. For a detailed description of the molecular mechanism, refer to text.

1.5 Salivary Gland Development

1.5.1 Developmental Origins

Ex vivo culture of the three major salivary glands from mice has provided valuable insight into salivary gland development. It has been well established that the underlying mesenchyme of all three major glands develops from the neural crest; conversely, the developmental origins of the epithelium remains nebulous, with respect to being derived from either the ectoderm or endoderm. Literature has yet to reach a consensus, as many suggest the parotid gland is of ectodermal origin, whereas the submandibular and sublingual glands develop from the endoderm[4,18]. During salivary gland initiation, the small outpouchings of precursor oral epithelium invade the surrounding mesenchyme. Comprising the oral epithelium is the oral ectoderm and the foregut endoderm where there is a junction formed by the orophayrngeal membrane. Discrepancies regarding which portion of the oral epithelium contribute to salivary gland initiation and subsequent development result from the inability to discern the exact position of the junction separating the ectoderm from the endoderm.

Lineage tracing analysis using Cre/LoxP transgenic mice has proven fruitful in mapping several germ layers of craniofacial tissues. Wnt1-Cre and Msep1-Cre mice have shown the role of the neural crest in the developing tooth and cranial base and skull vault, respectively[23,24]. Sox17 has been used to identify endodermal-derived tissues; Sox17-2A-iCre/R26R mice showed no labeling of the epithelium of the major salivary glands, suggesting they are of ectodermal origin[18]. Additionally, ectodysplasias, diseases affecting only ectodermal-derived tissues show abrogated salivary gland phenotypes[22], further alluding to their ectodermal origins. Future work should implore ectoderm-derived Cre drivers to further vindicate salivary gland precursors.

1.5.2 Salivary Gland Developmental Stages

Ex vivo organ culture has been widely used to investigate developmental phenomena during organogenesis of the lungs, mammary, prostate, kidneys, and

salivary glands. *Ex vivo* culture of the fetal SMGs of mice has been used for over 50 years due to ease in gland isolation while recapturing many aspects of salivary gland development seen *in vivo* (Figure 1.8)[20, 25]. Salivary gland development begins with a thickening of the oral epithelium and ultimately generates the complex, highly organized, branched architecture required for the efficient production and vectorial transport of the salivary secretome. Embryonic day 11 (E11.5) marks the onset of the Prebud stage in the mouse SMG (with the discovery of the coitial plug defining E0) as the primitive oral epithelium begins to thicken forming the salivary gland placode. At this time Wnt-1+ neural crest progenitor cells begin to coalesce into neuronal cell bodies that will form the parasympathetic ganglion which will develop in parallel with the salivary epithelium[22].

Additionally, the endothelial cell plexus is seen surrounding the condensing mesenchyme. During the Initial bud stage at E 12, the placode invades the surrounding first mandibular arch mesenchyme generating a distal terminal endbud with a proximal stalk. The primary distal endbud expands to undergo epithelial clefting to generate 3-5 daughter endbuds at E12.5. Rapid proliferation and epithelial morphogenesis occurs during the Pseudoglandular stage, from E12.5 to late E14. Epithelial branching morphogenesis results from reiterative rounds of cleft formation and progression accompanied by basement membrane remodeling and epithelial cell proliferation to generate an immature network of interconnected acinotubular network. Luminalization and cytodifferentiation from late E14 to E17 mark the Canalicular and terminal Bud stages, resulting in a contiguous branched network.

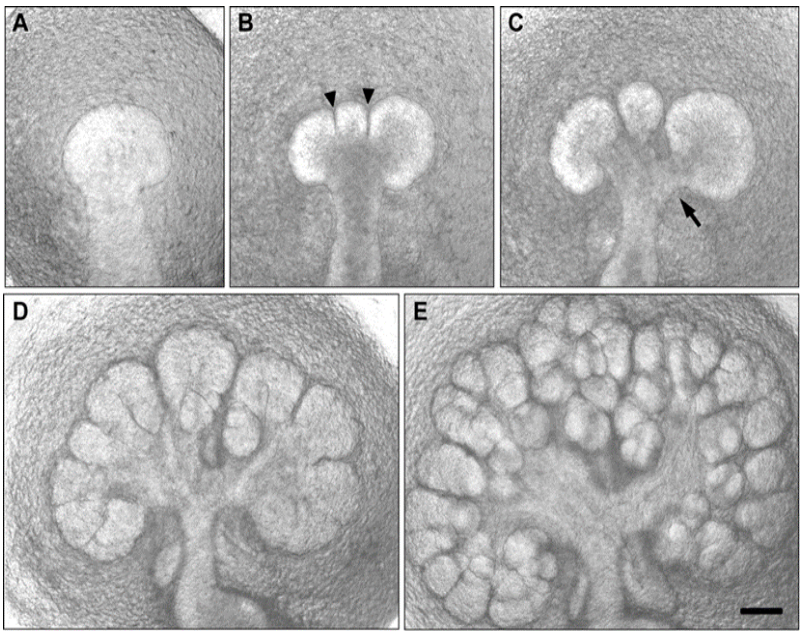

Figure 1.8 *Ex vivo* culture of the fetal SMGs of mice. Over the course of embryonic development, the oral epithelium will undergo drastic morphogenesis to generate highly branched contiguous acinar-tubular networks.

1.5.3 Stromal and Neural Induction of Salivary Morphogenesis

Salivary gland organogenesis is dependent on interactions between the various cell and tissue types comprising the gland to promote proliferation, survival, apoptosis, cell shape changes, adhesion, and motility. Epithelial, mesenchymal, endothelial, neuronal, and lymphatic cell populations all make unique contributions to the developing gland. The role of endothelial and lymphatic systems in salivary gland development are not well understood and require further investigation. In contrast, much emphasis has been placed on studies the roles of epithelial-mesenchymal, and more recently, epithelial-neuronal interactions. Such interactions have been studied using *ex vivo* SMG culture[20]. Furthermore, the SMG can be mechanically separated into individual epithelial, mesenchymal, and parasympathetic ganglion components, where they can be studied in isolation or through recombination experiments.

Ex vivo SMG culture using heterotypic tissue recombination systems have shed valuable insight into the roles of mesenchyme-, and neuronal-derived signaling molecules to promote epithelial clefting, end bud expansion, duct formation, and generation of luminal space during glandular induction and morphogenesis. E.13 SMG epithelium recombined with non-inductive, maxilla-derived mesenchyme failed to branch, whereas E.13 epithelium overlayed with metanephric mesenchyme formed tubules reminiscent of the collecting ducts within the kidney[26]. Additionally, E.13 salivary gland mesenchyme recombined with branching mammary epithelium formed salivary gland-like structures[27]. Using heterotypic tissue recombination experiments at various stages during SMG development, Wells and colleagues identified that the epithelial and stromal compartments within the fetal SMG contain a time-dependent, intrinsic reprogramming capacity. They found that the genetic program(s) required to mediate inductive events resides in both the epithelial and mesenchymal tissue compartments within the salivary gland before E.12.5. However, after E.12.5, the instructive information necessary to drive glandular morphogenesis is contained only within the mesenchyme[28].

In 1937, the seminal work done by Pavlov established the role of the autonomic nervous system (ANS) in salivary gland function. Despite this, the functions of the sympathetic and parasympathetic branches of the ANS nervous system during salivary gland development are only just beginning to be elucidated. During development, the peripheral fibers from the parasympathetic ganglion develop in parallel with the SMG, providing rationale that the PSG might function in salivary gland organogenesis. To investigate the role of the PSG in SMG organogenesis, Knox et. al. mechanically separated the PSG from fetal SMGs with epithelial and mesenchymal compartments still intact and placed in culture. Explants cultured without the PSG showed reduced branching morphogenesis with fewer epithelial end buds than fully intact SMGs, highlighting the role of neuronal input in salivary gland development[29]. Additionally, irradiated SMGs of fetal mice displayed reduced morphogenesis resulting from epithelial and neuronal apoptosis. Remarkably, irradiated glands treated with the neurotropic factor, neuturin which interacts with PSG fibers, completely restored PSG function and subsequently rescued SMG branching morphogenesis by increasing epithelial cell proliferation[30].

1.5.4 Branching Morphogenesis

Branched structures are seen in virtually all levels of organization, ranging from molecular and subcellular scales to cellular, tissue, and even whole-organism hierarchies. In higher organisms, the epithelium of the lung, kidney, prostate, mammary, and salivary glands all exhibit branched/tree-like architectures to facilitate the efficient production and vectorial transport of glandular secretions (Figure 1.9)[58]. Such physiological systems are dependent on the reticulate organization of their cellular and subcellular constituents to necessitate final tissue/glandular morphologies and emergent functions.

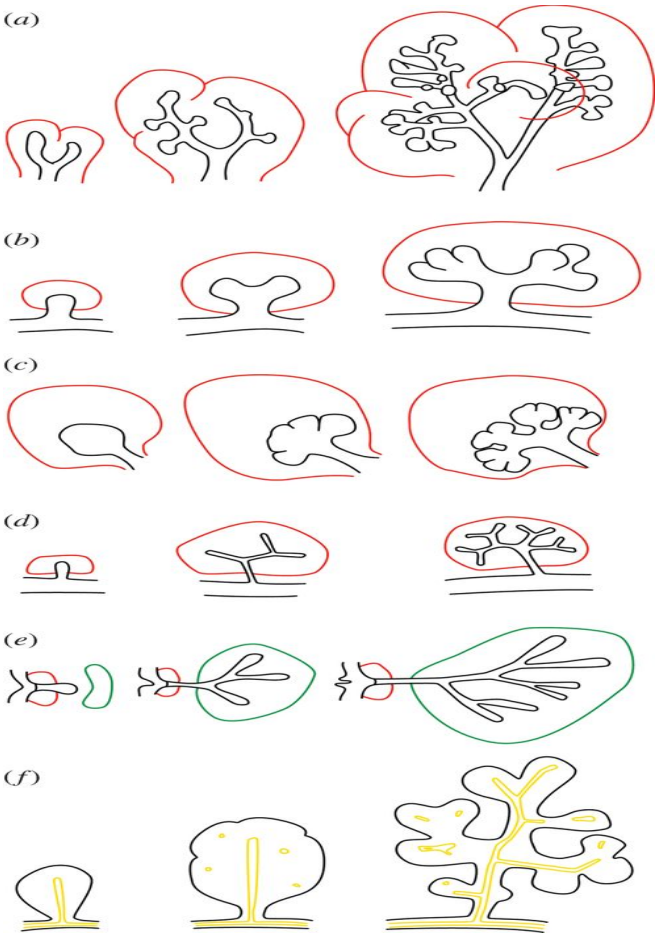

Figure 1.9 Branching morphogenesis in various exocrine glands. Lung (a), ureteric bud (b), salivary gland (c), prostate (d), mammary gland (e), and pancreas (f)

Organogenesis of branched organ structures is dependent on the reciprocal interactions between the epithelium and underlying stroma. The cell-type heterogeneity within the mesenchyme is indicative of its pleiotropic roles in providing an epithelial niche regulating cell proliferation, migration, stem/progenitor cell maintenance, cytodifferentiation, tissue morphogenesis and homeostasis. Neuronal, endothelial, and mesenchymal cell populations comprising the stroma and their concomitant biochemical and biophysical inputs highlight the highly evolved developmental synchrony required of coordinated morphogenic outputs.

Ex vivo recombination experiments highlight the key role of the juxtaposed mesenchyme in driving epithelial morphogenesis; fetal salivary epithelium cultured with either non-branching pharyngeal arch or lung mesenchyme either failed to branch or generated morphologies reminiscent of a branching lung, respectively. Interestingly, a recent study has shown the defined temporal nature of the reciprocal interactions between the epithelium and the mesenchyme, as embryonic salivary epithelium before embryonic day 12.5, was able to reprogram non-glandular mesenchyme to provide the instructive signals necessary for inducing salivary gland branching morphogenesis[28]. These results suggest that genetic program controlling morphogenic outputs is well defined; yet readily malleable by the regulatory signaling networks controlling organogenesis.

1.5.5 Organ/tissue patterning through branching morphogenesis

Any recurring characteristic or repeated regularity in a system in space and time results in pattern formation.[156] Biological patterns resulting from branching morphogenesis are highly conserved throughout vertebrate organogenesis. Tissues and organs including the lung, mammary, prostate, and salivary glands are all highly branched systems. Analysis of branched organ architectures has identified three major geometrical modes of organ morphogenesis: domain branching, planar bifurcation, and orthogonal bifurcation[58-62] (Figure 1.10).

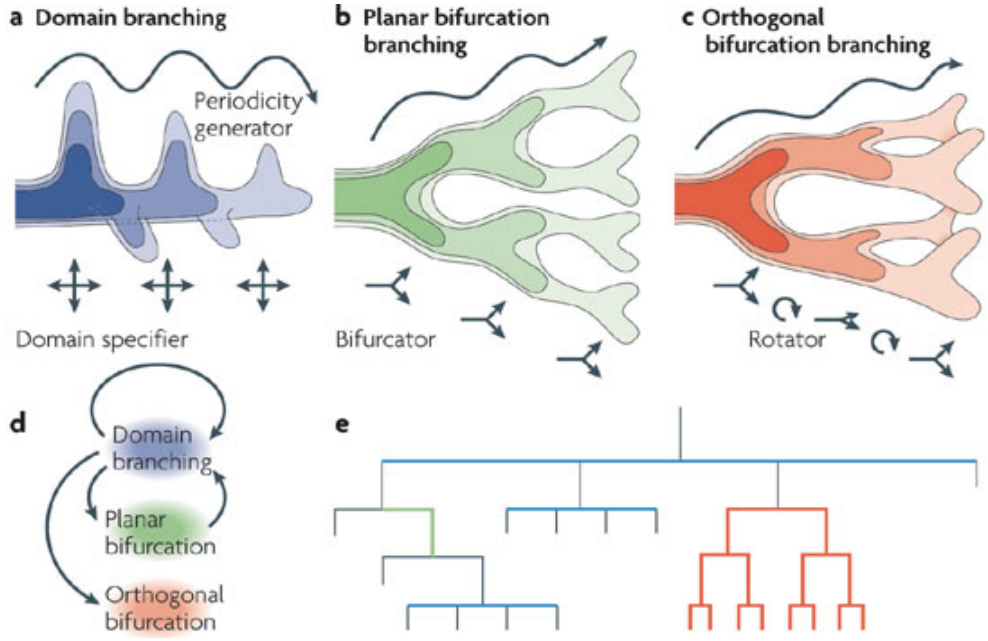

Figure 1.10. Geometrical modes of branching morphogenesis. Domain branching (a), planar bifurcation (b), orthogonal branching (c). The various modes of branching morphogenesis are utilized by different exocrine glands at different frequencies and periodicities to generate final organ/gland architecture (d,e).

Resultant organ architecture is ultimately dependent on the spatiotemporal sequence the geometric modes are used in, as well as the frequency and periodicity at which they occur[58]; it has long been suggested that signaling molecules are essential in generating patterned, well-branched tissue architectures. The mechanisms contributing to biological pattern formation have been under investigation for over 100 years.

Inductive cell signaling events spanning different tissue types are essential for organogenesis during development. Interestingly, the final morphologies of many branched organs are readily discernable at the micro and macroscopic scale, yet despite only subtle nuances in each system, the signaling molecules and their downstream pathways are highly conserved from organ to organ. During morphogenesis, the precursor epithelia of the lung and the salivary gland both invade their respective underlying stroma in response to Fibroblast Growth Factor 10 (FGF10). In the mammary gland FGF2 and FGF10 have been shown to regulate ductal elongation and bud formation, respectively[157]. However, in the salivary gland FGF7 contributes to bud formation, whereas FGF10 facilitates ductal elongation. How then, are the defined outputs of glandular patterns generated from almost identical inputs?

The term “morphogen” was first coined by Alan Turning when his seminal paper titled ”The Chemical Basis of Morphogenesis” was published in 1952. He described the capability of two homogenously distributed chemical species (morphogens) to self-organize into patterns when external perturbations (biological noise) induce initial morphogen distribution to deviate from equilibrium[158]. His *reaction-diffusion* model, Turing provides a mathematical description of pattern formation resulting from the activation and inhibitory responses of two diffusing morphogens with different diffusion characteristics. In 1969, Wolpert and colleagues developed French Flag Model for positional information, suggesting that morphogen production must be confined to an immobile source to permit a graded signal distribution over the target tissue[159]. The graded signal confers the dose-dependent

regulation of cell differentiation by altering the genetic programs controlling cell fate (Figure 1.11) [160].

It wasn't until the late 1980's when Bicoid, a transcriptional effector, was found to regulate anterior-posterior body symmetry in a concentration gradient-dependent manner in the developing Drosophila embryo[161]. Since the discovery of Bicoid in the late 1980's, multiple signaling molecules including the fibroblast growth factors, epidermal growth factors (EGF), Wnts, Transforming Growth Factor-β (TGF-β) superfamily members, and hedgehog have all been shown to induce concentration-dependent responses resulting in differential gene expression, cell lineage specification, and branching morphogenesis.

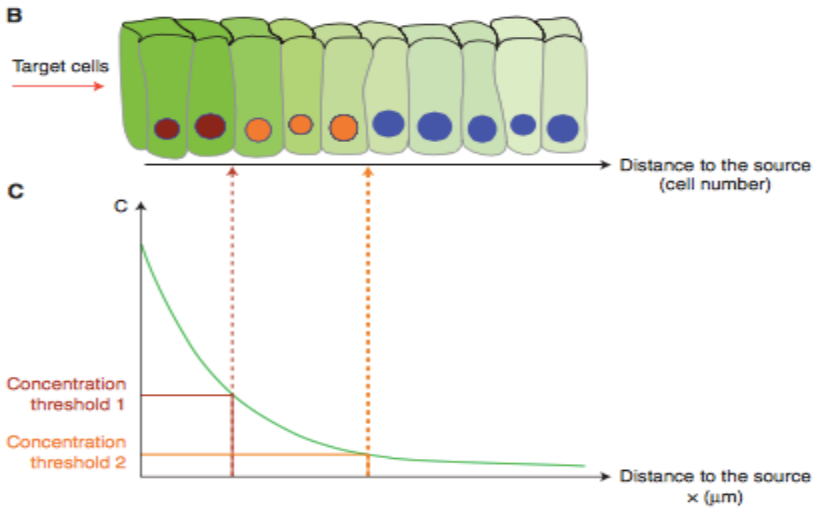

Figure 1.11 French Flag Model for morphogen gradient formation. A morphogen produced by a localized source diffuses over a target cell domain (b). Over time, a concentration field can arise by reaction-diffusion mechanisms. Concentration thresholds at a given position arise from graded morphogen distributions to regulate gene expression patterns, controlling cell differentiation and morphogenesis (c).

1.5.6 Growth Factor Signaling Pathways in Salivary Gland Branching Morphogenesis

Coordinated cell proliferation, survival, stem/progenitor maintenance and expansion, migration, ECM remodeling and turnover, and cell motility are essential during salivary gland branching morphogenesis[22]. SMG *ex vivo* culture experiments using isolated epithelium or homo/heterotypic tissue recombination have identified multiple signaling factors and pathways that facilitate the crosstalk between the epithelium and heterocellular stromal populations. Signaling during epithelial morphogenesis is complex; many growth factors and ECM protein signaling pathways are highly integrated and converge to regulate morphogenic events. Knockout mice and loss of function approaches implicate a comprehensive number of genes in the branching process.

Among the most well studied growth factor families in salivary organogenesis are the Fibroblast Growth Factor family (FGF) of signaling molecules. *Fgf10*$^{-/-}$ and *Fgfr2b*$^{-/-}$ mice do not form salivary glands, suggesting a role for FGF10:FGFR2b signaling in salivary gland initiation,[20]. Mice deficient in FGF7 do not display any severe phenotypes and have normal salivary glands suggesting that other FGF family members are capable of compensating FGF7 function. *Ex vivo* culture of isolated SMG epithelium stimulated with FGFR2b ligands, FGF7 and FGF10 were observed to have distinct effects on epithelial morphogenesis[139]. FGF7 treatment resulted in SMG budding, whereas FGF10 induced the formation of elongated ductal structures. FGF signaling has been implicated in regulating stem/progenitor cell maintenance and expansion in the branching SMG. Lombaert et. al., identified that FGF10:FGFR2b signaling upregulates an autocrine epithelial KIT signaling pathway such that FGFR2b/KIT stimulation, through separate MAPK and PI3K/AKT pathways, promotes KIT+K14+Sox10+ distal progenitor proliferation in the endbud[9]. Additionally, FGF10:FGFR2b signaling has been shown to amplify FGFR signaling by increasing *Fgfr1b,Fgfr2b, and Fgf1* transcription, which has been shown to be required for endbud expansion and differentiation[140,141].

The Wnt family secreted proteins play pivotal roles in cell-cell communication during embryogenesis and development. Wnt signaling has been shown to coordinate with FGF signaling in the developing SMG. Early during SMG development, Wnt signaling proteins localize to the mesenchyme, however, after E 14.5 Wnt/β-catenin and non-cannonical Wnt signaling is restricted to the ductal regions via FGF-mediated inhibition within the endbud[142]. Non-cannonical Wnt signaling via Wnt5b has been suggested to regulate the expression of ductal marker *Cp2l1*. Restriction of CP2l1 to ductal structures has been suggested to be mediated by the FGF-mediated inhibition of Wnt5b within the endbud. Additionally ectopic expression of Wnt/-catenin within the presumptive duct regions induced K5+ proliferation and drove ductal differentiation.

The ectodysplasin (Eda) pathway is required for the generation of many ectodermal organs and appendages. Eda belongs to the TNF superfamily of signaling molecules and manifests its signaling function through binding its receptor, Edar. In humans, mutations within the Eda:Edar pathway result in hypohidrotic ectodermal dysplasia, characterized by malformed teeth, hypoplastic sweat glands, and dysfunctional salivary glands[143,144]. *Eda*-null mice show SMG phenotypes with few ductal structures, whereas ectopic expression of *Eda* under the K14 promoter leads to SMGs with expansive lumens and increased branching. Upstream
Wnt/-catenin signaling amplifies *Eda* -transcription within the mesenchyme. Following secretion and binding Edar within the epithelium, NF-$_k$B-mediated downstream signaling results in elevated *Shh* levels. Shh signaling upregulates *Fgf8,* which positively regulates both *Fgf10* and *Shh* gene expression[143]. It has been suggested that Shh levels can also negatively regulate FGF10 expression in the mesenchyme to fine-tune the extent of FGF10-mediated proliferation within the epithelium.

EGF:EGFR signaling has been observed to proliferation during salivary gland branching morphogenesis as *EGFR*$^{-/-}$ mice display reduced branching resulting from decreased proliferation[145]. Furthermore, inhibition of MMP-mediated release from the cell surface, or addition of function blocking antibodies for EGFR ligand, HB-EGF, markedly inhibit branching by reducing the number of end buds and a complete absence

of ductal structures. EGFR ligands, EGF and TGF- have also been shown to function in promoting SMG morphogenesis, but their mechanisms have yet to be fully elucidated. Cholinergic input from the PSG expands epithelial K5+ proximal progenitors and promotes ductal differentiation through an ACH/M1:HB-EGF/EGFR-dependent mechanism[8].

1.5.7 Epithelial Clefting During Salivary Gland Branching Morphogenesis

By embryonic day 12, the primitive salivary epithelium has already invaded into the fibrous meshwork of the underlying stroma as a proximal elongated stalk and distal terminal endbud. Epithelial clefting begins at E 12.5 with cleft initiation, characterized by emerging furrow-like membrane deformations along the periphery of the endbud. During branching morphogenesis, distal epithelial cell clusters will undergo reiterative rounds of epithelial clefting to separate endbud structures into individual hemispheres. Live cell imaging studies show that epithelial clefts are highly dynamic structures, with some regressing back to their original position, while others progress and deepen[146,147]. Ultrastructural analysis of embryonic SMG clefts by electron microscopy identified the presence of actin-rich membrane protrusions extending at the base of clefts at the onset of cleft progression. Defined as a "shelf", this cytoplasmic ridge is hypothesized to mediate integrin-dependent contact with the basement membrane, activating contractile actomyosin machinery to induce a downward acting mechanical force for cleft progression[146].

The role of actomyosin machinery in epithelial clefting during branching morphogenesis was established when E.13 SMGs treated with either myosin II or ROCK inhibitors showed aberrant cleft progression. Interestingly, both inhibitors had no effect on cleft initiation, as SMG epithelia treated with either inhibitor showed an increase in the number of forming clefts, implying that the role of actomyosin machinery in epithelial clefting is restricted to cleft progression and not cleft initiation. ROCK or myosin II inhibition also resulted in decreased β1-integrin activation levels, shown by confocal microscopy pixel intensity levels using

fluorescently tagged antibody shown to specifically bind active conformations of β1-integrin[147]. Reduced β1-integrin activation was concurrent with decreased localization of focal adhesion proteins including, focal adhesion kinase (FAK), talin, and vincullin to sites of basal cell-ECM interactions at the endbud periphery. These results indicate that cleft progression is in part, dependent on ROCK/myosinII-induced activation of β1-integrin to recruit of focal adhesion proteins to cell-matrix attachment sites in order to drive cleft progression.

E.13 SMGs subject to FAK inhibition using either pharmacological agents or siRNA knockdown displayed phenotypes similar to SMGs treated with ROCK and myosin II inhibitors, with an increase in the number of initiated clefts at the endbud periphery and decreased branching morphogenesis. Interestingly, perturbation of ROCK-1 resulted in impaired basement membrane secretion and assembly with basement membrane proteins accumulating within the terminal cell cluster in developing SMG. ROCK-1 was found to be responsible for regulating the localization of polarity protein PAR1b to the correct membrane microdomain to facilitate polarized basement membrane and extracellular matrix protein secretion[148]. Dysfunctional FAK signaling was also associated with decreased epithelial cell proliferation and fibronectin deposition/assembly. The role in fibronectin in salivary gland branching morphogenesis was established when developing SMGs treated with fibronectin-targeting siRNAs showed disrupted branching morphogenesis[147,149]. Exogenous addition of fibronectin was able to rescue branching defects induced by siRNA-treatment. It was identified that fibronectin levels are positively regulated by downstream FAK activation, leading to increased fibronectin secretion at the cell surface. Fibronectin accumulation at sites of cell-ECM contact triggers activation of β1-integrin, which is hypothesized to function with α5 integrin as the functional α5β1-heterodimer to facilitate fibronectin adhesion. Additional integrin clustering and activation by focal adhesion proteins triggers ROCK/actomyosin-mediated contraction to promote fibronectin fibrillogenesis through the mechanical stretching of fibronectin to reveal a cryptic self-assembly motif. Live cell imaging studies using fluorescently-

tagged fibronectin reveal that fibronectin deposition within forming clefts drives progression. As fibronectin accumulates at the base of the cleft, cell-cell contacts within the cleft are replaced by cell-fibronectin contacts, triggering the expression of BTBD7 within the progressing cleft. BTBD7 positively regulates the expression of Snail2 to repress E-cadherin, thereby depleting the number of cell-cell contacts within the cleft region, allowing cleft progression to proceed (Figure 1.12) [25,150].

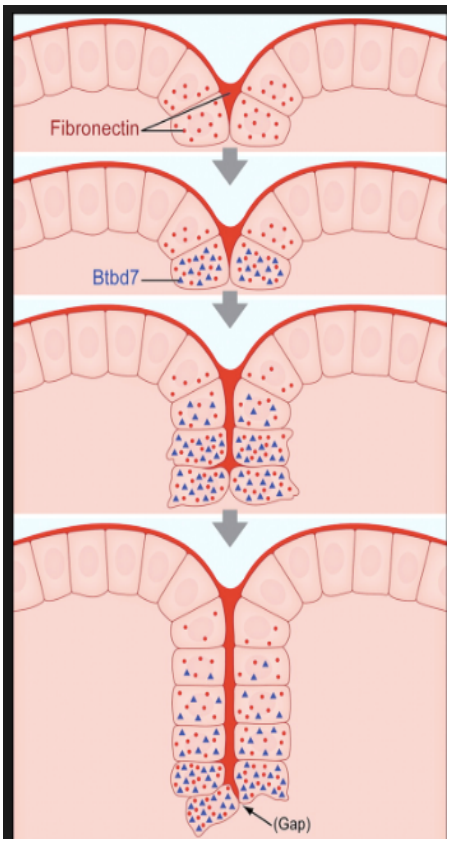

Figure 1.12 Fibronectin and Btbd7 are required for salivary gland clefting during branching morphogenesis. Fibronectin accumulates at nascent clefting sites. Downstream fibronectin signaling upregulates Btbd7 activity to replace cell-cell interactions with cell-matrix adhesions.

1.5.8 Salivary Gland Lumen Formation

The creation of hollow interiors within the highly branched acinotubular networks of many branched glands, including the lungs, collecting ducts of the kidneys, and salivary glands are essential for glandular function. Within the salivary gland, lumen formation occurs within endbud and ductal structures, resulting in the generation of a contiguous branched system to provide directional salivary flow into the oral cavity. The diversity in tubular structures and their mechanisms provides a challenge in determining organ/gland-specific modes of tube formation. Blood vessel lumen formation has been hypothesized to occur through cord hollowing, where lumen formation occurs at the apical domains of adjacent endothelial cells by organizing increased vesicular trafficking to apical membranes[167,168]. Elevated vesicular delivery of polarity complexes required for lumen expansion to the apical membrane domains leads to an increase in membrane surface area and the formation of microluminal structures. Microlumens within single cells then fuse with those of neighboring endothelial cells forming continuous lumens. Conversely, within the developing Drosophilia trachea, lumen formation occurs as a consequence of cell invagination. As the tracheal epithelial cells respond and elongate to a gradient of FGF ortholog, branchless, they begin to thicken and invaginate inwards to arrange themselves into a hollow tube[63].

Tubulogenesis within the salivary gland is not well understood. Like most morphogenic events, tube formation suggested to result from epithelial-mesenchymal cell crosstalk. Granted, that ductal tube formation occurs alongside SMG innervation by the parasympathetic branch, but not sympathetic branch of the autonomic nervous system, Knox and colleagues predicted that the PSG might contribute to lumen formation within ductal structures during salivary gland development. Neurturin (NRTN), a neurotrophic factor produced within the salivary endbuds, has been shown to be required for recruiting neuronal outgrowth towards the developing epithelium. Function blocking antibodies for NRTN significantly reduced the number of PSG varicosities interacting with the epithelium and inhibited branching morphogenesis[29].

Additionally, inhibiting NRTN-dependent PSG-epithelial interactions resulted in increased primitive duct with accompanied by dysregulated ZO-1 localization along the ductal midline implicating that neuronal input from the PSG aids in proper duct formation by coordinate sites of ductal lumen formation.

Acetylcholine (ACh) is the dominant neurotransmitter in manifesting PSG-induced functions. In concert with previous studies chemical inhibition of ACh signaling resulted in an overall decrease in E 13 *ex vivo* SMG explants, however, ZO-1 localization and duct width were similar to untreated controls. Rather, inhibition of vasoactive intestinal peptide receptor (VIPR) on the SMG epithelium using a VIPR antagonist, showed phenotypes similar to NRTN-function blocking antibody experiments with an increase in duct length, mislocalized ZO-1 staining, and an overall decrease in epithelial morphogenesis. VIPR1 binds vasoactive intestinal peptide (VIP), a PSG-derived neuropeptide whose expression patterns cluster tightly with secondary duct formation and ductal biomarkers K19 and K7. VIPR1 is a G_s-coupled GPCR that induces elevated cyclic AMP (cAMP) levels to activate protein kinase A (PKA), which has been shown to be responsible for regulating multiple cell functions. Isolated E 13 SMG epithelial explants were cultured in the presence of VIP or membrane permeable cAMP analog (8-bromoadenosine cyclic adenosine monophosphate), showed the same effects, with SMG epithelium undergoing rapid proliferation, ductal elongations, and the formation of a contiguous lumen. Untreated glands showed the formation of microlumens with atypical protein kinase C (aPKC) and subapical golgi marker GM130 staining, however, no continuous lumen was observed in these SMGs, implying that VIP/VIPR signaling is responsible for contiguous ductal lumen formation in a cAMP/PKA-dependent manner.

1.5.9 Salivary Gland Progenitor Cell Populations in Development

It's well established that epithelial morphogenesis is dependent on progenitor cell populations. *Ex vivo* SMG homo- and heterotypic tissue recombination experiments at various stages of salivary gland development highlight the plasticity and

reprogramming ability of embryonic mesenchymal and epithelial tissue compartments. Wells and colleagues identified the capability of the epithelium and mesenchyme to reprogram glandular and nonglandular mesenchyme, however, this was shown to be developmental-stage specific, suggesting that progenitor populations with the SMG decrease over the course of development and undergo cytodifferentiation to give rise to acinar, ductal, and myoepithelial cell lineages[28]. Cell fate decisions during development are accompanied by alterations in patterns of gene expression, which are regulated by several growth factor, ECM, and additional homo/heterocellular-based interactions within the local microenvironment.

Characteristic gene expression patterns of embryonic stem cells were compared to those within the SMG epithelial endbud and ducts. Oct3/4, the transcriptional effector characterized as the master regulator of pluripotency in ES cells was undetectable using qPCR methods. Nanog, which is typically affiliated in ES cell maintenance, was also absent within the SMG epithelium during development. On the contrary, Sox2, Klf4, and c-Myc, were all found to reside within the epithelium at E.13, although their localization within epithelial subcompartments were different. *Sox2* expression was localized to the ductal compartment at E 13, followed by a gradual decrease in transcript levels during development and into adulthood. Like *Sox2*, *Klf4* mRNA also localized to ductal structures, however, unlike *Sox2*, *Klf4* expression increased during development[151]. One possible explanation for this observation is that *Krtn19* expression, a ductal differentiation marker, has been suggested to be under Klf4-dependent transcriptional regulation. *c-Myc* gene expression is found within both endbud and ductal structures at E 13, however, its expression is increased at E15, during the rapid branching phase of salivary gland development, which is accompanied by large scale cell proliferation and migration. In sum, the expression profiles gathered from this study suggest that the salivary epithelium does not contain a reservoir of ES cells, but rather progenitor cell populations.

Lombaert et. al., have suggested that two different pools of epithelial progenitors reside within the SMG; distal endbud and proximal stalk progenitors[9]. Knox et. al.,

showed that branching morphogenesis is perturbed when the parasympathetic ganglion of E13 SMGs is mechanically separated from epithelial and mesenchymal compartments[8]. The dominant neurotransmitter released by the PSG is acetylcholine, which in the salivary gland binds muscarinic receptors one and three (M1 and M3), a family of G_q- coupled GPCRs. Chemical inhibitors targeting ACh/M1 signaling in whole organ explants were shown to abrogate branching morphogenesis in a similar fashion compared to removal of the PSG. qPCR for progenitor markers *Krt5*, *Krt15,* and *Apq3* was used to examine the effect of PSG removal on progenitor populations. All three markers were downregulated in the absence of PSG-mediated ACh/M1 stimulation, suggesting that parasympathetic innervation is important for regulating salivary gland epithelial progenitor levels.

Ex vivo culture of isolated epithelium treated with ACh analog, carbachol (CCh) increased the number of K5+ epithelial progenitors and was able to rescue branching morphogenesis in explants where the PSG had been removed. Genetic lineage tracing analysis has confirmed that K5 is a basal epithelial progenitor localized within the intercalated ducts of salivary glands and Fluorescence Assisted Cell Sorting (FACS) of adult human salivary glands shows that approximately 1.6% of the total epithelial cell population are K5+, suggesting that adult salivary glands maintain a small reservoir of progenitor cells. Studies from prostate epithelium have identified ACh/M1 signaling as a transactivator of EGFR signaling by facilitating the MMP-2 mediated release and activation of HB-EGF from the plasma membrane[151,152]. Isolated SMG epithelia treated with EGFR inhibitor and CCh did not branch, implying that ACh/M1-mediated morphogenesis is dependent on downstream EGFR activation. In normal SMG development, K5+ progenitors differentiate into keratin 19+ cells to drive differentiation towards the ductal cell lineage. To investigate the effects of CCh and HB-EGF on K5+ cell proliferation and differentiation, isolated SMGs were stimulated with either CCh or HB-EGF. Exogenous CCh doubled the K5+ progenitor population while also increasing the K5+K19+ cell populations, indicating that both K5+K19- and K5+K19+ populations are capable of responding to ACh/M1 signaling. HB-EGF

stimulation increased the number of proliferating K5+K19+ and K5-K19+ cells, highlighting a role for HB-EGF-mediated signaling in driving ductal differentiation within the salivary gland. This data suggests a role for PSG ACh/M1 signaling in promoting branching morphogenesis by promoting progenitor cell expansion and differentiation, while also identifying an important role for neuronal input in maintaining a pool of proximal K5+ epithelial progenitors in adult salivary glands.

KIT (c-Kit or CD117) is a receptor tyrosine kinase that has been studied extensively within hematopoietic progenitor cell populations[153]. KIT signals through binding its ligand, stem cell factor (SCF) to activate downstream MAPK, PI3K/AKT, and PLCpathways. Within the developing SMG, *Kit* transcripts localize within the endbud, while mRNA for SCF (*Kitl*) was predominantly found within the mesenchyme with some transcripts detected within the endbud. FACS analysis during E13-E16 showed that the KIT+ cell population increased from 10% to 20% relative to the entire epithelial cell compartment within the SMG, with 70% of the KIT+ cells undergoing proliferation, shown by ki67 co-staining[9].

1.6 Branching Morphogenesis in Other Exocrine Organs

1.6.1 Branching of the Drosophila Tracheal System

One of the most characterized, multicellular-branched organs is the tracheal system of invertebrate species Drosophila melanogaster. This tubular epithelial network is highly ramified, ensuring that molecular oxygen reaches every cell within the organism by passive diffusion[63]. Early during larval development, roughly 10-sac like invaginations of approximately eighty epithelial cells form along the embryo. Tracheal cells begin to organize themselves into bud-like structures in response to a mesoderm-derived, Branchless (Bnl) concentration gradient. An FGF ortholog, Bnl exists at the top of the signaling hierarchy controlling tracheal branching through binding Breathless (Btl), its cognate receptor expressed at the basolateral surfaces of tracheal epithelial cells. Bnl:Btl ligand-receptor interactions promote outgrowth of the tracheal bud via

collective cell migration and rearrangement preceded by extensive filopodia formation. Extending branches are further fine-tuned through reciprocal Bnl:Btl/Detla:Notch regulatory feedback signaling networks (Figure 1.13).

Epithelial cells closest to the source of diffusing Bnl (tip cells) begin to produce Notch as to activate Delta:Notch signaling in epithelial cells most distal to the Bnl source to induce stalk cell differentiation along the growing branch. To form the fully functional branched tracheal system, tubular extensions must converge, fuse, and form lumens to form contiguous networks. Spatial organization of the Drosophila tracheal system is regulated through the availability of molecular oxygen species.

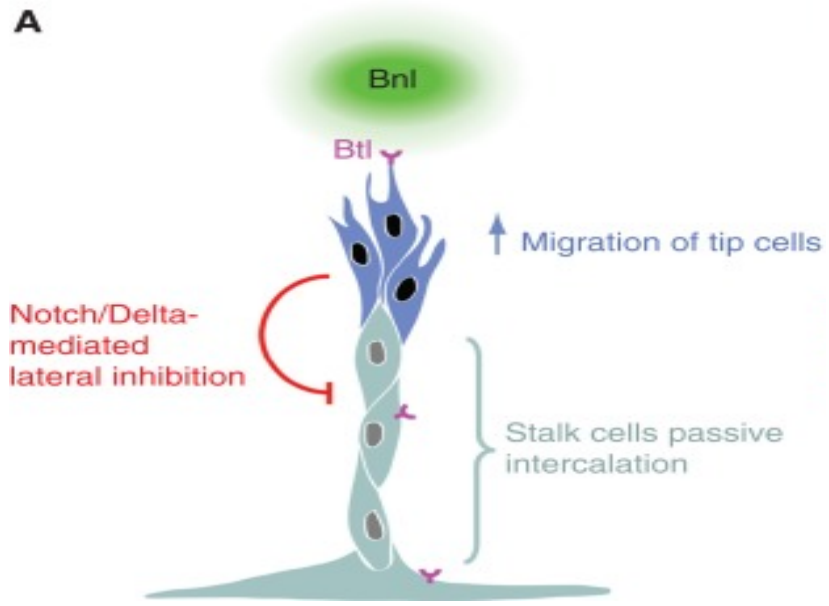

Figure 1.13 Branching morphogenesis of the Drosophila trachea. Dynamic cell shape changes begin with breathless expressing epithelial cells responding to a diffusing branchless gradient. Under hypoxic conditions, Bnl expression is upregulated, pr omoting tracheal bud outgrowth and branch extension. As oxygen begins to diffuse through the developing branched network, Bnl expression is downregulated thereby abolishing Bnl-inductive branching events.

1.6.2 Branching Morphogenesis of the Lung

The lungs function to exchange oxygen from the external environment with carbon dioxide in the cardiovascular system. The left and right lungs are comprised of two and three lobes, respectively, with the former to spatially accommodate the heart. After molecular oxygen is inhaled through atmospheric air, it travels through the bronchial tree and terminates at alveolar air sacs within the lobules of the lungs to facilitate gas exchange. The bronchial tree is a highly branched, tubular structure resulting from reciprocal signaling interactions between cell populations within the ventral foregut endoderm and ventral anterior mesoderm during development[59].

The lung primordium is derived from the ventral foregut endoderm, which gives rise to other organs including the respiratory system, thyroid, liver, and esophagus. Lung specification begins at the embryonic stage of lung development (E 9.0) when the anterior foregut endoderm evaginates to generate the lung primordium. From E 9.5 to E 12.5 (embryonic stages) the lung primordium consists of the primitive trachea and two primary lung buds, the later of which will give rise to the left and right lobes of the distal lung. From E 12.5 to E 16.5 (pseudoglandular stage) the two lung buds will begin to extend distally, followed by reiterative rounds of branching morphogenesis, forming the bronchial tree. During the canalicular (E16.5-E17.5) and sacular (E17.5-postnatal day 5) stages, branches of the bronchial tree luminize, while the terminal branches become increasingly more narrow and form aggregates of epithelial sacs which will eventually form alveoli[59,65-67].

Ex vivo culture of lung explants in combination with loss of function and / or knockdown approaches has provided insight into the molecular mechanisms responsible for lung morphogenesis. Wnt signaling has been shown to positively regulate the expression of the transcriptional effector and respiratory endodermal progenitor marker Nkx2.1 within the anterior foregut[65]. *Wnt2*$^{-/-}$ and *Wnt2b*$^{-/-}$ mice show concomitant loss of Nkx2.1 expression within the foregut resulting in the absence of branching lungs and trachea. Bmp signaling has also been shown to contribute to regulating bronchial tree formation. Bmp4, localized to the ventral mesenchyme surrounding the anterior foregut

has been identified to repress Sox2 expression, thereby promoting Nkx2.1 expression and function in lung morphogenesis[66,68].

The fibroblast growth factor family of signaling molecules has been found to play an extensive role in lung development. Haploinsufficiency in either *Fgf10* or its cognate receptor, *Fgfr2* do not develop lungs, suggesting a key role for FGF10:FGFR2b signaling in lung morphogenesis[66]. Early during primary bud formation (~ E 9 to ~ E 9.75) FGF10 expression is detected around the developing primary lung buds[67]. FGF10 localization within the mesenchyme to specific sites surrounding the epithelium highlights the role for FGF10 in contributing to regulating sites of branch initiation and overall lung architecture. Recent evidence suggests that bronchial tree pattern emerges from reaction-diffusion signaling events through FGF10 and SHH ligand-receptor based Turning models[70]. However, the role of signaling molecules in regulating pattern formation is currently under investigation.

1.6.3 Renal Branching Morphogenesis

The kidneys are an arborized network comprised of collecting ducts, calyces, the renal pelvis, and ureter. The kidneys function in multifarious physiological roles including maintenance of bodily fluid homeostasis through balancing electrolyte and water content, removal of metabolic waste, vitamin D production, and regulation of blood pressure[71]. The functional unit of the kidney is the nephron, which filters blood to generate a "filtrate" consisting of water and solutes. The filtrate produced by the nephrons accumulates in the ducts to coalesce at the renal pelvis from where it will exit the kidney through the ureter. Within the human kidney, roughly 785,000 nephrons furcate and fuse to approximately 60,000 collecting ducts.

At embryonic day 8, distinct cell populations within the intermediate mesoderm undergo mesencymal-to-epithelial signaling crosstalk to epithelialize to form the nephric duct via BMP4 and retinoic acid gradients produced by the axial and paraxial mesoderm. The primitive nephric duct containing Pax2+Lhx+Gata3+ cells will eventually give rise to the renal collecting system and ureter through branching

morphogenesis[72]. From E. 10.5/E. 11 the ureteric bud begins to emerge from the nephric duct already containing a continuous lumen, and grows dorsally into the MM. During elongation differences in gene expression patterns give rise to two different domains within the elongating bud. The distal tip of the ureteric bud will undergo branching morphogenesis to generate the collecting system, while the tubular portion of the bud will form the ureter. The nephric duct responds to diffusing GDNF through Ret signaling via co-receptor GFR1. Ret mice fail to form branched ureteric branches.

Downstream GDNF:GFR1/Ret signaling results in the secretion of epithelial-derived Wnt11, creating a positive feedback loop between the mesenchyme and epithelium. Downstream GDNF:GFR1/Ret targets include Etv4 and Etv5, which are common transcriptional effectors of FGF:FGFR signaling, which could partially explain functional compensation through FGF10:FGFR2b signaling in *Ret*-deficient kidneys. GDNF signaling to the epithelium is regulated by BMP4 signaling which inhibits mitogenic GDNF signaling at the distal bud, but induces proximal stalk elongation. Mice deficient in *Ret, Gdnf,* or *Gata3* show no abnormalities in the early stages of nephric duct formation and elongation, however, at later stages the nephric duct fails to fully extend to the appropriate level. This may be a consequence of functional compensation by FGF10:FGFR2b signaling, which has been shown to play a role in salivary gland induction. Additionally, $Ret^{-/-}$ mice fail to form filopodial structures implying that cell migration is required for full nephric duct extension.

1.6.4 Mammary Gland Branching Morphogenesis

Mammogenesis is a defining characteristic within the evolutionary history of mammals functioning primarily to provide nourishment to newborn progeny[73]. Epithelial-derived secretory acini, comprised of basal myoepithelial, with luminal ductal and acinar cell populations facilitate the unidirectional secretion of milk into an interconnected ductal system. Fluid flow converges at the lactiferous duct where it will eventually arrive at the nipple. The bilayered, acinotubular secretory network of the mammary gland is surrounded by an underlying inductive stroma. Induction of

mammary morphogenesis is in part, attributable to the signaling factors produced by the mesenchyme, however, unlike many other branching exocrine organs, hormonal factors have been shown to drive large scale morphogenic events. Unique to other branching epithelia, the mammary gland development and expansion is defined in three major stages: Embryonic, pubertal, and reproductive.[73,74].

Mammary epithelial morphogenesis occurs during embryonic and pubertal stages; the former being responsible for establishing the branching foundation required for large scale morphogenic expansion of branching architectures[74]. The rudimentary branched structure remains quiescent until puberty, wherein a rapid branching phase generates most of the acinotubular structures in the mammary gland. Additional morphogenesis occurs during pregnancy. Mammogeneisis begins with specification and establishment of the mammary line, a multilayed ectoderm that runs from forelimb bud to the hindlimb bud on the ventral side of the embryo along the anterior-posterior axis. After cell lineage specification occurs at E 10.5, mesenchyme-dependent dorsal ventral patterning of the epithelium establishes the formation of five pairs of symmetrically localized mammary placodes, which will expand into the underlying stroma by E 14 to form a stalk and terminal cell cluster. By E 16, a cord extends into the fat pad contained within the stroma, where the epithelium will begin to undergo branching morphogenesis generating a primary ductal system of ten to fifteen distal ducts and proximal endbuds via planar bifurcation. Lumen formation within the primitive ductal network begins at E16 and is completed by E 18[75].

Parathyroid hormone-like hormone (PTHLH) signals through its type I receptor (PTH1R) to help form the initial ductal system during the embryonic stage of mammogenesis[74,76]. *Pthlh* expression is localized to the epithelium from where it signals to the mesenchyme to modulate Wnt signaling mechanisms. Wnt signaling plays a pivotal role in establishing the mammary line during embryogenesis and has been linked to *Tbx3* expression. At E 10.5 transcriptional effector TBX3 is restricted to the mesenchyme where it surrounds the presumptive mammary line[77]. Ectopic expression of of Wnt inhibitor Dickopf (DKK1) within mammary ectoderm resulted in

gland hypoplasia, accompanied with the loss of *Wnt10b and Tbx3* expression, implying that Wnt signaling upstream of *Wnt10b* and *Tbx3* regulates mammary line specification[77]. *Wnt10b* and *Tbx3* expression appear to be linked as $Tbx3^{-/-}$ mice do not express *Wnt10b* and overexpression of *Tbx3* results in a concomitant increase in *Wnt10b* transcription. It has been proposed that transcriptional regulation by TBX3 localizes Wnt signaling to define the mammary line. Expressed along the ventral border of the mammary line is BMP4. BMP4 and TBX3 have been identified as antagonists of one another to control mammary gland specification and dorsal-ventral placode patterning. Also shown to play a role in dorsal-ventral placode patterning is FGF10. *Fgf10* mice either hetero- ($Fgf10^{+/-}$) or homozygous ($Fgf10^{-/-}$) do not develop all 5 placodes and are characterized by the absence of *Wnt10b* levels[78]. Mutant *Fgf10* phenotypes were observed to be similar to those of mice expressing nonfunctional $Gli^{Xt/Xt}$ mutant[78-80]. Predominantly identified as a transcriptional effector within the hedgehog pathway, Gli is predicted to positively regulate *Fgf10*, however, concrete evidence demonstrating this has yet emerge.

The ductal system generated during embryogenesis undergoes rapid expansion during puberty to form branched lobulo-alveolar networks within the stromal fat pad (Figure 1.15)[81]. Under the control of hormonal and growth factor input, the branching mammary epithelium arises from combined proliferation, migration, ECM remodeling, and differentiation of epithelial cells within the primary ductal system. Cells along the outermost periphery of the primary ducts differentiate into the myoepithelial cell lineage. Sprouting laterally from primary ducts are the secondary ducts, which will expand to form lobular like structures. Pituitary gland derived factor, growth hormone has long been implicated as a global regulatory factor required during mammary gland development.

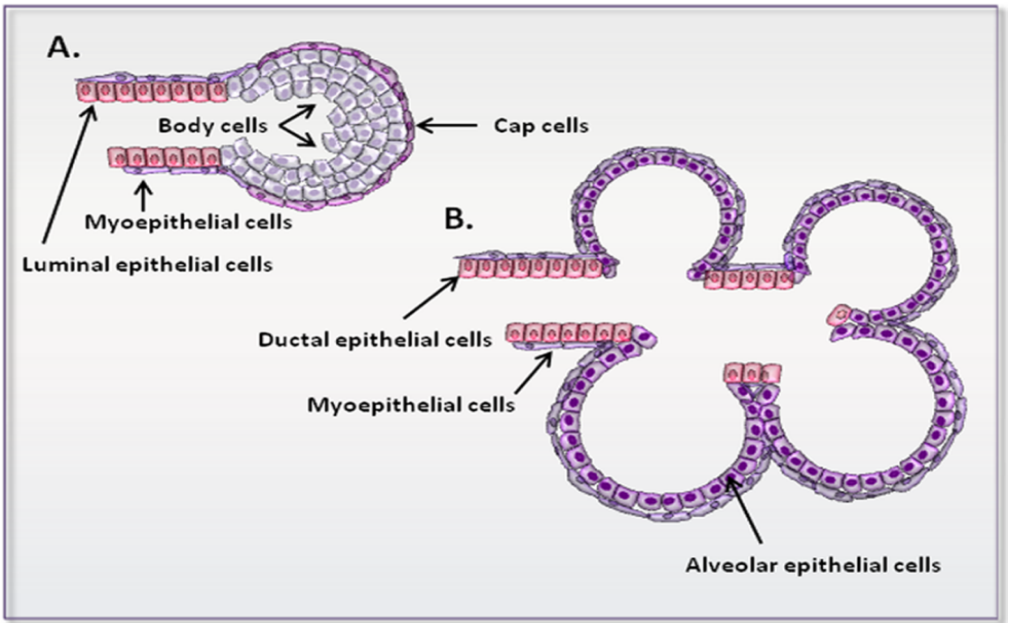

Figure 1.14. Initial bud and early branching stages of mammary gland organogenesis. Mammogenesis begins as the epithelium protrudes as a stalk and terminal end bud. Ductal epithelial cells remain relatively stationary, whereas myoepithelial cells have been shown to line the duct and migrate along the cap cells to drive the formation of lobular structures.

Genetic ablation of growth hormone receptor, *Ghr*, results in impaired mammary branching and a 90% decrease in insulin growth factor-1 levels[82]. Recent studies have highlighted the role of stromal-derived IGF-1 in regulating developmental processes within the mammary gland. Growth hormone:growth hormone receptor signaling has been suggested to be upstream of IGF-1 signaling as *Igf*$^{-/-}$ mice exhibit no defects in growth hormone levels despite severe defects in mammogenesis[74,82].

Estrogen is one of the most important hormones in pubertal mammary branching, as mice lacking estrogen receptor 1 (ESR1) only form the rudimentary ductal system *in utero*[83-85]. Interestingly, only 40% of the luminal cell population express ESR1, which has led investigators to hypothesize the existence of a paracrine signaling mechanism between ESR1+ and ESR1- epithelial cells. The favored signaling factor secreted by ESR1+ cells to ESR1- cells is amphiregulin, a member of the EGF family of secreted ligands[74]. During puberty, amphiregulin is tethered to the extracellular face of the plasma membrane. Studies investigating ampiregulin have shown that A Disintegrin and Metalloproteinase (ADAM) family member, ADAM17 cleaves amphiregulin from epithelial plasma membranes, allowing its diffusion into the surrounding mesenchyme to bind its congate receptor, EGFR to continue ductal outgrowth by stimulating the production of FGF2, which has been observed to contribute to ductal outgrowth[86-88]. Additional EGF family members, including EGF, TGF, and neuregulin have also been implicated in mammary ductal tree formation. Investigation of downstream MAPK signal transduction and transcriptional events following TGF and/or FGF7 stimulation in mouse mammary epithelia revealed their antagonist effects on mammary morphogenesis[89]. Proteins known to function in neuronal positioning during nervous system patterning, netrin, slit2, and reelin have also been identified as factors contributing to branching morphogenesis within the mammary gland[74,89-91].

1.7 The Fibroblast Growth Factor Family of Signaling Molecules

1.7.1 Fibroblast Growth Factors: An Overview

Fibroblast growth factors (FGFs) are small (~150-300 amino acids) mitogenic polypeptides that function as signaling factors[97]. 22 and 23 FGFs have been identified in humans and mice, respectively. However, FGF15 in mice is the ortholog of FGF19 in humans. In humans, the twenty-two FGFs are partitioned into seven subfamilies with respect to sequence similarity, signaling modality, function, and phylogeny (Figure 1.15) [98]. FGFs within the FGF11 subfamily (FGF11-14) are structurally similar to the FGF family, however they demonstrate no functional similarity, as they are not secreted and function only within the cells that they are produced[98]. For this reason, they are usually referred to as FGF-like molecules and will not be considered in the following text. The remaining six of the seven subgroups are all secreted into the extracellular space to induce cell-cell communication; five subgroups signal using paracrine-based mechanism, where the distance between the source (producing the FGF) and the target (receiving the FGF) is fairly small; one subgroup signals in an endocrine fashion where the distance between the source and target is large.

FGF1 and FGF2 were the first FGFs identified when their isolation from bovine brain extracts promoted cultured fibroblast proliferation[100]. In humans, the FGF family of secreted glycoproteins spans twenty two genes coding for FGF protein products with pleiotropic functions in both developing and adult tissues. FGFs exert their functions through specific interactions with their cognate receptors (FGFRs1-4), to regulate a vast array of cellular processes including cell proliferation, survival, apoptosis, migration, phosphate metabolism, stem cell maintenance, and morphogenesis.

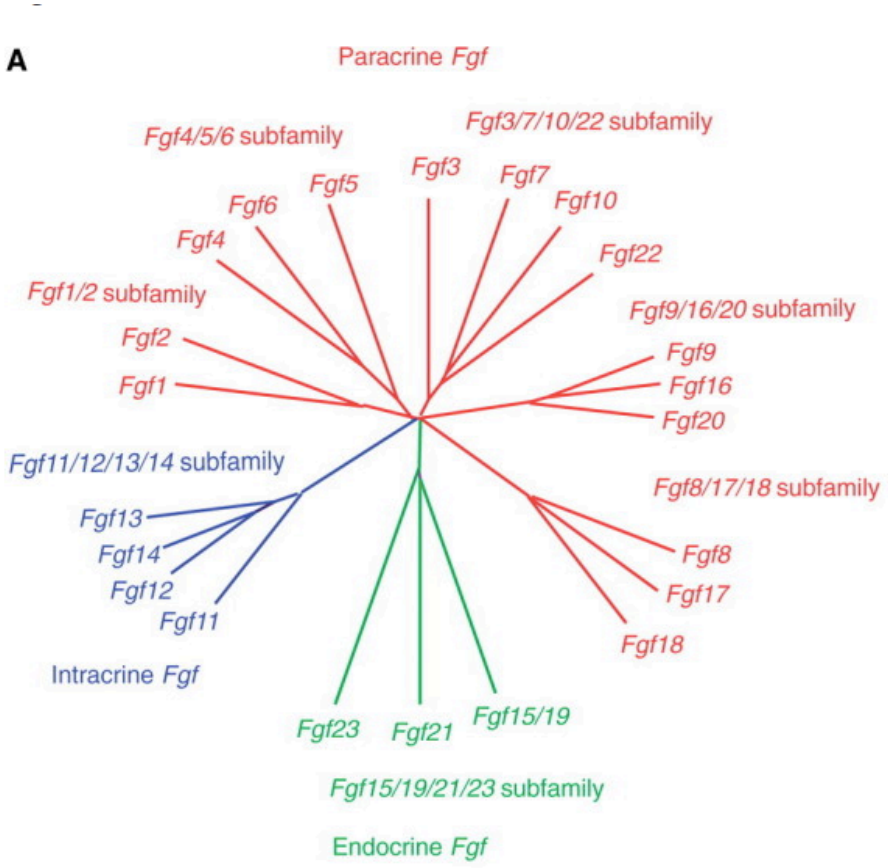

Figure 1.15. Phylogenetic tree of the fibroblast growth factor family of signaling molecules.

1.7.2 FGF:FGFR Structure and Ligand-binding Specificity

Crystal structures of at least one FGF from each subfamily have shown that 150 to 300 amino acids contribute to the primary structure of FGFs[103]. 120 amino acids comprise a conserved β-trefoil core domain showing 30-60% sequence homology across FGFs. The globular tertiary structure of the - trefoil within paracrine FGF family members results from 12 antiparallel β-strands folding into three similar β-β-β-loop-β secondary structures[103,104]. Endocrine FGFs have an atypical β-trefoil core domain, owing to the absence of the β11 strand (Figure 1.16). Paracrine signaling FGFs require cofactor heparan sulfate (HS) to mediate FGF:FGFR binding and confer FGF-specific functions[105] The HS binding site within FGF molecules locates to a polybasic region within the β1-β2loop and extended β10 -β12regions to bind polyanionic residues along the HS polymer. Differences in FGF binding affinity for HS affect the mobility of the FGF through the extracellular space, which can lead to diverse bioactivities. Marenkova et. al., showed that the distinct biological activity of FGF10 can be traced to a single amino acid within its HS binding domain. Ex vivo culture of isolated lacrimal gland explants placed 0.1mm from a point source of either heparin-linked FGF10 or FGF7 induced elongation or budding, respectively. Site-directed mutagenesis of Arg187 within the FGF10 HS-binding domain, to valine, the corresponding residue in FGF7 induced lacrimal gland explants promoted end bud formation when placed the same distance from the HS-FGF10Arg187V source.

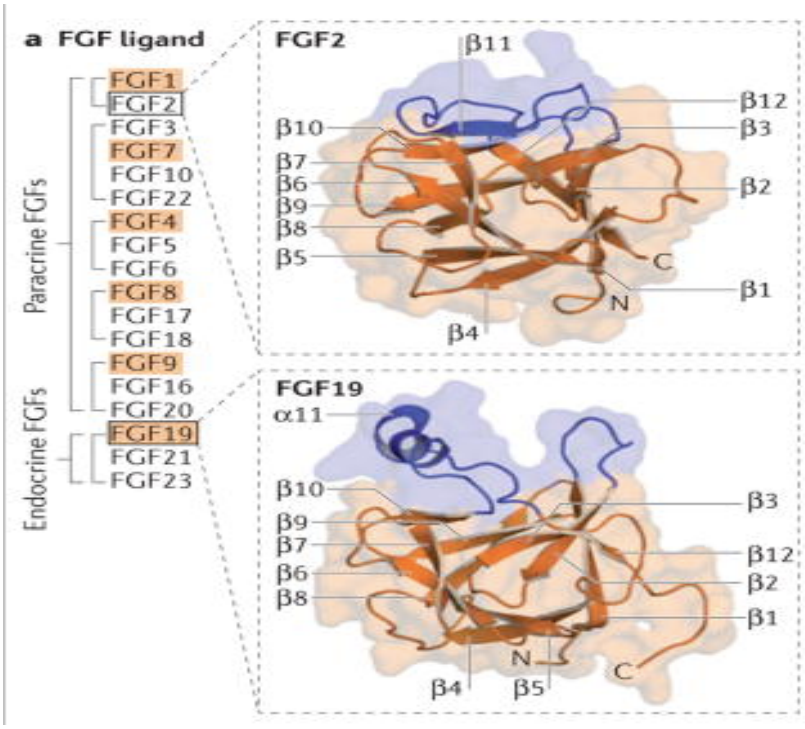

Figure 1.16 Paracrine and endocrine FGF conserved core structures. The various biological activities of FGFs may arise from the primary structure sequence within the heparan sulfate binding site located within the β1-β2loop and extended β10-β12 region of the FGF molecule.

This data implies that a divergence in primary structure within the conserved core domain of FGF molecules confers ligand-specific interactions with heparan sulfate and distinct modes of morphogenesis[106]. Additionally, the specific bioactivities of FGFs result from differences in primary structure altering their affinity for specific FGFRs, as well as the highly divergent N and C terminal domains flanking the core domain.

The four FGFR genes in the human genome encode single pass transmembrane receptor tyrosine kinases containing intracellular kinase domain and juxtaposed membrane domains, three IgG-like extracellular domains (D1-D3), and a stretch of acidic amino acids referred to as the acid box, spanning D1 and D2 linker regions. FGFR isoforms arising from alternative splicing of FGFRs1-3 include receptors lacking either the D1 extracellular domain or both the D1 and acid box domains, which have been shown to modulate interactions with CAMs as well as regulate receptor auto-inhibition (Figure 1.17a)[106-110].

As no crystal structure for any non-ligand bound FGFR exists, structural insights to uncomplexed FGFR conformation have been reliant on nuclear magnetic resonance (NMR) solution studies. NMR analysis of the D2-D3 domains indicate that in the absence of ligand the D3 domain is flexible. Crystal structures of ligand:FGFR complexes show that the D3 domain adopts a stable, extended conformation, suggesting that FGFR conformation is dictated through ligand binding events[109]. Available crystal structures for FGF1:FGFR1c,2c,3c, FGF1:FGFR2b, FGF2:FGFR2c, FGF8:FGFR2c, and FGF10:FGFR2b have illuminated conserved similarities and differences in ligand:receptor interactions. Alternative splicing of βC'-βE and βF-βG loops within the C-terminal D3 domain is responsible for FGF:FGFR binding specificity and promiscuity (Figure 1.17b)[103,108]. The FGF3 subfamily of paracrine FGFs are functionally distinct, in that they all bind FGFR2b.

Mouse knockout models and loss of function approaches have provided valuable insight into the pleiotropic roles of FGF:FGFR signaling during development. *Fgfr1* $^{-/-}$ mice display severe growth defects including reduced limb

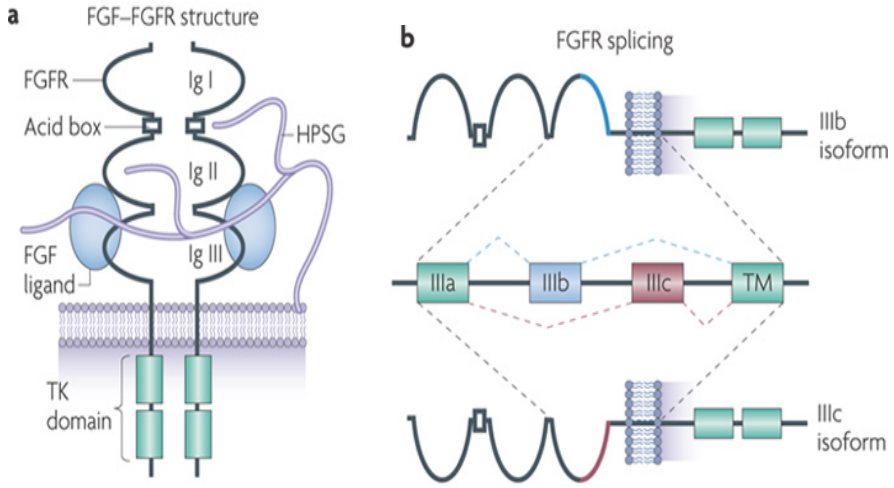

Figure 1.17 Ligand binding specificity of FGF:FGFR signaling is conferred following the alternative splicing of exon coding regions at the C-terminal half of the extracellular IgGIII domain. Containing a portion of the FGF binding site, the C-terminal half of IgGIII spans the D2, D3 extracellular domains and the D2-D3 linker region. Isoforms IIIb/IIIC of FGFR1-3 establish and fine-tune the reciprocal interactions between communicating cells required to maintain whole-organism homeostasis during organogenesis in developmental and physiological function(s) of adult tissues alike. b.). Primary transcripts coding for FGFR1-3 undergo alternative splicing. Invarient exon 7 (labeled IIIa) encodes the N-terminal portion of the D3 domain, while exon 8 and exon 9 (coding for IIIb or IIIc portions of D3, respectively) undergo alternative splicing to generate FGFRIIIb or FGFRIIIc isoforms.

skeletons, misshapen fore-, and hindlimbs, and die in gastrulation stages during embryonic development owing to failed mesodermal cytodifferentiation. In humans, haploinsufficiency in *Fgf10* or *Fgfr2b* have been implicated in the pathologies of lacrimo-auriculo-dento-digital (LADD) syndrome and hypohidrotic ectodermal dysplasia (HED). *Fgf8*$^{-/-}$ mice are embryonic lethal have severe defects in limb bud formation as well as hypoplastic salivary glands and pharyngeal arches.

Downstream FGF signaling begins following the ligation of an FGF to its cognate FGFR, leading the ligand:receptor complex to dimerize with a juxtaposed FGF:FGFR complex. Receptor dimerization results in transphosphorylation within the FGFR intracellular kinase domain and receptor activation. Intracellular downstream phosphorylation events within juxtaposed membrane domains and C-terminal regions of activated FGFRs recruits adapter protein including FRS2 and PLC , respectively. FRS2 recruits additional adapter proteins including Shp2, Grb2, Gab1 to propagate downstream MAPK, PI3K/AKT, and PLC/PKC signaling pathways to regulate proliferation, survival, motility, progenitor cell maintenance and expansion, and ECM biosynthesis and deposition (Figure 1.18).

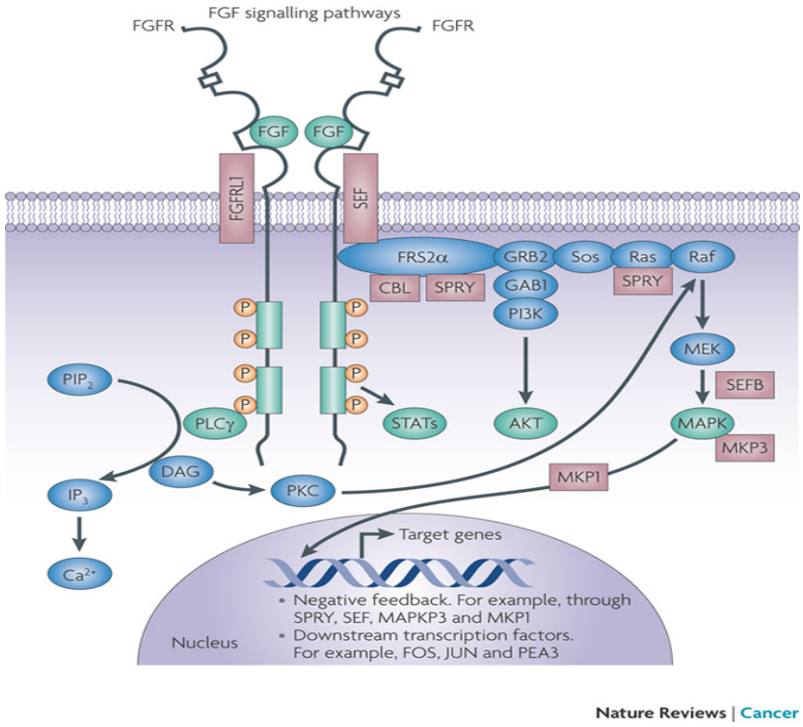

Figure 1.18. Downstream FGF:FGFR signaling includes activation of MAPK, PI3K/AKT, and PLC pathways.

1.8 Extracellular Matrix and Integrin Functions in Epithelial Morphogenesis

1.8.1 The Extracellular Matrix and Integrins: An Overview

The extracellular matrix (ECM) is an interconnected meshwork of fibrillar and nonfibrillar scaffolding proteins and glycosaminoglycans (GAGs) chains, wherein lipids, remodeling enzymes, and growth factor signaling molecules are widely interspersed. Similar to the genes coding for the FGF family of signaling molecules, extracellular matrix (ECM) gene products appear to have arisen during metazoan evolution[111-113]. Although the first studies regarding ECM structure and function were investigated using vertebrate model organisms, the emergence of cDNA and genomic sequencing technologies revealed their ancient evolutionary origins. Sequence similarity and phylogenetic analysis has shown that the genomes of many bilaterian organism ranging from mammals, to fruit flies, to worms, contain a common array of ECM proteins including αβγ laminin chains, type IV collagen -chains, nidogen, perlecan, and fibrillar collagens[113].

The evolutionary landscape comprising single celled organisms to complex multicellular organisms is largely attributed to the ECM milieu. Exon shuffling during metazoan evolution has been suggested to contribute to a variety of multidomain protein structures, generating the vast heterogeneity observed in the extracellular matrices within vertebrate tissues. ECM heterogeneity within various tissue types is responsible in forming epithelial basement membranes, interstitial fibrous meshworks, tendons, cartilage, and bones.

Cellular interactions with the underlying ECM are mediated by a large variety of adhesion receptors including integrins, syndecans, alpha dystroglycan, and lutheran blood glycoproteins. Since their discovery in 1987, integrins have been identified as the major receptors for cell-ECM adhesion, functioning as a mechanical clutch by providing a linkage between the cellular cytoskeleton and ECM[119,120] Integrin ligation to ECM induces downstream activation of MAPK, PI3K/AKT, JNK,PLC-y signaling

pathways essential for various developmental, immune, and hemostatic processes. Dysregulation of integrin signaling has been implicated in a number of human diseases including muscular dystrophy and cancer. Integrin-ECM adhesions work synergistically with intracellular actomyosin networks to facilitate adhesion assembly, disassembly, and traction force generation onto the ECM. Cell- and tissue-specific expression of integrin subunits confers differential binding specificities towards cognate ECM substrates.

1.8.2 ECM and Integrin Function in Morphogenesis

Evolutionary expansion, diversification, and specification of the ECM during metazoan evolution have given rise to structural and functional heterogeneity required of multicellular life[111]. Extracellular matrix function has been attributed to cell adhesion, polarity, proliferation, and differentiation, while also providing structural support, growth factor reservoirs, and integration of mechanosensory input from the immediate microenvironment. Dynamic morphogenic events during organogenesis are accompanied by rapid ECM turnover, suggesting that the final glandular morphologies resulting from branching morphogenesis are, in part dependent upon remodeling of the ECM. Moreover, synthesis, deposition, and degradation of the extracellular matrix are under tight spatiotemporal regulation during the developmental stages of tissue morphogenesis, highlighting the role of the ECM in shaping branched tissue architectures. Physical and biochemical properties of the ECM are largely dependent on the composition and organization of the network, conferring a vast array of cell-, tissue-specific responses. The extracellular matrix is typically divided into two groups on the basis of location and spatial organization within various tissue types: the basement membrane and the interstitial matrix within connective tissues.

A variety of collagenous and non-collagenous proteins including collagen isoforms I, III,IV,V,VI, laminins, fibronectin, as well as the nonsulfated GAG, hyaluronic acid, encapsulate cell populations within the mesenchyme to function in tissue mechanics and cell signaling; triple helical collagen assembles and osmotically

active GAG chains, impart viscoelastic properties allowing the stroma to resist and withstand tensile and compressive forces, respectively.

The basement membrane is a fundamental component underlying all epithelial tissues, however basement membranes have also been identified in endothelial, muscle, fat, and schwann cell types[121]. Interestingly, the first proteins synthesized within the vertebrate embryo are components of the basement membrane, highlighting its importance in the evolution of multicellular organisms. Consisting of laminins, collagen IV, nidogen, and perlecan, the epithelial basement membrane is arranged into a sheet roughly 150-300 nm in thickness. The basement membrane underlying basolateral membrane domains of epithelial and endothelial cells plays a key role in establishing mechanical stability, polarity, and differentiation of tissue microstructures through interactions with various cell surface adhesion receptors[118].

Determining the function of ECM proteins during branching morphogenesis have proved challenging, as many *ex vivo* organ and organoid cultures imploring both gain- and loss-of-function approaches often inhibit branching. *Ex vivo* cultures of embryonic salivary submandibular gland gland explants treated with the C-terminal LG4-domain of the laminin α5 chain perturbed branching morphogenesis with control glands having a higher number of end buds[124]. Similarly, addition of synthetic peptides contained wtihin the alpha 1 chain of the laminin G-domain that bind syndecans also inhibit Brm of the SMG[125]. Cells from the lung and salivary glands grown in three-dimensional collagen gels treated with collagenase was shown to inhibit branching, whereas exogenous stimulation with TGF to upregulate collagen expression and secretion inhibited mammary morphogenesis[126-128]. Difficulty in identifying ECM function during branching suggests fine-tuned developmental stage-specific ECM biosynthesis and turnover resulting from the dynamic alterations in gene expression profiles during the branching process.

Mouse knockout models of ECM components highlight their importance during embryogenesis and development. *Fibronectin*$^{-/-}$ mice are embryonic lethal at E.10.5 and show defects in mesoderm specification during development and alveolar-lobular

hypoplasia in the mammary gland[114,115]. *Lama1*$^{-/-}$ mice are embryonic lethal at E. 6.5, showing epiblast polarization defects, endodermal differentiation abnormalities, and unregulated induction of apoptosis[116-118]. Salivary gland organogenesis is dependent on collective cell adhesion and migration to undergo branching morphogenesis. Function blocking antibodies to integrin binding sites on laminin-111 or laminin-binding subunit α6-integrin showed disrupted branching morphogenesis[129,130]. Interestingly, genetic ablation of 3-integrin decreased branching morphogenesis, whereas α6-null SMGs showed no defects. However, *Itga3*$^{-/-}$:*Itga6*$^{-/-}$ double knockout mice resulted in a more severe SMG phenotype, suggesting that integrins function in a synergistic fashion to promote epithelial morphogenesis in the salivary gland[131].

1.8.3 ECM Dynamics in Morphogenesis

Frequent changes in ECM architecture, biosynthesis, and degradation within a physiological system are typically reflective of dynamic tissue remodeling capacity. Variability within ECM organization and associations via covalent and non-covalent crosslinking provides an attractive mechanism to regulate cell-and tissue-specific cell behaviors, including proliferation, differentiation, self-assembly, and stem/progenitor cell self-renewal. Alterations in the reticulate ECM organization can occur through multiple mechanisms; cytoskeletal-generated forces can be transmitted via physical coupling of integrins to the ECM to induce the mechanical stretching of ECM proteins; ECM accumulation and degradation at specific membrane domains to either impart stability in tissue structure or to create space for cells to migrate; and cleavage-mediated release of extra-,pericellular matrix immobilized growth factors to mediate defined spatiotemporal signaling events.

Among the most commonly recognized protein clades functioning in remodeling the ECM are the matrix metalloproteinase (MMP) family. The first MMP collagenase was identified in tails of tadpoles undergoing metamorphosis as the enzyme capable of degrading the fibrillar collagen[132-134]. In humans, 23 MMPs have been identified and exhibit multifunctional roles, resulting from promiscuous substrate specificity, as MMP

substrates also include growth factors, receptor tyrosine kinases, cell adhesion molecules, and other MMPs[135]. Most MMPs are secreted, free to diffuse within the extracellular space, however, some are linked to the membrane, either as transmembrane or GPI-anchored proteins.

Named after the divalent zinc ion and conserved methionine residue within the active site, MMPs share several other conserved structural features[136]. Primary MMP transcripts are are synthesized as zymogens, containing an auto inhibitory prodomain that lay across the catalytic active site. When the prodomain is removed/cleaved, the active site is available to bind and catalyze substrate-specific enzymatic reactions. Most, but not all MMPs contain a four bladed -propeller hemoplexin domain to facilitate MMP:protein interactions, MMP localization, internalization, substrate recognition, and degradation.

Physical properties of the ECM including stiffness, porosity, surface topography, and insolubility are obligatory in providing a scaffold to support tissue structure and morphogenesis. MMP function extends far beyond degrading structural components within the ECM; MMP-mediated cleavage of ECM proteins alters the physicochemical and bioactive properties of the local niche to control cell/tissue structure and function. ECM protein cleavage products promote the release of bioactive ECM peptide sequences which can influence cell behavior, increases porosity within the meshwork to provide space for single- and multicelluar migration, modulate the integrity of cell-cell adhesions, and targets growth factors contained within the ECM to modulate their activity[137].

Within the fetal salivary gland, type two transmembrane MMP (MT_2-MMP or MMP15) cleaves the C-terminal noncollagenous domain 1 (NC1) of collagen IV to promote β1-integrin-dependent proliferation[138]. During puberty, mammary gland ductal tree expansion into a ramified lobulo-tubular network results from two distinct branching processes: terminal endbud (TEB) elongation and branching of the secondary ductal system. TEB extension through the fat pad determines the length of the ductal network, whereas generation of secondary ductal branches arises from primary duct

biplanar bifurcation. Both modes of mammary branching are dependent on synergistic MMP activity. *Mmp2*$^{-/-}$ mice are deficient in TEB elongation with an excess of secondary ductal branches. Conversely, *Mmp3*$^{-/-}$ mice show aberrant secondary duct formation with no defects in TEB elongation[138]. Therefore, aberrant MMP expression and localization is key in regulating branching morphogenesis.

Juxtaposed to the membrane domains of branching organs, MMPs typically localize to specific sites along basement membrane to regulate matrix organization. Alterations in local ECM accumulation and organization around branching epithelia have been suggested to control branch point formation and expansion. At the tips of many branching organs, MMPs mediate ECM remodeling to create space for the expanding epithelium to allow for collective cell migration and proliferation. In contrast, ECM deposition and accumulation along the ducts and flanks of the endbuds stabilize the epithelium to restrict domain expansion and branching, implying that cells have an innate ability to sense the composition of their immediate microenvironment to drive or limit the growth of epithelial branching domains (Figure 1.19)[123]

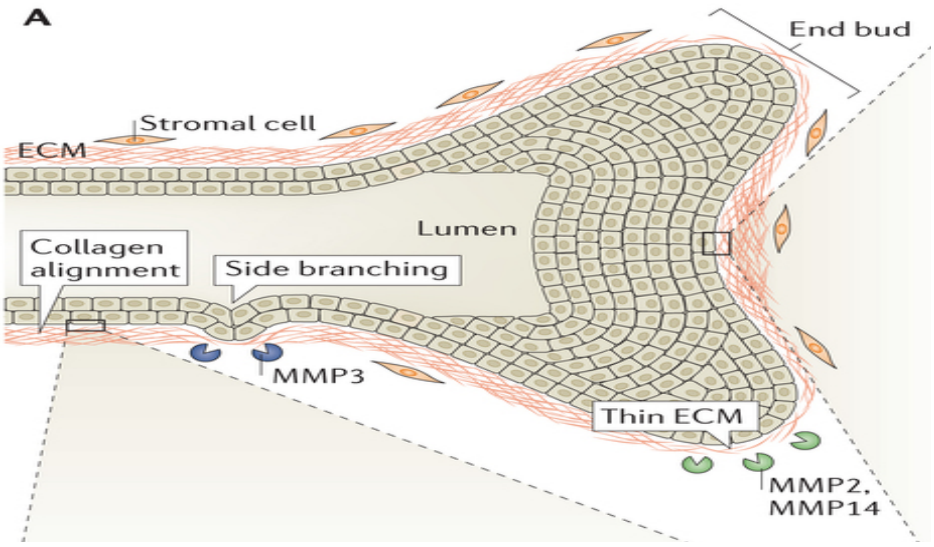

Figure 1.19. ECM remodeling by MMPs during epithelial morphogenesis. MMP localization and ECM turnover have been suggested to contribute to the final branched geometries during organ/gland morphogenesis through regulating ECM accumulation and degradation. Within the mammary gland MMP3 is responsible for regulating secondary duct development, whereas MMP2 and MMP14 (MT1-MMP) have been shown to regulate end bud expansion through ECM degradation.

Chapter 2

THE EFFECTS OF FGF7 AND FGF10 ON SALIVARY GLAND PROGENITOR CELLS GROWN IN 3D HYALURONIC ACID, LAMININ-MODIFIED HYDROGELS

2.1 Abstract

Radiation therapy used to treat head and neck cancers results in salivary gland dysfunction and xerostomia. Salivary gland hypofunction is concurrent with a steady decline in oral health. The creation of a bioengineered salivary gland would provide a potential long term treatment option for those suffering from xerostomia, or dry mouth. Here we report the effects of fibroblast growth factors, FGF7 and FGF10 on human salivary gland acinar-like cells (hSACs) grown in three-dimensional hyaluronic acid:laminin hydrogels. hSAC spheroids encapsulated in our culture system self-assemble into spheroid structures 20-40 microns in diameter after one week. Stimulation with FGFR2b ligands, FGF7 or FGF10 showed sustained hSAC proliferation and specific modes of morphogenesis. FGF7 treatment promoted the formation of epithelial cleft-like and lobule-like structures, whereas the addition of FGF10 to hSAC structures induced duct-like elongations. We found that hSACs treated with FGF7 and FGF10 upregulate fibronectin protein levels and deposition within the hydrogel network; however, FGF7 but not FGF10 increased protein levels of fibronectin-binding α_5-integrin, suggesting that FGF7 is responsible for inducing the expression of cellular machinery required for cleft formation during hSAC morphogenesis. FGF10 treatment followed by FGF7 addition resulted in more complex morphogenesis than either ligand alone. Interestingly, simultaneous stimulation with FGF7 and FGF10 had a minimal effect on overall hSAC morphogenesis, suggesting that these two ligands bind FGFR2b competitively. In summary, FGFR2b ligands FGF7 and FGF10 are capable of inducing morphogenesis of primary salivary gland cells into

structures reminiscent of native salivary gland architectures, which can be used to restore glandular function in tissue engineering applications.

2.2 Introduction

Radiation-induced atrophy of the salivary glands during head and neck cancer treatments leads to dry mouth or xerostomia[1]. Patients suffering from xerostomia face several oropharyngeal

maladies including dental carries, dysphagia, and increased susceptibility to microbial infection. To date, there is no cure for xerostomia and current treatments are unsatisfactory. Generation of a bioengineered, implantable, fully-functional salivary gland could provide a long-term cure and improve the quality of life in those suffering from dry mouth. Several attempts have been made to generate an artificial salivary gland.

Salivary gland ductal cells have been isolated from both primate and human tissues[2,3]; however, ductal cells are not responsible for generating salivary fluid flow and protein secretion necessary for maintaining glandular homeostasis. Previous work by our lab has shown the successful isolation of human salivary gland acinar-like cells (hSACs). hSACs encapsulated in hyaluronic acid-based hydrogels were found to self-assemble into spheroid structures and respond to both parasympathetic and sympathetic neural input shown by the rapid increase in cytosolic Ca2+ concentrations and an increase in zymogen granule content, respectively[4]. To restore glandular function to those suffering from xerostomia, salivary spheroids must undergo branching morphogenesis to generate functional acinar-tubular networks with contiguous lumens, reminiscent of native glandular structures.

Branching morphogenesis is a fundamental developmental process wherein rapid glandular expansion is coordinated with collective migratory events, apoptosis, extracellular matrix (ECM) deposition and turnover to form well-organized, contiguous epithelial networks as to promote the most efficient means for vectorial transport of glandular secretions. Many developing glands require crosstalk between epithelial and stromal tissue compartments to facilitate collective cell assembly into higher ordered, branched architectures[6]. Mesenchymal, endothelial, immune, and neuronal cell populations residing

within the underlying stroma make unique contributions in regulating epithelial morphogenesis. Mesenchymal fibroblast growth factor, FGF10 binding to its receptor FGFR2b has been shown to play a key role in inducing collective cell morphogenesis to help generate the final morphologies observed in many exocrine organs and glands including the lungs, kidneys, prostate, mammary and salivary glands[7-11]. *Fgf10*$^{-/-}$ and *Fgfr2b*$^{-/-}$ mice exhibit lung and salivary gland aplasia, highlighting their contribution to organogenesis and creation of branched acinar-tubular networks[12-13].

The Fibroblast Growth Factor (FGF) family of signaling molecules spans 22 genes within the human genome. Their gene products are known to regulate pleiotropic functions throughout the developing vertebrate embryo and into adulthood to maintain tissue homeostasis. First identified in bovine pituitary extracts, FGF1 and FGF2 were found to exert strong mitogenic effects on cultured fibroblasts *in vitro*[14]. Various approaches using loss of function and disease and knockout mouse models have provided valuable insight into the abundant and non-overlapping functions of FGFs. FGFs manifest their functions by binding their cognate FGFRs, inducing context-dependent activation of downstream MAPK, PI3K/AKT, and PLC pathways to regulate cell processes including proliferation, survival, stem/progenitor cell maintenance, and motility.

Owing to their various bioactivities, FGFs have been used in many tissue engineering applications including wound healing, tissue regeneration, and the creation of functional neotissues. Controlled release of FGF2 complexed to freeze dried gelatin microspheres was shown to significantly increase dermal wound closure, capillary formation, and epithelialization in healing impaired diabetic mice[15]. FGF7 was shown to be responsible for the regenerative capability within the liver by regulating the expansion of liver progenitor cells (LPCs), as FGF7-null mice showed a large decrease in LPC populations accompanied by dysfunctional hepatic regeneration[16].

We recently reported that these human salivary acinar-like cells express a variety of stem/progenitor cell markers including KIT, musashi, and keratin 5, suggesting that these cells have the ability to undergo branching morphogenesis. Reports by Lombeart et. al., and Knox et. al., have identified two distinct progenitor populations, distal endbud KIT+K14+ cells and proximal duct KIT+K5+ cells, respectively, within the fetal SMGs of mice. Loss

of either progenitor population results in perturbed branching morphogenesis, suggesting the importance during gland development[17,18]. Lombeart and colleages identified that FGF10:FGFR2b signaling is responsible for propagating an autocrine epithelial KIT pathway in ex vivo SMG cultures. Independent downstream signaling from both pathways converge to amplify the transcription of a cassette of FGF:FGFR-affiliated transcriptional effectors to promote distal progenitor expansion and branching morphogenesis.

In this study we report the effects of FGFR2b stimulation using ligands FGF7 and FGF10, on salivary gland progenitor cells cultured in a hyaluronic acid:laminin-modified hydrogels. We found that both ligands induce salivary gland progenitor cell proliferation, consistent in their role as potent mitogens. Interestingly, FGF7 and FGF10 induce distinct types of morphogenesis, with FGF7 inducing epithelial lobule formation and FGF10 promoting duct-like elongations. We also observed that simultaneous stimulation of FGFR2b with FGF7 and FGF10 inhibits overall morphogenesis, but addition of FGF10 followed by FGF7 promotes more complex morphogenesis. Stimulating FGFR2b with either FGF7 or FGF10 with FGF:FGFR signaling cofactor, heparin increases FGFR2b-mediated morphogenesis in a dose-dependent fashion. Addionally, extended culture of these structures results in apoptosis-dependent lumen formation within duct- and endbud-like structures.

2.3 Materials and Methods

Tissue Procurement

Human tissue specimens of parotid and submandibular glands were obtained from patients undergoing head and neck surgery. Informed consent and a tissue procurement protocol were approved by the Institutional Review Board from both the Christiana Care Health System (CCHS) and the University of Delaware. Following surgical excision, tissue specimens were placed on ice and stored at four degrees Celsius until quality control processing and for use in the laboratory.

Cell Explant Culture

After obtaining an IRB approved protocol from both Christiana Care Health System and the University of Delaware, healthy tissue specimen from human parotid

and submandibular glands were obtained from patients undergoing head and neck surgery. Salivary tissue was placed in betadine solution at a dilution of 1/10 for approximately 2 minutes and washed in chilled Dulbecco's Modified Eagle Medium (Life Technologies, Frederick, MD). Salivary epithelium was mechanically separated from surrounding connective tissue and finely minced. Epithelial rudiments were then suspended in Hepato-STIM medium (BD Biosciences Discovery Labware, Bedford, MA) supplemented with 100 U/mL of penicillin G sodium and 100 ug/mL of streptomycin sulfate in 0.085% (w/v) saline and 2.5 ug/mL amphotericin B and cultured into 6-well tissue culture treated plates. Salivary epithelial rudiments were maintained at 37 degrees Celsius in a humidified atmospheric chamber with 5% (v/v) CO2.

Two-Dimensional Cell Culture

Salivary acinar-,ductal-,and myoepithelial-like cells emerging from cultured tissue explants were allowed to reach 50-60% confluency. Media was aspirated and cells were washed with phosphate buffered saline (PBS) (Life Technologies). 0.250 uL of 0.05% (w/v) trypsin with EDTA (Fisher Scientific, Pittsburgh, PA) was added to the 6-well culture plates and incubated at 37 degrees Celsius for 5 minutes. Cells were re-suspended in 2.50 mL of Hepato-STIM media and 0.250 uL of trypsin soybean inhibitor (Sigma-Aldrich, St. Louis, MO) and centrifuged at 3000 RPM for 5 minutes. Supernatant was aspirated and the cell pellet was re-suspended in 3mL of Hepato-STIM cell culture media. Cells were split at a dilution of 1/10 for subsequent experiments.

Three-Dimensional Cell Culture

Lyophilized poly-ethylene glycol diacrylate (PEGDA) and hyaluronic acid functionalized with reactive thiol groups (HA-SH) were synthesized following a previously reported procedure (Citation Prestwhich) (ESI BIO, Alemeda, CA). Prior to any cell culture, HA-SH was dissolved in degassed, deionized (DI) water and incubated

at 37 degrees Celsius for 20 minutes. PEGDA was readily reconstituted in DI water at room temperature. Both solutions were mixed at a crosslinking density of 1:4 (PEGDA:HA-SH) at a final volume of 50 uL to form a thin, gel-only layer on cell culture inserts (Millipore, Billerica, MA, diameter: 12mm, pore size: 0.4 um).

Pure acinar-like cell populations cultured in either T-25 or T-75 tissue culture flasks with Hepato-STIM media were allowed to reach confluency. 0.05% trypsin (w/v) with EDTA (Fisher Scientific, Pittsburg, PA) was added to tissue culture flasks and incubated at 37 degrees Celsius for five minutes. Cells were pelleted following resuspension in trypsin soybean inhibitor (Sigma-Aldrich, St. Louis, MO) and media. The cell pellet was resuspended in fresh cell culture medium and counted using a hemacytometer. 1 x 105 cells were added to 1.5mL eppendorf tubes and pelleted at 3000 RPM for 3 minutes. Supernatant was discarded and the pellet was resuspended in HA-SH (ESI BIO) and 6 mg/mL laminin-111 (Sigma) at a 1:1 ratio and incubated at room temperature for 10 minutes. Poly-ethylene glycol diacrylate was added to the suspension at a 1:4 ratio relative to thiolated hyaluronic acid. The solution was mixed thoroughly and added to cell culture inserts (Millipore) and placed in 37 degrees Celsius. After 40 minutes, cell culture medium was added outside the cell culture inserts. Due to variability in crosslinking kinetics, cell culture media was added on top of the cell-laden hydrogel upon gelation. For growth factor/heparin treatments, 100ng/ml of FGF7 FGF10 and/or 0.05, 0.1, 0.5 ug/mL heparin were added to the interior of the cell culture inserts at day seven.

Edu Cell Proliferation Assay

10 uM of Edu solution (Click-iT Edu Imaging Kit) (Invitrogen) diluted into cell culture media was added to hSAC spheroids growing in three-dimensional culture at 37 degrees Celsius for 8 hours. hSACs were fixed in 4% paraformaldehyde (PFA) at room temperature for 30 minutes. hSACs were quickly washed in 1X PBS and then permeabilized with 0.2% (v/v) Triton X-100 for 30 minutes at room temperature. Triton solution was quickly washed in 1X PBS and the Click-iT reaction cocktail was added to

each hydrogel in cell culture inserts. hSACs were incubated with the reaction cocktail in the dark at room temperature for 30 minutes. Reaction cocktail was removed and hydrogels were washed briefly in 1X PBS. Hydrogels were placed in 8-well nunc chamber slides (Lab-tek Products, Nalge Nunc International, Naperville, IL).
3% BSA (v/v) and a drop of antifade (Invitrogen) were added to hydrogels. Hydrogels were protected from light and stored at four degrees Celsius until imaging.

Western Blot

hSACs grown in three-dimensional culture as described above. The HA:ECM-modified hydrogel was degraded following 30 minutes of hyaluronidase treatment (75 U/mL, Sigma). hSACs were lysed in RIPA buffer (150mM NaCl, 1% (v/v) NP-40, 0.5% (w/v) deoxycholic acid, 0.1% (v/v) SDS, 50 nM Tris pH 8.0) with protease inhibitor cocktail and phosphatase inhibitors and placed on ice for 45 minutes. Lysates were centrifuged for 10 minutes at 13,000 RPM (Eppendorf 5402 centrifuge) at 4 degrees Celsius. The pellet was discarded and the protein concentration within the supernatant was measured using a bicinchoninic acid (BCA) assay. 50 ug of protein was loaded onto 10% NuPAGE Bis-Tris precast gels (Life Technologies) and separated using 1X MES running buffer (50mM MES, 50 mM Tris-Base, 0.1% SDS, 1mM EDTA, pH 7.3) at a voltage of 160V for 35 minutes. Protein was then transferred to a methanol fixed PVDF membrane at room temperature for one hour at 20V. The membrane was blocked in 3% BSA (w/v) solution while shaking overnight at 4 degrees Celsius. Primary antibodies for phospho-Erk1/2 (1:2000), total Erk1/2 (1:2000), Phospho-Akt (Ser 273) (1:2000), total Akt (1:2000) (Cell Signaling, Danvers, MA), beta-actin (1:10000) (AbCAM), fibronectin (1:500) (AbCAM), and alpha 5 integrin (1:1000) in 3% BSA were added to the PVDF membrane and incubated at room temperature for one hour while shaking. The membrane was washed in 1X TBST for 3 minutes and repeated five more times. Secondary IgG antibodies conjugated to horseradish peroxidase raised against mouse, rabbit, or goat IgG were added to the membrane for one hour at room temperature while shaking. Wash steps were repeated

as described above. Protein bands were visualized using chemiluminescent substrate (Thermo-Fisher Scientific).

Immunocytochemistry

Cell culture medium was aspirated from cell-seeded hydrogels. Hydrogels were fixed in 4% paraformaldehyde (PFA) solution for 30 minutes at room temperature. 1X PBS was used to wash the hydrogels following fixation. Cells were permeabilized with 0.2% (v/v) Triton X-100 solution for 30 minutes at room temperature. After washing with 1X PBS, hydrogels were blocked in 3% (w/v) bovine serum albumin (BSA) in PBS overnight at 4 degrees Celsius. Hydrogels were then placed into 8-well nunc chamber slides (Lab-tek Products, Nalge Nunc International, Naperville, IL). Primary antibodies for FGFR2b (goat, Santa Cruz Biotechnology, Dallas, TX), fibronectin (rabbit, AbCAM, Cambridge, MA), ki67 (AbCAM), CK19 (AbCAM), beta catenin and active caspase 3 (AbCAM) were added to cell-laden hydrogels for 2 hours at 37 degrees Celsius, while shaking. Primary antibody solution was removed and hydrogels were washed in 1X PBS for twelve minutes. Washing steps following primary antibody incubation were repeated 3 times. Secondary antibodies conjugated to Alexa 488 and Alexa 568 fluorophores (raised against mouse or rabbit IgG) (Invitrogen, Carlsbad, CA) were added to hydrogels for 1 hour and thirty minutes. Hydrogels were washed as described above. Either Draq 5 (Biostatus, Leicestershire, United Kingdom) or NucBlue (Invitrogen) were added to hydrogels. Following a quick wash with 1X PBS, hydrogels were placed in 3% BSA (w/v) with one drop of antifade solution (Invitrogen) and stored at four degrees Celsius before imaging. All imaging was done using Zeiss 510 or 710 laser scanning confocal microscopes.

2.4 Results

FGFR2b stimulation with FGF7 or FGF10 induces hSAC proliferation in three dimensional culture

To investigate the role of FGF7 and FGF10 on hSAC spheroids, we first encapsulated single hSACs into a three-dimensional hyaluronic acid:laminin-modified

hydrogel scaffold (Figure 1A). Exogenous FGF7 or FGF10 were added to the culture media following hSAC self-assembly into spheroids and cell proliferation was investigated (Figure 1B-I). Both FGF7 and FGF10 increased cell proliferation after 8 hours (Figure 2.1 C, D), shown by incorporation of fluorescent thymine, indicating that FGFR2b stimulated cells are progressing through the cell cycle. ki67 staining (Figure 2.1 F-H), which exclusively marks actively proliferating cells at all phases of the cell cycle highlights sustained cell proliferation at 24 hours within FGF7 and FGF10 treated hSAC spheroids.

Erk1/2 and AKT are canonical downstream effectors in mediating FGF:FGFR functions and are common targets for phosphorylation following FGFR activation. Therefore, we sought to investigate the downstream phosphorylation events resulting from FGFR2b stimulation with either FGF7 or FGF10. After 8 hours, both FGF7 and FGF10 show an increase in the phosphorylation of AKT compared to untreated control (Figure 2.1J). ERK1/2 phosphorylation is unchanged in treated and untreated hSAC spheroids after 8 hours post-treatment. After 24 hours, FGF7 and FGF10 treated hSACs show an increase in phospho-Erk1/2 levels relative to controls; however AKT phosphorylation is observed only in FGF10 treated hSACs.

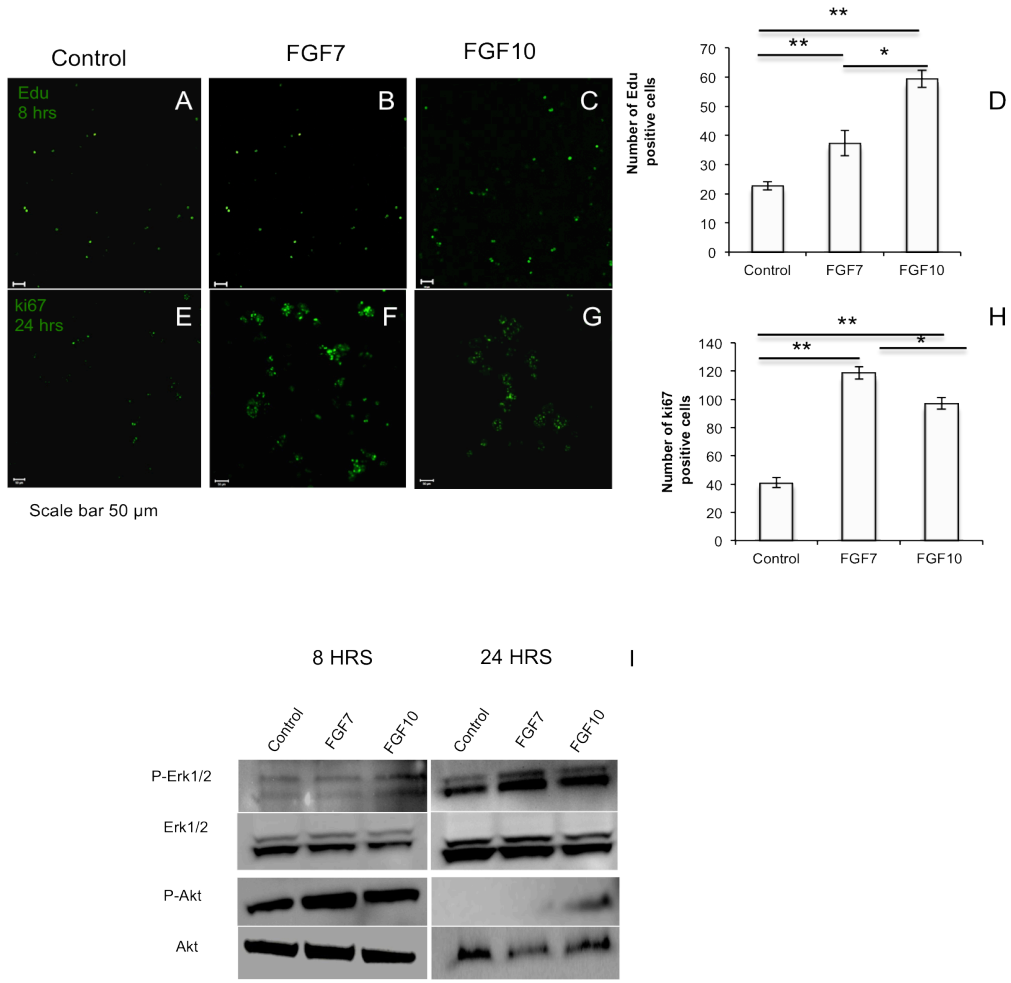

Figure 2.1. hSAC spheroids undergo proliferation in response to FGFR2b stimulation with ligands FGF7 and FGF10. hSAC spheroids grown in hyaluronic acid:laminin hydrogels after 1 week (A) Scale bar 50 µm. Edu labeling shows hSAC proliferation in unstimulated (B), FGF7 (C), and FGF10 (D) treated samples 8 hours after growth factor addition. Scale bar 20µm The number of Edu positive cells was quantitated (E) (Student's t-test with standard error ** $P<0.01$, * $P<0.05$) n=3 biological replicates. ki67 immunostaining in unstimulated (F), FGF7 (G), and FGF10 (H) stimulated hSACs 24 hours after growth factor addition. Scale bar 20µm. The number of ki67 positive cells were quantified (I) (Student's t-test **$P<0.05$) n=3 biological replicates. Immunoblot of and p-ERK1/2. ERK1/2, p-AKT, and AKT 8 and 24 hours after addition of FGF7 or FGF10 (J).

FGF7 and FGF10 promote distinct hSAC morphogenesis

To examine the effects of FGF7 and FGF10 on hSAC morphogenesis, hSAC spheroids were incubated for 48 hours following FGFR2b stimulation with either FGF7 or FGF10. FGFR2b localization and the structural deviation from spheroid morphology were examined using immunofluorescence and confocal microscopy. FGF7 treated hSAC spheroids showed various morphologies including membrane furrowing reminiscent of epithelial clefting and lobular structures (Figure 2B,F), whereas FGF10 treatment resulted in elongated duct-like structures (Figure 2C,G), consistent with previous reports of isolated SMG epithelial rudiments treated withFGF7 and FGF10, respectively. Consistent with previous reports, both untreated and treated hSAC spheroids ubiquitously expressed FGFR2b at the cell surface (Figure 2.2A-F) 48 hours after exogenous addition of FGF7, FGF10, and carrier controls, suggesting that FGFR localization does not mediate ligand-specific cell behaviors.

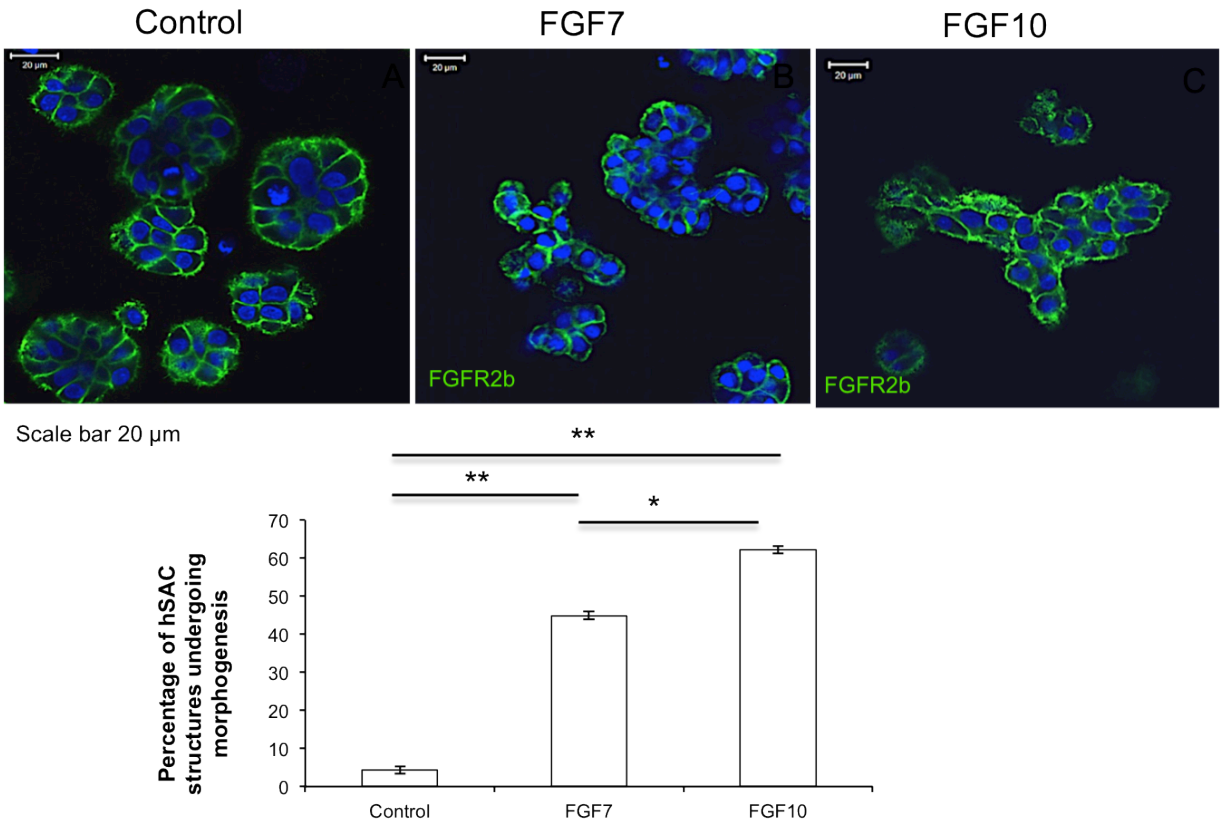

Figure 2.2. hSAC spheroids undergo distinct morphogenesis in response to FGFR2b ligands FGF7 and FGF10. hSACs self-assemble into spheroid structures and express FGFR2b (green) when cultured in hyaluronic acid:laminin hydrogels (A,D). Stimulation of FGFR2b with FGF7 induces the formation of lobule-like structures with short extensions (B,E). FGF10 treatment promotes elongation of spheroid structures (C,F). The percentage of hSAC spheroids responsive to either FGF7 or FGF10 was quantified (G) (n=3 biological replicates, Student's T-test with standard error ** $P<0.01$, * $P<0.05$).

FGF7 and FGF10 Upregulates Fibronectin Expression and Secretion, but only FGF7 Upregulates 5-Integrin

We examined the effects of FGF7 and FGF10 on fibronectin and fibronectin-binding integrin subunit, α_5-integrin. Both fibronectin and α_5-integrin are expressed at high levels at the onset of gland initiation and epithelial clefting stages of SMG development, so we hypothesized that FGF7 or FGF10 might be responsible for their expression. Western blot and confocal microscopy analysis showed that hSAC spheroids treated with FGF7 or FGF10 upregulated total fibronectin protein levels and increased extracellular fibronectin deposition (Figure 2.3).

We noticed that hSACs treated with FGF7 displayed membrane furrows that were reminiscent of epithelial clefting. Previous reports have suggested a role for α_5-integrin subunit to participate in fibronectin binding and transmission of an actomyosin mechanical unraveling of fibronectin to reveal a cryptic self-assembly site necessary for fibronectin accumulation within cleft sites and cleft progression. We found that hSACs treated with FGF7, but not FGF10, showed higher levels of α_5-integrin compared to control, suggesting that FGF7 is responsible for upregulating the machinery needed for cleft formation and progression in salivary gland branching morphogenesis.

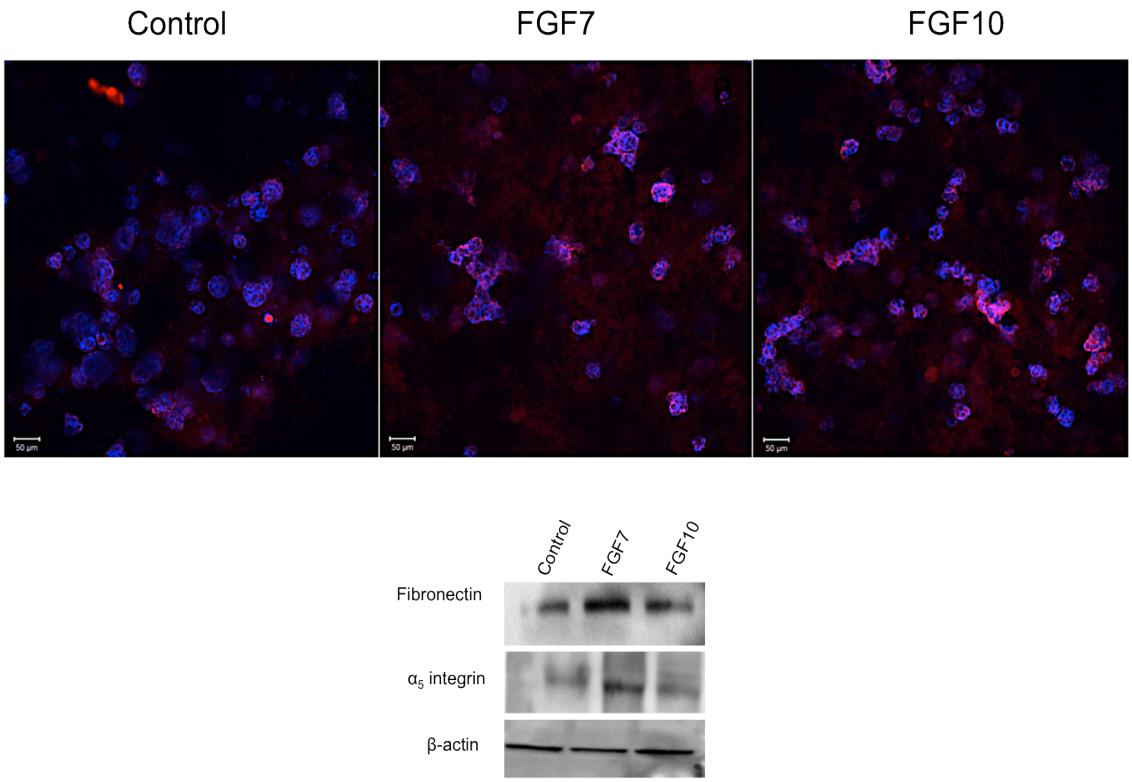

Figure 2.3. Downstream signaling events mediated by FGF7 and FGF10 are linked to extracellular matrix protein synthesis, deposition, and cell adhesion. hSACs encapsulated in hyaluronic acid:laminin hydrogels (blue, phallodin) secrete fibronectin (red) in response to FGFR2b ligation to FGF7 or FGF10 (A-C). Total fibronectin levels are increased following treatment with either FGF7 or FGF10 (D panel 1) but only FGF7 upregulates α_5-integrin levels (D panel 2).

Temporal addition of FGF10 followed by FGF7 results in more complex hSAC morphogenesis

We analyzed a pre-existing microarray data set to examine the expression patterns of *Fgf7* and *Fgf10* during submandibular gland (SMG) development. Relative gene expression analysis of *Fgf10* shows that it is highly expressed within the mesenchyme at the onset of gland initiation (Figure 4A). Additionally, the epithelium of *Fgf10*$^{-/-}$ mice fail to invade into the underlying stroma as a proximal stalk and distal terminal endbud at embryonic day 12. Therefore, we hypothesized that hSACs treated with FGF10 followed by FGF7 would undergo dynamic cell rearrangements into structures reminiscent of native salivary gland architectures.

hSAC spheroids were treated with FGF10 and allowed to undergo FGF10-dependent morphogenesis for 24 hours. FGF7 was then added to hSACs treated with FGF10 for 24 hours and were incubated for another 24 hours. Morphometric analysis revealed that these structures had longer ductal extensions and an increase in endbud-like structures when compared to untreated hSACs and hSACs treated with FGF10 and FGF7 at the same time. (Figure 4B-E). Interestingly, simultaneous addition of both FGF7 and FGF10 perturbed the extent of FGFR2b-dependent morphogenesis. FGFR2b stimulation using both ligands at the same time promoted hSAC spheroids to assume morphologies with a less-than intermediate phenotype characterized by membrane furrowing and short duct-like extensions, suggesting that FGF7 and FGF10 competitively bind FGFR2b.

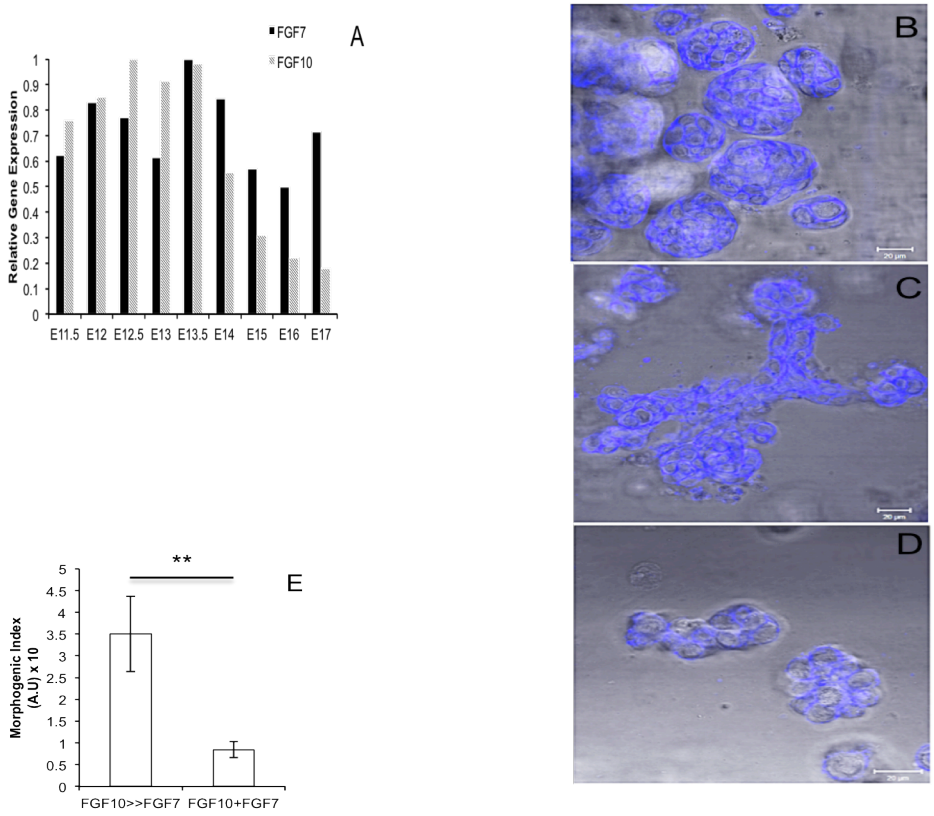

Figure 2.4. Addition of FGF10 followed by FGF7 treatment induces more complex hSAC morphogenesis than simultaneous addition of FGF10 and FGF7. Relative gene expression analysis (normalized to the highest expression level) from a microarray data set during submandibular gland development from embryonic days 11.5 to 17 (A). Untreated hSAC spheroids highlighted by actin staining (blue) (B). hSAC spheroids treated with FGF10 followed by FGF7 addition have longer ducts and an increase in the number of endbud-like structures (C) when compared to controls and hSACs treated with FGF10 and FGF7 at the same time (D). The extent of morphogenesis was quantified by multiplying the number of endbud-like structures by the duct length (E) (n=3 biological replicates, Student's T-test with standard error, ** $P<0.01$).

2.5 Discussion

Since their discovery, members of the fibroblast growth factor family of signaling molecules have been implicated in functioning as potent mitogens[14]. During organogenesis, however, the downstream signaling events mediated by activated FGF:FGFR signaling are vast, including stem cell self-renewal and expansion, organization of cytoskeletal networks, integrity of cell-cell adhesions, and ECM dynamics[18-21]. Coordination of these processes is essential for generating the branched architectures of various organs during development. Animal models investigating FGF:FGFR signaling have made the FGF family one of the most well studied groups of signaling factors. FGF and FGFR knockout and disease models highlight their pleiotropic functions; however, the role of FGF:FGFR signaling in primary cells and tissues is not well understood. Herein, we report the effects of FGFR2b ligands, FGF7 and FGF10 on primary salivary gland progenitor cell proliferation and morphogenesis, in 3D hydrogel microenvironments.

Fgf10$^{-/-}$ and *Fgfr2b*$^{-/-}$ mice do not develop salivary glands, highlighting their contribution to salivary gland organogenesis[12,13]. *Fgf7*$^{-/-}$ mice show no SMG phenotype[22], suggesting functional compensation by other FGFs. When FGF7 and FGF10 were initially characterized on the basis of their biochemistry and mitogenic activities, FGF10 was found to bind heparin with higher affinity than that of FGF7[23-25]. This led to the initial hypothesis that FGF10 activities were more tightly regulated by heparin than FGF7. Previous studies show that variations in HS sulfation patterns contribute to distinct modes of morphogenesis. Additionally, the difference between FGF7 and FGF10-induced morphologies in ex vivo SMG culture were traced to a single amino acid residue within the HS-binding region of FGF7 and FGF10. Site directed mutagenesis of Arg 187 in FGF10 to Val 187, the corresponding residue in FGF7, induced epithelial budding when isolated SMG epithelial rudiments were treated with the FGF10^{R187V} mutant, highlighting a key role for HS-mediated growth factor gradients in determining the type of morphogenic response by regulating the diffusion radius of HS-binding growth factors[26].

Our experiments show that salivary gland progenitor cells cultured in 3-dimensional hyaluronic acid:laminin-modified hydrogels self-assemble into spheroids 30-40 microns in diameter by day seven an express FGFR2b at the cell surface. FGF7 and FGF10 both induced sustained salivary gland progenitor cell proliferation shown by ki67 staining and incorporation of fluorescent thymine, indicative of entry into S-phase of the cell cycle, consistent with the role of FGFs in acting as mitogens. Differences in the number of proliferating cells with either FGF7 or FGF10 treatment may be a consequence of endogenous perlecan (HSPG2) contained within the laminin component of the hydrogel system. Previous work has identified 2% perlecan by weight within laminin-111, owing to the inability to completely purify laminin from other basement membrane components[27]. Increased proliferation at later timepoints and sustained AKT phosphorylation with FGF10 treatment might result from initial FGF10 trapping events mediated by transient binding interactions with the HS-chains of perlecan.

The distinct morphologies observed by treating spheroids with FGF7 or FGF10 are similar to previous reports using ex vivo SMG culture,with exogenous addition of FGF7 inducing lobular morphologies and FGF10 inducing elongated morphologies. Distinct morphologies resulting from stimulation of FGFR2b with either FGF7 or FGF10 may also be a consequence of endogenous HS chains within the laminin and spheroid-derived perlecan. Previous work from our lab shows that spheroids secreted large amounts of HSPG2, further contributing to HS content within the hydrogel system, which can impact the intrinsic bioactivities of theses growth factors. Heparanase treatment 24 hours after exogenous addition of FGF7 or FGF10 lead to an increase in FGF10 duct lengths and FGF7 lateral extensions, suggesting that there are FGF species bound to HS chains present within our hydrogel system which can be released through the proteolytic cleavage of HS chains (Cannon unpublished).

A previous study identified the differential FGFR2b downstream phosphorylation dynamics in HeLA cells treated with either FGF7 or FGF10. Using mass spectrometry-qualitative-based proteomics, Francavilla and colleagues were able to identify that upon FGF10:FGFR2b ligation, but not FGF7:FGFR2b, tyrosine 734

(Y734) embedded deep within the kinase domain becomes a phosphorylation target. This phosphorylation event triggers receptor internalization and recycling to the plasma membrane, whereas FGFR2b lacking Y734 phosphorylation, as in the case of FGF7:FGFR2b signaling, leads to receptor internalization and degradation. FGF7:FGFR2b signaling lead to increased transcription of genes involved in cell proliferation, whereas, FGF10:FGFR2b signaling increased expression of genes associated with cell migration[28]. This data beings to answer the puzzling question as to how different ligands binding the same receptor elicit different responses. Our results do not show altered levels of FGFR2b, as the time course over which our experiments were performed might not capture this signaling events. Further work would have to investigate the defined temporal dynamics of FGF7- and FGF10:FGFR2b signaling and how this model contributes to heparan sulfate dependent morphogen gradients inducing differences in morphogenic outcomes.

Several reports have shown the reciprocal regulation of growth factor and extracellular matrix signaling during glandular development. EGFR ligand, transforming growth factor, was shown to upregulate fibronectin in primary mammary organoids cultured in Matrigel[29]. Interestingly, FGF7 stimulation within mammary organoid cultures was shown to decrease fibronectin levels. The 5-chain of laminin was found to be required for epithelial clefting and endbud expansion during SMG epithelial morphogenesis through binding 1-integrin by amplifying *Fgfr1b/Fgfr2b/Fgf1* transcription[30]. This signaling response was found to be reciprocally regulated, as FGFR2b stimulation with FGF10 was shown to upregulate *Lama5* levels and rescue SMG epithelium treated with siRNA targeting laminin α_5-chain primary transcripts. Here we showed that FGF7 and FGF10 both upregulate fibronectin levels, leading to increased extracellular deposition. Interestingly, we saw an accumulation of fibronectin at the cell periphery and at sites resembling clefts in lobular like structures, but not in control spheroids, suggesting that deposited fibronectin was undergoing remodeling, but this requires further investigation. Interestingly, FGF10 treated hSAC spheroids showed no preferential fibronectin distribution and assembly, as fibronectin was ubiquitously

distributed throughout intra- and extracellular compartments. It's possible that fibronectin may self-assemble at the cell periphery, induced by the mechanical unraveling of individual fibronectin molecules. Our findings showing that FGF7, but not FGF10, upregulate integrin suggest that FGF7 is responsible for upregulating the machinery needed for cleft formation and progression in salivary gland branching morphogenesis.

We observed that hSAC spheroid treatment with FGF10 preceding FGF7 addition lead to more complex morphogenesis than hSAC spheroids treated with both FGFR2b ligands simultaneously. Our data suggests the both ligands bind FGFR2b competitively and that presentation of the correct growth factor and/or ECM cues at defined temporal scales is important for obtaining hSAC morphogenesis that resemble native gland morphologies. Within the developing SMG, laminin-111 polymerization provides the framework for basement membrane structure and is later replaced by laminin-511 during development. Incorporating laminin-111 within our HA-based hydrogel system is required for FGF7- and FGF10-dependent hSAC morphogenesis, as HA-based hydrogels lacking laminin fail to form bud- and duct-like morphologies (Pradhan-Bhatt and Cannon unpublished). These results imply that laminin-111 functions as an inductive signaling cue for hSAC morphogenesis. Additionally, the laminin-111 within our hydrogel system is not covalently crosslinked, which may impart a unique topography within the polymer network, providing the required space for hSAC structures to migrate. However, this requires further investigation.

Previous work in our lab has identified that acinar cells isolated from primary tissue have the capability to self-assemble into spheroids in HA-based hydrogel networks, secrete major salivary enzyme amylase, and respond to cholinergic and adrenergic stimulation[4]. This work has implications in tissue engineering applications seeking to restore salivary function to those suffering from salivary gland dysfunction. The data presented here provides a proof of principle study, wherein hSACs derived from primary tissue display remarkable progenitor cell characteristics on the basis of their gene expression profiles and ability to organize into higher ordered

structures reminiscent of native tissue architectures. In conclusion, our study provides a basis for implantation studies seeking to provide the most efficient means of restoring salivary gland function.

Chapter 3

HUMAN SALIVARY-LIKE ACINAR CELLS UNDERGOING MORPHOGENESIS FORM LUMENS AND ARE CAPABLE OF DIFFERENTIATION

3.1 Abstract

Radiation-induced atrophy following head and neck cancer treatments results in salivary gland hypofunction. Decreased salivary flow is concurrent with xerostomia, or dry mouth, leading to a poor prognosis in oral health. Current treatments are unsatisfactory; therefore, we envision the creation of a bioengineered, artificial salivary gland to restore glandular function. Prior reports from our lab have shown the successful isolation and culture of human salivary acinar-like cells (hSACs) in both 2D and 3D culture systems. We have identified that hSACs express several stem/progenitor cell biomarkers and undergo epithelial morphogenesis into higher ordered structures in response to FGFR2b ligands, FGF7 and FGF10 when grown in hyaluronic acid/laminin-modified hydrogels. Here, we report that hSAC spheroids grown in HA/laminin hydrogels treated with FGF10 followed by FGF7 form lumens after twelve days in culture. Lumen formation in hSAC structures is apoptosis-mediated, as active caspase-3 localizes within the interiors of tubular and endbud-like structures. These structures express salivary-specific enzyme α-amylase, suggesting our culture conditions promote acinar-cell differentiation. Remarkably, these structures are also capable of ductal cell cytodifferentiation. hSACs cultured with conditioned media from isolated dorsal root ganglia or by stimulation of EGFR with exogenous heparin-binding epidermal growth

factor (HB-EGF) promote cytokeratin 19 expression, a hallmark of the salivary ductal cell lineage.

3.2 Introduction

Stem/progenitor populations within developing organs/glands including the lungs, kidneys, mammary glands, and salivary glands are required for organogenesis. Abrogating the biophysical and biochemical cues regulating stem/progenitor cell survival during glandular development often result in organ/gland hypoplasia or aplasia, leading to severe physiological abnormalities[1]. FGF signaling has been shown to play a key role in progenitor cell maintenance and organogenesis of the lungs and salivary glands, as disrupting FGF10:FGFR2b signaling using siRNA or pharmacological inhibitors reduces progenitor marker *Sox9* expression is distal epithelial lung progenitors and KIT+K14+ distal endbud progenitors in the SMG[2-4]. Importantly, *Fgf10*$^{-/-}$ and *Fgfr2b*$^{-/-}$ mice demonstrate lung and salivary gland agenesis[5,6].

Epithelial morphogenesis is dependent on the reciprocal cross talk with the underlying heterogeneous stromal cell populations. Mesenchymal, neuronal, endothelial, and leukocyte cell populations contained within the condensing stroma during development all make unique contributions to shape the final architecture of many branched organs, including the salivary gland. Mesenchymal FGF7 and FGF10 have been shown to induce distinct modes of salivary gland morphogenesis within the developing fetal SMG epithelium, end bud formation and ductal elongations respectively[7]. Additionally, reports have highlighted the concerted actions of the parasympathetic branch of the autonomic nervous system and mesenchymal cell populations in maintaining epithelial progenitor cell maintenance and expansion, induction of branching morphogenesis, and ductal tubulogenesis[7-11]. These studies identify the key role for other cell populations within different tissue compartments in driving final glandular morphologies and efficient functions during organogenesis.

Identification of organ/gland specific-progenitor cells and their role during organogenesis provides a potential means to restore gland function following damage. Patients with head and neck cancers undergoing radiation therapy exhibit significantly reduced salivary flow as a consequence the salivary glands lying in close proximity to directed ionizing beam radiation. Scattered radiation has been shown to induce the salivary gland atrophy and necrosis of saliva producing units, leading to dry mouth or xerostomia[12,13]. Loss of saliva within the oral cavity has been shown to result in multiple oropharyngeal defects including dental caries, difficulty in mastication, dysphasia, and increased susceptibility to infection by microorganisms. Current treatments including over the counter oral sialagogues to stimulate salivary flow are futile, as these cholinomimetics target receptors found on the surface secretory acini, which are destroyed following radiation treatment. Therefore, the creation of an artificial salivary gland would greatly improve the quality of life in patients suffering from xerostomia.

We have successfully identified a progenitor population in our primary cultures that display characteristic expression of progenitor markers including KIT, musashi, keratin 5, and keratin 14 (Pradhan-Bhatt unpublished). Human acinar-like cells (hSACs) exhibit morphologies akin to terminally differentiated acinar cell populations within the native salivary gland, however gene expression profiling has revealed their potential multipotency to give rise to differentiated salivary gland acinar, ductal, and myoepithelial cell populations. We have previously reported that hSAC spheroids grown in three-dimensional hyaluronic acid:laminin-111 modified hydrogels are capable of undergoing morphogenesis in response to fibroblast growth factors, FGF7 and FGF10, suggesting their capability to organize into higher ordered structures reminiscent of those seen during native salivary gland development.

Herein, we report that hSAC spheroids grown in three-dimensional hyaluronic acid:laminin modified hydrogels are capable of forming higher ordered structures that form lumens, express salivary-specific enzyme -amylase, and have the potential to differentiate into ductal structures. Our findings have implications in tissue engineering

applications attempting to generate higher ordered, three-dimensional neotissues that can be implanted into patients suffering from xerostomia to restore salivary gland function.

3.3 Materials and Methods

Tissue Procurement

Human tissue specimens of parotid and submandibular glands were obtained from patients undergoing head and neck surgery. Informed consent and a tissue procurement protocol were approved by the Institutional Review Board from both the Christiana Care Health System (CCHS) and the University of Delaware. Following surgical excision, tissue specimens were placed on ice and stored at four degrees Celsius until quality control processing and for use in the laboratory.

Cell Explant Culture

After obtaining an IRB approved protocol from both Christiana Care Health System and the University of Delaware, healthy tissue specimen from human parotid and submandibular glands were obtained from patients undergoing head and neck surgery. Salivary tissue was placed in betadine solution at a dilution of 1/10 for approximately 2 minutes and washed in chilled Dulbecco's Modified Eagle Medium (Life Technologies, Frederick, MD). Salivary epithelium was mechanically separated from surrounding connective tissue and finely minced. Epithelial rudiments were then suspended in Hepato-STIM medium (BD Biosciences Discovery Labware, Bedford, MA) supplemented with 100 U/mL of penicillin G sodium and 100 ug/mL of streptomycin sulfate in 0.085% (w/v) saline and 2.5 ug/mL amphotericin B and cultured into 6-well tissue culture treated plates. Salivary epithelial rudiments were maintained at 37 degrees Celsius in a humidified atmospheric chamber with 5% (v/v) CO2.

Two-Dimensional Cell Culture

Salivary acinar-,ductal-,and myoepithelial-like cells emerging from cultured tissue explants were allowed to reach 50-60% confluency. Media was aspirated and cells were washed with phosphate buffered saline (PBS) (Life Technologies). 0.250 uL of 0.05% (w/v) trypsin with EDTA (Fisher Scientific, Pittsburgh, PA) was added to the 6-well culture plates and incubated at 37 degrees Celsius for 5 minutes. Cells were re-suspended in 2.50 mL of Hepato-STIM media and 0.250 uL of trypsin soybean inhibitor (Sigma-Aldrich, St. Louis, MO) and centrifuged at 3000 RPM for 5 minutes. Supernatant was aspirated and the cell pellet was re-suspended in 3mL of Hepato-STIM cell culture media. Cells were split at a dilution of 1/10 for subsequent experiments.

Three-Dimensional Cell Culture

Lyophilized poly-ethylene glycol diacrylate (PEGDA) and hyaluronic acid functionalized with reactive thiol groups (HA-SH) were synthesized following a previously reported procedure (Citation Prestwhich) (ESI BIO, Alemeda, CA). Prior to any cell culture, HA-SH was dissolved in degassed, deionized (DI) water and incubated at 37 degrees Celsius for 20 minutes. PEGDA was readily reconstituted in DI water at room temperature. Both solutions were mixed at a crosslinking density of 1:4 (PEGDA:HA-SH) at a final volume of 50 uL to form a thin, gel-only layer on cell culture inserts (Millipore, Billerica, MA, diameter: 12mm, pore size: 0.4 um). Pure acinar-like cell populations cultured in either T-25 or T-75 tissue culture flasks with Hepato-STIM media were allowed to reach confluency. 0.05% trypsin (w/v) with EDTA (Fisher Scientific, Pittsburg, PA) was added to tissue culture flasks and incubated at 37 degrees Celsius for five minutes. Cells were pelleted following resuspension in trypsin soybean inhibitor (Sigma-Aldrich, St. Louis, MO) and media. The cell pellet was resuspended in fresh cell culture medium and counted using a hemacytometer. 8 x 104 cells were added to 1.5mL eppendorf tubes and pelleted at 3000 RPM for 3 minutes. Supernatant was discarded and the pellet was resuspended in HA-SH (ESI BIO) and 6 mg/mL laminin-111 (Sigma) at a 1:1 ratio and incubated at

room temperature for 10 minutes. Poly-ethylene glycol diacrylate was added to the suspension at a 1:4 ratio relative to thiolated hyaluronic acid. The solution was mixed thoroughly and added to cell culture inserts (Millipore) and placed in 37 degrees Celsius. After 40 minutes, cell culture medium was added outside the cell culture inserts. Due to variability in crosslinking kinetics, cell culture media was added on top of the cell-laden hydrogel upon gelation. For growth factor/ dorsal root ganglion conditioned media treatments, 100ng/ml of FGF7 FGF10 were added to the interior of the cell culture inserts at day seven.

Whole-cell fluorescent labeling and immunocytochemistry

Cell culture medium was aspirated from cell-seeded hydrogels. Hydrogels were fixed in 4% paraformaldehyde (PFA) solution for 30 minutes at room temperature. 1X PBS was used to wash the hydrogels following fixation. Cells were permeabilized with 0.2% (v/v) Triton X-100 solution for 30 minutes at room temperature. After washing with 1X PBS, hydrogels were blocked in 3% (w/v) bovine serum albumin (BSA) in PBS overnight at 4 degrees Celsius. Hydrogels were then placed into 8-well nunc chamber slides (Lab-tek Products, Nalge Nunc International, Naperville, IL). Primary antibodies for FGFR2b (goat, Santa Cruz Biotechnology, Dallas, TX), CK19 (AbCAM), beta catenin and active caspase 3 (AbCAM) were added to cell-laden hydrogels for 2 hours at 37 degrees Celsius, while shaking. Primary antibody solution was removed and hydrogels were washed in 1X PBS for twelve minutes. Washing steps following primary antibody incubation were repeated 3 times. Secondary antibodies conjugated to Alexa 488 and Alexa 568 fluorophores (raised against mouse or rabbit IgG) (Invitrogen, Carlsbad, CA) were added to hydrogels for 1 hour and thirty minutes. Hydrogels were washed as described above. Draq 5 (Biostatus, Leicestershire, United Kingdom) or NucBlue (Invitrogen) were added to hydrogels. If applicable, hSAC structures were incubated with Syto13 (Invitrogen) for 15 minutes at room temperature in the dark. Following a quick wash with 1X PBS, hydrogels were placed in 3% BSA (w/v) with one drop of antifade solution (Invitrogen) and stored at four degrees Celsius

before imaging. All imaging was done using Zeiss 510 or 710 laser scanning confocal microscopes.

3.4 Results

Prolonged Culture of hSACs Treated with Heparin-FGF10 Followed by FGF7 Treatment Undergo Apoptosis-Dependent Lumen Formation

Lumen formation is essential during salivary gland development. Preceded by branching morphogenesis, lumen formation within endbud and ductal structures is essential for saliva collection and directed flow into the oral cavity. We observed that sustained culture of hSAC spheroids treated with heparin-FGF10 and FGF7 structures lead to the formation of lumens within endbud- and duct-like structures. Confocal microscopy identified active caspase 3 activity within presumptive lumens (Figure5 A-B) implying that lumen formation during hSAC spheroid morphogenesis is driven by an apoptosis-dependent mechanism.

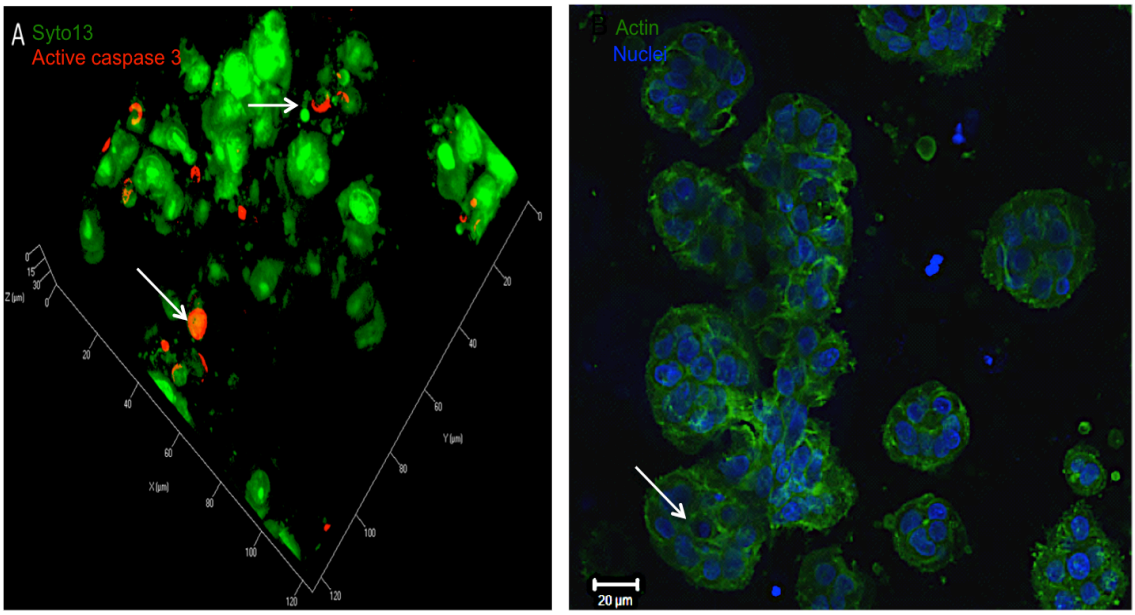

Figure 3.1 Extended culture of hSAC structures treated with FGF10:heparin followed by FGF7 form lumens through an apoptosis-dependent mechanism. hSAC structures (Syto13, green) cultured for longer than 12 days begin to form hollow tubes seen by active caspase 3 (red) (A). Maximum intensity projection of hSAC structure. Actin (green) and nuclei (blue) highlight hSAC acino-tubular morphologies (B).

hSAC Structures Are Capable of Differentiation

Previous reports from our lab showed that salivary acinar cells self-assembled into spheroid structures and secreted α-amylase into the extracellular space when cultured in HA-based hydrogels. hSAC spheroids cultured in HA:laminin-111 hydrogels treated with heparin-FGF10, followed by FGF7 treatment also secreted -amylase into the extracellular space. Interestingly, α-amylase staining was also observed within endbud- and duct-like structures (Figure 3.2A), suggesting that our culture conditions are promoting differentiation towards the acinar cell lineage.

Ex vivo culture of fetal mouse SMGs treated with acetylcholine, the major neurotransmitter of the parasympathetic branch of the nervous system drove keratin 5 progenitor expansion and differentiation into keratin 19 positive ductal cell lineage through ACh/M1-mediated transactivation of HB-EGF/EGFR signaling. Our results show that hSAC spheroids treated with temporal addition of heparin-FGF10 and FGF7, followed by HB-EGF treatment after 24 hours upregulated keratin 19 expression throughout hSAC strucutres, suggesting that hSAC stuctures are capable of responding to HB-EGF treatment to drive differentiation towards keratin-19 positive ductal cell lineage (Figure 3.3 A,B).

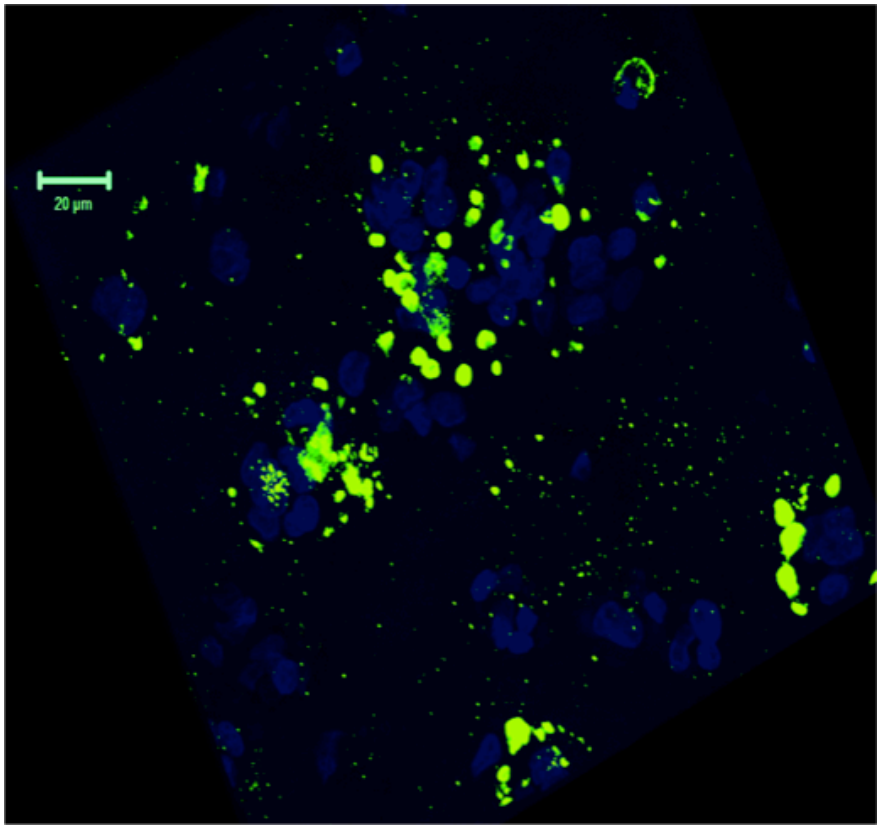

Figure 3.2 hSAC structures treated sequentially with FGF10-heparin and FGF7 express acinar cell biomarker α-amylase. Nuclei (blue) amylase (green).

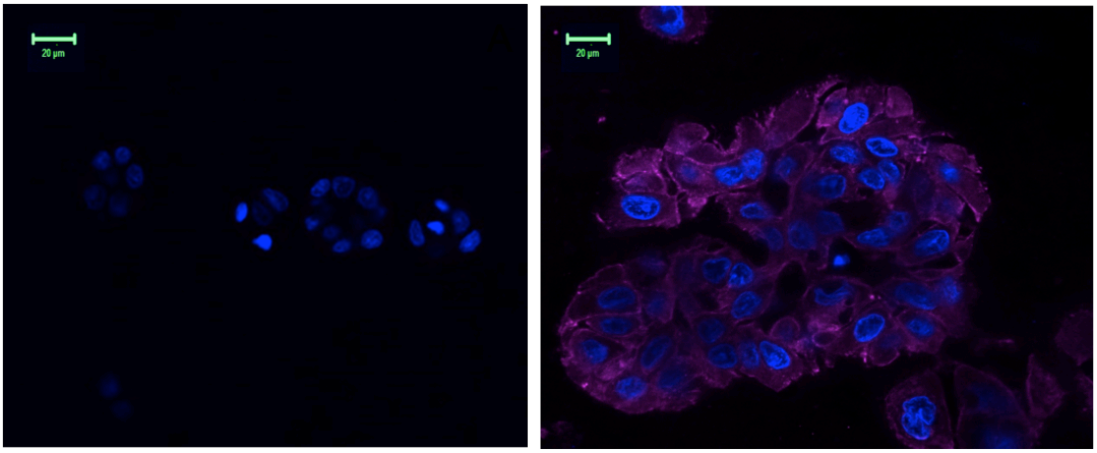

Figure 3.3. hSAC spheroids sequentially treated with heparin-FGF10, FGF7, and HB-EGF show increased cytokeratin 19 expression when compared to untreated controls. Untreated hSAC spheroids highlighted using a nuclear stain do not express ductal marker CK19 (Panel 1). Heparin-FGF10 followed by FGF7 and HB-EGF treatment show elevated levels of ductal biomarker CK19 (magenta) when compared to control (Panel 2).

3.5 Discussion

Epithelial lumen formation within the fetal SMGs of mice begins at the onset of cytodifferentiation at embryonic day 16, suggesting that after the rapid proliferation and branching phases of SMG development, epithelial progenitor populations are subject to alterations in gene expression patterns to drive lumen formation and cell differentiation. Here we show that hSAC spheroids, which express a variety of progenitor biomarkers, are capable of organizing into higher ordered structures that contain lumens, secrete acinar-cell specific salivary enzyme α-amylase, and are capable of differentiation towards ductal cell lineage through HB-EGF stimulation.

Epithelial compartments within tissues and organs are typically organized with well-defined apical-basal polarized membrane microdomains. Apical-basal polarity is a prerequisite to lumen formation and is usually governed by subcellular mechanisms including cell-matrix and cell-cell interactions[14,15]. Formation of cell-matrix interactions is usually mediated by α/β integrin heterodimers, whereas cell-cell contacts are established by homophilic cadherin-cadherin interactions. Whole organism knockouts of integrin subunits including β1-integrin typically result in embryonic lethality[16,17]; however, tissue specific knockouts highlight integrin function in controlling epithelial cell polarization, lumen formation, and arrangement into complex three-dimensional tissue/organ morphologies. The collecting ducts of the kidneys of β*1-/-*mice still exhibit lumens with no signs of aberrant polarization, however, lumens were found to be dilated when compared to wildtype controls[18]. Endothelial cells devoid of β1-integrin showed reduced levels of polarity protein, Par3. Ectopic overexpression of Par3 was able to partially rescue lumen occlusion in developing vasculature networks, implying that downstream β1-integrin signaling targets polarity promoting protein complexes[19,20]. Future work will examine the localization of polarity promoting complexes and integrin /subunits to investigate polarity within branched hSAC structures.

Currently, there is no literature describing the role for FGF:FGFR signaling in contributing to glandular lumen formation during organogenesis. However, FGF10:FGFR2b signaling has been shown to positively regulate the expression of sonic

hedgehog signaling within the salivary epithelium. Shh has been suggested to mediate salivary lumen formation[21,22], however, additional studies are required to provide evidence that this is the case. Our data show that hSAC spheroids undergoing FGF10-heparin/FGF7-mediated morphogenesis begin to form hollow lumens after twelve days in culture. We show that lumen formation in our cultures is driven through activation of the apoptotic pathway, as shown by active caspase 3 staining and confocal microscopy. Interestingly, these express acinar cell-specific salivary enzyme α-amylase, suggesting that our culture conditions are conducive to driving cytodifferentiation towards the acinar cell lineage. We are unsure as to whether the extracellular and intracellular localization of α-amylase suggests any type of directional secretion, as even if -amylase exocytosis is directed into a duct-like lumen, it will accumulate within the extracellular space within the hydrogel network. Future work will investigate the directionality of α-amylase secretions.

Recent reports have shown the role of VIP/VIPR1 in mediating SMG lumen formation and expansion in *ex vivo* cultures[15]. Inhibition of VIPR1, which is expressed on the developing epithelium, fail to form contiguous lumens and show aberrant localization of occluding junction marker, ZO-1, wherein wildtype SMGs ZO-1 is found to coalesce at the presumptive ductal midline. VIPR1 is contained within the G_s-GPCR family of transmembrane receptors whose downstream activation results in increased cytosolic cAMP levels, leading to downstream PKA activation and PKA-mediated phosphorylation events. Isolated epithelial SMG rudiments treated with VIP or membrane-permeable cAMP analog 8-bromoadenosine cyclic adenosine monophosphate showed similar effects with elongated duct-like morphologies, accompanied by ductal lumen formation suggesting that VIP/VIPR1 mediated lumen formation occurs in a cAMP/PKA-dependent manner. We have preliminary data suggesting that hSAC spheroids treated with FGF10-heparin and FGF7, followed by VIP treatment exhibit elongated ductal structures. However, lumen formation within these structures is currently uninvestigated. Future work will examine the ability of these structures to form hollow tubes.

Co-cultures of isolated SMG epithelium with PSG showed the role of neuronal input in contributing to cell proliferation and the formation of ductal tubes[15,23,24]. Additionally, the contribution to ductal tube formation and growth made by the PSG was found to be independent of direct contact between the epithelium and neuronal axon fibers, and instead mediated through the diffusion of biochemical signals from the PSG to the epithelium.

Previous reports have shown that within developing SMGs, ACh/M1 signaling transactivates EGFR signaling by facilitating the MMP-2 mediated release and activation of HB-EGF from the plasma membrane to promote ductal differentiation[25]. HB-EGF addition to branched hSAC structures previously treated HS-FGF10 and FGF7 showed upregulation of K19 compared to FGFR2b stimulated hSAC structures. HB-EGF binds EGFR with higher affinity than other EGF family members, including TGF and EGF, which bind the other EGFR family members including ErbB3 and ErbB4[26]. Downstream HB-EGF: EGFR signaling has been previously shown affect ductal morphogenesis in the prostate[27].

Previous work from our lab has shown the successful isolation and expansion of human salivary acinar-like cells (hSACs) in hyaluronic acid-based hydrogels. The remarkable breadth stem/progenitor markers expressed within our hSACs in three-dimensional culture suggests the inhertent capability of hSAC differentiation into any of the three major epithelial cell types within the salivary gland. Our data suggests that hSACs are capable of undergoing dynamic reorganization into higher ordered structures, lumen formation, and differentiation into acinar and ductal cell lineages. This work is a proof of principle study, highlighting the potential of hSACs to organize into functional salivary neotissue. In sum, the results obtained here could help provide a template for tissue engineering applications attempting to generate artificial glandular structures.

Chapter 4

GLOBAL DISSCUSSION

The overarching goal of tissue engineering is to restore organ/gland function following irreparable damage. Tissue engineering applications are reliant on identifying the most suitable cell population(s), designing the appropriate niche or scaffold, and providing the appropriate biophysical and biochemical cues in a defined spatiotemporal manner to drive the creation of three dimensional neotissues to restore organ/gland-specific functions and physiological homeostasis. Salivary gland dysfunction resulting from the destruction of secretory acini units from ionizing beam radiation used to treat head and neck cancers leads to xerostomia, or dry mouth. In lieu of the unsatisfactory treatments for xerostomia, including cholinomimetics and artificial saliva, we envision the creation of an artificial salivary gland.

We have identified a population of human salivary acinar-like cells (hSACs) that exhibit progenitor cell characteristics, as shown through their gene and protein expression profiles, capability to assembly into higher ordered architectures that contain lumens following stimulation of FGFR2b with ligands FGF7 and FGF10, and differentiation capacity following HB-EGF stimulation or DRG-neuronal input to drive keratin 19 expression and cytodifferentiation towards the ductal cell lineage. Progenitor cell populations are essential during organogenesis, as a reduction in progenitor populations in various glands including the lung, kidney, intestine, mammary, prostate, and salivary glands results in organ/glandular dysfunction and even aplasia. Within many developing organs and glands, it is the epithelial compartment that is responsible for undergoing large-scale alterations in structure, which ultimately generate the final characteristic three-dimensional morphologies of a given physiological system.

However, the underlying stroma, a heterogenous tissue compartment containing mesenchymal, neuronal, endothelial, and immune cell populations is responsible for containing the instructive signals to drive epithelial morphogenesis.

Among the most well studied signaling molecules are those within the fibroblast growth factor (FGF) family. Ranging from 17-34 kDs, the 22 members of the human FGF family are small, freely diffusible polypeptides that bind to specific FGFRs, regulating an array of cellular functions to contribute to organogenesis and physiological homeostasis. FGF:FGFR signaling is fine-tuned by alternative splicing of exon sequences on FGFR transcripts coding for the C-terminal portion of the D3 extracellular domain and through specific interactions with diverse heparan sulfate polymers. These posttranscriptional and posttranslational modifications regulate ligand binding specificity, diffusive mobility of the ligand, and the type of/extent of morphogenic responses.

Individual hSACs encapsulated within three-dimensional HA:laminin-111 hydrogel networks self-assemble into hSAC spheroids ranging from 30-40 microns in diameter and express the epithelial FGFR2 isoform, FGFR2b. Ligands for FGFR2b including FGF1, FGF3, FGF7, FGF10, and FGF22. Stimulation of FGFR2b on hSAC spheroids with ligands FGF7 and FGF10 increased proliferation rates compared to untreated controls showing sustained proliferation after 8 and 24 hours of culture, as shown by incorporation of fluorescent thymine molecules and ki67 staining. Elevated $Erk^{1/2}$ phosphorylation levels were detected in FGF7 and FGF10 treated hSAC spheroids after 8 hours. Interestingly, sustained Akt phosphorylation at Ser 273 (mTOR phosphorylation site) suggests that sustained FGF10:FGFR2b signaling acts through both MAPK and PI3K/Akt downstream pathways. 2 hours after isolated SMG epithelial rudiments were treated with either FGF7 and FGF10 show that FGF7:FGFR2b signaling acts through PI3K/Akt and MAPK pathways, whereas the effects of FGF10:FGFR2b signaling are MAPK dependent. Together, these results suggest that FGFR2b downstream signaling is regulated in a fine-tuned temporal fashion. Future

work will investigate the downstream transcriptional events altered by FGFR2b stimulation by FGF7 and FGF10.

One of the major enigmas in cell signaling paradigms is: how do two different ligands that bind the same receptor induce different cell responses? Marenkova et. al., proposed that the heparan sulfate binding affinity of FGFR2b ligands FGF7 and FGF10 is at least, in part, responsible for modulating the distinct mode of morphogenesis in the developing SMG and lacrimal glands. As FGF10 binds heparan sulfate with higher affinity than FGF7, with its radius of diffusion being more restricted than that of FGF7. By mutating a single amino acid within the HS-binding domain of FGF10, $FGF10^{R187\rightarrow V}$ was converted into a functional mimic of FGF7 as shown through surface plasmon resonance (SPR) analysis and by tracking the release and diffusion of fluorescently labeled FGF7, FGF10, and $FGF10^{R187\rightarrow V}$ from heparin-coated beads through cell culture media over time. SMG epithelial rudiments treated with FGF7 and $FGF10^{R187\rightarrow V}$ showed the same budding morphologies, while FGF10 induced duct-like elongations.

Moreover, downstream FGF7/FGF10:FGFR2b downstream signaling was investigated in HeLa cells. Authors found that a tyrosine residue embedded deep within the kinase domain of FGFR2b, Y734, becomes phosphorylated upon FGF10 binding, whereas Y734 is not phosphorylated in HeLa cells following FGF7-mediated stimulation of FGFR2b. Phosphorylation of Y734 within FGFR2b following FGF10 treatment leads to the recruitment and binding of PI3K via its SH2 domain on the p85 subunit, which recruits adaptor protein SH3B4 to effectively traffick internalized FGFR2b to Tfr-positive endosomes leading FGFR2b recycling to the plasma membrane.

Work in our lab has yet to characterize the diffusion of FGF7 and FGF10 through the HA:laminin-111 hydrogel system. Identifying the mobility of these two FGFR2b ligands within our system would provide a defined starting point for our lab to investigate the temporal nature of FGF7-, and FGF10:FGFR2b downstream signaling. Our results do not show altered FGFR2b levels and/or localization following treatment with FGF7 or FGF10; however, the time course over which our experiments were

performed might not capture FGFR2b internalization and/or recycling. Further work would have to investigate the defined temporal dynamics of FGF7- and FGF10:FGFR2b signaling and how this model contributes to heparan sulfate dependent morphogen gradients inducing differences in morphogenic outcomes.

Fgf1,Fgfr1b,Fgfr2b have been shown to be reciprocally regulated by α_5-chain containing laminin, laminin-511 at the cell periphery in *ex vivo* culture of developing SMGs. Growth factor:ECM crosstalk has been identified in other branching glands including the lacrimal and mammary glands. Within the developing lacrimal gland, FGF10:FGFR2b signaling converges with Barx2-regulated transcriptional events. Barx2, a homeodomain transcription factor was shown to be responsible for FGF10-mediated ductal elongation by co-regulating the expression of matrix metalloproteinases *Mmp2* and *Mmp*9, as well as fibronectin binding integrin subunit *Itga5*. EGFR ligand, transforming growth factor,was shown to upregulate fibronectin in primary of mammary organoids cultured in Matrigel. Interestingly, FGF7 stimulation within mammary organoid cultures was shown to decrease fibronectin levels.

Our data suggests that hSACs treated with FGF7 and FGF10 both upregulate total fibronectin protein levels and deposition. However, FGFR2b stimulation with FGF7, but not FGF10 was found to upregulate α_5-integrin protein levels. Therefore, we have identified a novel link between FGF signaling and ECM deposition and potentially organization within our hSAC cultures. We have yet to investigate the effects of FGF7-, and FGF10:FGFR2b on the regulation of MMPs, however future work will investigate the crosstalk between growth factor, ECM, and ECM remodeling enzymes. *Ex vivo* culture of fetal mouse SMGs investigating cleft formation and progression revealed fibronectin accumulation at sites of cell-ECM contact triggers activation of β_1- integrin, which is suggested to function with α_5 integrin as the functional $\alpha_5\beta_1$ integrin-heterodimer to facilitate cell adhesion to fibronectin. Integrin clustering into focal adhesions and downstream signaling induces ROCK/actomyosin-mediated contraction required for the mechanical unraveling of fibronectin, revealing a cryptic self-assembly motif to promote fibronectin fibrillogenesis and accumulation at sites of

epithelial clefting. Future work will further investigate the effects of FGF7 and FGF10 on fibronectin assembly and accumulation along the cell periphery during hSAC morphogenesis.

Our data suggests that the defined temporal addition of FGF7 and FGF10 may be important for inducing specific gene expression patterns to drive hSAC morphogenesis into structures most representative of the native salivary gland structure. Using a publicly available microarray dataset, we analyzed the expression profiles of FGF7 and FGF10 over the course of SMG development. FGF10 is detected at much higher levels than FGF7 within the mesenchyme at the onset of salivary gland initiation, implying that FGF10:FGFR2b signaling is required for the invasion of the primitive oral epithelium into the underlying mesenchyme as a proximal stalk and distal endbud. *Fgf7,Fn1*, and *Igta5* are highly expressed at embryonic days 12.5 and 13, when epithelial clefting and endbud formation begins. To coordinate morphogenic events in parallel with those during organogenesis, we decided to treat hSAC spheroids with FGF10 followed by FGF7. We observed that hSAC spheroids stimulated with FGFR2b ligands at specific timepoints had longer ducts and more lobular-like structures than hSAC spheroids treated with either growth factor alone, simultaneous addition, or untreated. Our data suggests that both ligands bind FGFR2b competitively and that downstream signaling from FGF7- or FGF10-binding FGFR2b regulate differential expression patterns to coordinate organized hSAC morphogenesis.

Patel et. al., have showed that specific heparan sulfate structures modulate endbud expansion, ductal elongation and differentiation within the developing SMG. FGF10:FGFR2b signaling modulated by HS chains containing IdoA2S:GlcNAc6S sulphation patterns resulted in downstream amplification of *Fgfr1, Fgf1,* and *Apq5* transcriptional activity accompanied by endbud expansion and differentiation towards the aquaporin 5 expressing basal cell lineage. Conversely, FGF10:FGFR2b signaling regulated by HS chains with IdoA2OH-GlcNAc6S sulfphation patterns result in the upregulation of grainy head transcription factor Cp2l1, a marker of the ductal cell lineage. hSAC spheroids treated with FGF10 followed by FGF7 treatment showed

FGF1 expression. However, untreated hSAC spheroids also showed FGF1 within structures. Interestingly, FGF10/FGF7 treated hSACs showed extracellular staining of FGFR2b and FGF1, which colocalized within the hydrogel network compared to controls, where it was absent. These results suggest that a portion of the extracellular domain(s) of FGFR2b may be cleaved where freely diffusing endogenous FGF1 molecules can bind to regulate the extent of FGFR signaling within hSAC structures. However, future work is required to investigate the nature of this possible mode of FGF:FGFR signaling and its effects on hSAC morphogenesis and differentiation.

Chapter 5

CONCLUSIONS AND FUTURE WORK

Here we report the effects of fibroblast growth factors, FGF7 and FGF10 on human salivary acinar-like cells (hSACs) grown in three-dimensional hyaluronic acid:laminin hydrogels. hSACs express FGFR2b on the cell surface and stimulation with cognate ligands FGF7 and FGF10 induce sustained cell proliferation and downstream phosphorylation events consistent with the role of FGF ligands functioning as potent mitogens. Isolated SMG epithelia treated with FGF7 or FGF10 in *ex vivo* culture display distinct modes of morphogenesis. Consistent with the literature, activation of FGFR2b with either FGF7 or FGF10 results in distinct hSAC architectures, with FGF7 inducing lobular-like structures and FGF10 promoting the formation of elongated structures.

A recent study has shown that ligand-dependent downstream FGFR2b phosphorylation events are capable of modulating receptor dynamics; FGF7 stimulation results in FGFR2b endocytosis with internalized FGFR2b vesicular maturation into late endosomes and subsequent degradation. In contrast, FGF10-mediated FGFR2b activation promotes receptor endocytosis into recycling endosome compartments with subsequent trafficking back to the plasma membrane. Interestingly, we observed no differences in FGFR2b localization at the cell membrane when comparing treated or untreated samples. Due to the time scale over which we performed our experiments, such signaling events may not have been observed. Future work will examine the defined timescale of downstream FGF7/10:FGFR2b signaling in hSAC structures undergoing morphogenesis.

We have identified a novel link between FGFR2b and extracellular matrix signaling. FGF7 and FGF10 both increase total fibronectin protein levels and deposition into our hydrogel scaffold. Interestingly, FGF7, but not FGF10, increases total α_5-integrin levels. α_5-integrin is the major α-subunit in the α/β integrin heterodimer that binds fibronectin. Future work would include an ECM array to measure the changes in gene expression in response to FGF7 and FGF10 to identify additional growth factor:ECM crosstalk.

We observed that treating hSAC spheroids with FGF10 followed by FGF7 resulted in more complex morphogenesis as shown through immunofluorescence and morphogenic index analysis. In contrast, simultaneous addition of both FGFR2b ligands resulted in less hSAC morphogenesis than with either ligand alone. This data suggests the competitive binding of FGF7 and FGF10 to FGFR2b and that the time scale over which hSAC spheroids respond to growth factor treatments are important for creating complex gland-like architectures. Additionally, *ex* vivo cultore of SMGs shows that FGF ligand-dependent gradient formation plays a role in generating distinct gland morphologies. Future work will incorporate defined growth factor gradients presented on defined temporal time scales to induce hSAC structures that most resemble organized glandular morphologies reminiscent.

Interestingly, we observed that prolonged culture of growth factor-treated hSAC structures begin to form lumens after twelve days in culture. Lumen formation in our culture system is apoptosis-mediated, shown by active caspase-3 localization at presumptive sites of lumen formation. Recent literature has shown the effect of vasoactive intestinal peptide (VIP) on ductal tube formation in the fetal SMGs of mice. We have preliminary data showing the morphological effects of recombinant VIP on hSAC spheroids already treated with FGFs 7 and 10. Future work will investigate the roles of VIP on hSAC morphogenesis and lumen formation.

The stem/progenitor expression profile within hSACs suggests their capability for generating the three cell types within the salivary epithelium. Treatment of hSACs with HB-EGF or culture in conditioned media from isolated rat dorsal root ganglia increased keratin 19 protein levels, as shown through immunofluorescence and confocal microscopy. Keratin 19 is a hallmark of the salivary ductal cell lineage, confirming that hSAC structures are capable of cytodifferentiation. Future work will investigate the ability of hSACs to differentiate into acinar, ductal, and myoepithelial cell types. Recombination of these cells types within the appropriate scaffold could lead to the creation of an artificial salivary gland. Additionally, hSACs subject to the correct growth factors and their gradients on defined timescales could also lead to the generation of glandular architectures with localized expression of differentiation markers.

REFERENCES

1.) Amano O, Mizobe K, Bando Y, Sakiyama K. Anatomy and Histology of Rodent and Human Major Salivary Glands: —Overview of the Japan Salivary Gland Society-Sponsored Workshop—. Acta Histochemica et Cytochemica2012;45(5):241-250. doi:10.1267/ahc.12013

2.) Frommer, J. The human accessory parotid gland: its incidence, nature, and significance. Oral Surg Oral Med. Oral Pathol 1977;43: 671–676.

3). Gibson, M.H. The prenatal human submandibular gland: a histological, histochemical and ultrastructural study. Anat Anz 1983;153:91–105

4.) Witt, R. Salivary Gland Diseases: Surgical and Medical Management. Thieme Medical Publishers. New York. 2005.

5.) Whelton H.P. Anatomy and Physiology of the Salivary Glands' Saliva and Oral Healt. 1977 2nd Ed.

6.) Proctor GB, Carpenter GH. Regulation of salivary gland function by autonomic nerves. Autonomic neuroscience : basic & clinical. 2007;133(1):3-18. Epub 2006/12/13.

7.) Ferreira, J.N., Hoffman, M.P. Interactions between developing nerves and salivary glands. Organogenesis 2013;Vol 9, Iss.3 199-203

8.) Knox SM, Lombaert IM, Reed X, Vitale-Cross L, Gutkind JS, Hoffman MP. Parasympathetic innervation maintains epithelial progenitor cells during salivary organogenesis. Science. 2010;329:1645–7. doi: 10.1126/science.1192046.

9.) I.M. Lombaert, S.R. Abrams, L. Li, V.P. Eswarakumar, A.J. Sethi, R.L. Witt, M.P. Hoffman Combined Kit and FGFR2b signaling regulates epithelial progenitor expansion during organogenesis. Stem Cell Rev., 1 (2013), pp. 604–619

10.) Lombaert, I.M., Knox, S.M., and Hoffman, M.P. (2011). Salivary gland progenitor cell biology provides a rationale for therapeutic salivary gland regeneration. Oral Dis. 17, 445–449.

11.) Nagler, R.M., and Baum, B.J. Prophylactic treatment reduces the severity of xerostomia following radiation therapy for oral cavity cancer. Arch Otolaryngology Head Neck Surg 129, 247, 2003.

12.) Helton, K., Yager, P. 2007. Interfacial instabilities affect microfluidic extraction of small molecules from non-Newtonian fluids. *Lab on a Chip*,**7**, 1581-1588 10.1039/B709585F

13.) Han, P., Suarez-Durall, P., Mulligan, R. Dry mouth: A critical topic for older adult patients. Journal of Prosthodontic Research. 2014; Epub.

14.) Turner RJ, Sugiya H. Understanding salivary fluid and protein secretion. Oral Dis. 2002;8(1):3-11. Epub 2002/04/09.

15.) Melvin JE, Yule D, Shuttleworth T, Begenisich,T. Regulation of fluid and electrolyte secretion in salivary gland acinar cells. Annu Rev Physiol 2005;67:445-469

16.) Baker, Olga J. et al. "Rat Parotid Gland Cell Differentiation in Three-Dimensional Culture." Tissue Engineering. Part C, Methods 16.5 (2010): 1135–1144. PMC. Web. 6 Jan. 2015

17.) Ekstrom, J., Khosravani, N., Castagnola, M., Messana, I. Saliva and the control of its secretion. Dysphagia, Medical Radiology. Diagnostic Imaging, DOI: 10.1007/174_2011_481, Springer-Verlag Berlin Heidelberg 2012

18. Rothova, M., Thompson, H., Lickert, H. and Tucker, A. S. (2012), Lineage tracing of the endoderm during oral development. Dev. Dyn., 241: 1183–1191. doi:10.1002/dvdy.23804

19.) R. Dudek, J.D. Fix Embryology (2nd ed.)Williams and Wilkins, Baltimore (1998)

20.) Knosp WM, Knox SM, Hoffman MP. Salivary gland organogenesis. WIREs. Dev Biol. 2012;1:69–82

21.) Tucker, A.S. Salivary Gland Development. Seminars in Cell and Developmental Biology. 2007;18(2):237–244

22.) Patel, V., Hoffman, M.P. Salivary gland development: A template for regeneration. Seminars in Cell and Developmental Biology 2014;25-26:52-60.

23.) Chai Y, Jiang X, Ito Y, Bringas P Jr, Han, J, Rowitch DH, Soriano P, McMahon, AP, Sucov HM. 2000. Fate of the mammalian cranial neural crest during tooth and mandibular morphogenesis. Development 127:1671–1679.

24.) Yoshida T, Vivatbutsiri P, Morriss-Kay G, Saga Y, Iseki S. 2008. Cell lineage in mammalian craniofacial mesenchyme. Mech Dev 125:797–808.

25.) Harunaga, J., Hsu, J.C., Yamada, K.M. Dynamics of salivary gland morphogenesis. J Dent Res 90(9):1070-1077, 2011.

26.) Grobstein C. Epithelio-mesenchymal specificity in the morphogenesis of mouse submandibular rudiments in vitro. J Exp Zool. 1953;124:383–444

27.) Kratochwil K. (1969). Organ specificity in mesenchymal induction demonstrated in the embryonic development of the mammary gland of the mouse. Dev. Biol. 20, 46–71 10.1016/0012-1606(69)90004

28.) Wells, K.L., Gaete, M., Matalova, E., Deutesh, D., Rice, D., Tucker, A.S. Dynamic Relationship of the Epithelium and Mesenchyme During Salivary Gland Initiation: The Role of Fgf10. Biology Open 2.10 (2013): 981–989. PMC.

29.) Nedvetsky, P.I., Emmerson, E., Finley, J.K., Ettinger, A., Cruz-Pacheco, N., Prochazaka, J., Haddox, C.L., Northrup, E., Hodges, C., Mostov, K., Hoffman, M.P., Knox, S. Parasympathetic Innervation Regulates Tubulogenesis in the Developing Salivary Gland. Dev Cell. 2014;30(4):449-462.

31.) Patel, V., Hoffman, M.P. Salivary gland branching morphogenesis. Differentiation (2006) 74:349–364.

32.) Proctor GB, Carpenter GH. Regulation of salivary gland function by autonomic nerves. Autonomic neuroscience : basic & clinical. 2007;133(1):3-18. Epub 2006/12/13.

33.) Ferreira, J.N., Hoffman, M.P. Interactions between developing nerves and salivary glands. Organogenesis 2013;Vol 9, Iss.3 199-203

34.) Knox SM, Lombaert IM, Reed X, Vitale-Cross L, Gutkind JS, Hoffman MP. Parasympathetic innervation maintains epithelial progenitor cells during salivary organogenesis. Science. 2010;329:1645–7. doi: 10.1126/science.1192046.

35.) I.M. Lombaert, S.R. Abrams, L. Li, V.P. Eswarakumar, A.J. Sethi, R.L. Witt, M.P. Hoffman Combined Kit and FGFR2b signaling regulates epithelial progenitor expansion during organogenesis. Stem Cell Rev., 1 (2013), pp. 604–619

36.) Lombaert, I.M., Knox, S.M., and Hoffman, M.P. (2011). Salivary gland progenitor cell biology provides a rationale for therapeutic salivary gland regeneration. Oral Dis. 17, 445–449.

37.) Nagler, R.M., and Baum, B.J. Prophylactic treatment reduces the severity of xerostomia following radiation therapy for oral cavity cancer. Arch Otolaryngology Head Neck Surg 129, 247, 2003.

38.) Helton, K., Yager, P. 2007. Interfacial instabilities affect microfluidic extraction of small molecules from non-Newtonian fluids. *Lab on a Chip*,**7**, 1581-1588 10.1039/B709585F

39.) Han, P., Suarez-Durall, P., Mulligan, R. Dry mouth: A critical topic for older adult patients. Journal of Prosthodontic Research. 2014; Epub

40.) Turner RJ, Sugiya H. Understanding salivary fluid and protein secretion. Oral Dis. 2002;8(1):3-11. Epub 2002/04/09.

41.) Melvin JE, Yule D, Shuttleworth T, Begenisich,T. Regulation of fluid and electrolyte secretion in salivary gland acinar cells. Annu Rev Physiol 2005;67:445-469

42.) Ekstrom, J., Khosravani, N., Castagnola, M., Messana, I. Saliva and the control of its secretion. Dysphagia, Medical Radiology. Diagnostic Imaging, DOI: 10.1007/174_2011_481, Springer-Verlag Berlin Heidelberg 2012

43.) Pradhan S, Zhang C, Jia X, et al. Perlecan domain IV peptide stimulates salivary gland cell assembly in vitro. Tissue Eng Part A 2009

44.) Kagami, H., Wang, S., and Hai, B. Restoring the function of salivary glands. Oral Diseases 14, 15, 2007.

45.) Nguyena, M.K., Alsberg, E. 2014. Bioactive factor delivery strategies from engineered polymer. *Prog Polym Sci*; 39(7): 1236–1265. 10.1016/j.progpolymsci.2013.12.001

46.) Dreifus, M., Wichterle, O. 1964. Clinical Experiences with Hydrogel Contact Lenses. *Cesk Oftalmol.* 20:393-9.

47.) Dicker, K., Gurski, L., Pradhan-Bhatt, S., Witt, R., Farach-Carson, M.C., Jia, X. Hyaluronan: A simple polysaccharide with diverse biological functions. Acta Biomaterialia. 2014; 10(4):1558-1570

48.) Fraser, J.R., Laurent, T.C., Laurent, U.B. Hyaluronan: its nature, distribution, functions and turnover. J Intern Med. 1997;247: 27–33

49.) Xu X, Jha AK, Harrington DA, Farach-Carson MC, Jia X. Hyaluronic acid-based hydrogels: from a natural polysaccharide to complex networks. Soft Matter. 2012;Epub.

50.) H.G. Garg, C.A. Hales Chemistry and biology of hyaluronan (1st ed.)Elsevier, Oxford (2004)

51.) J.A. Burdick, G.D. Prestwich Hyaluronic acid hydrogels for biomedical applications Adv Mater, 23 (2011), pp. H41–H56

52.) N. Itano, T. Sawai, M. Yoshida, P. Lenas, Y. Yamada, M. Imagawa. 1999. Three isoforms of mammalian hyaluronan synthases have distinct enzymatic properties. J Biol Chem, 274, pp. 25085–25092

53.) E.A. Turley. Hyaluronan-binding proteins and receptors. Adv Drug Deliv Rev, 7 (1991), pp. 257–264

54.) Soscia, D. A., Sequeira, S. J., Schramm, R. A., Jayarathanam, K., Cantara, S. I., Larsen, M., & Castracane, J. (2013). Salivary gland cell differentiation and organization on micropatterned PLGA nanofiber craters. Biomaterials, 34(28), 6773–6784. doi:10.1016/j.biomaterials.2013.05.061

55.) Tran, S.D., Sugito, T., Dipasquale, G., Cotrim, A.P., Ban- dyopadhyay, B.C., Riddle, K., Mooney, D., Kok, M.R., Chiorini, J.A., and Baum, B.J. Re-engineering primary epithelial cells from rhesus monkey parotid glands for use in developing an artificial salivary gland. Tissue Eng 12, 2939, 2006

56.) Ogawa, M., Oshima, M., Imamura, A., Sekine, Y., Ishida, K., Yamashita, K., … Tsuji, T. (2013). Functional salivary gland regeneration by transplantation of a bioengineered organ germ. Nature Communications, 4, 2498. doi:10.1038/ncomms3498

57.) Pradhan-Bhatt, S., Harrington, D. A., Duncan, R. L., Jia, X., Witt, R. L., & Farach-Carson, M. C. (2013). Implantable Three-Dimensional Salivary Spheroid Assemblies Demonstrate Fluid and Protein Secretory Responses to Neurotransmitters. Tissue Engineering. Part A, 19(13-14), 1610–1620. doi:10.1089/ten.tea.2012.0301

58.) Iber, D., Menshyakau, D. The control of branching morphogenesis. 2013. *Open Biology;* 10.1098/rsob.130088.

59.) Metzger RJ, Klein OD, Martin GR, Krasnow MA. 2008 The branching programme of mouse lung development. Nature 453, 745–750. (doi:10.1038/nature07005)

60.) Watanabe T, Costantini F. 2004 Real-time analysis of ureteric bud branching morphogenesis in vitro. Dev. Biol. 271, 98–108. (doi:10.1016/j.ydbio.2004.03.025)

61.) Meyer TN, Schwesinger C, Bush KT, Stuart RO, Rose DW, Shah MM, Vaughn DA, Steer DL, Nigam SK. 2004 Spatiotemporal regulation of morphogenetic molecules during in vitro branching of the isolated ureteric bud: toward a model of branching through budding in the developing kidney. Dev. Biol. 275, 44–67.

62.) Lu P, Werb Z. 2008 Patterning mechanisms of branched organs. Science 322, 1506–1509.

63.) Affolter M, Caussinus E 2008. Tracheal branching morphogenesis in Drosophila: New insights into cell behaviour and organ architecture. Development 135: 2055–2064

64.) Ochoa-Espinosa, A., & Affolter, M. (2012). Branching Morphogenesis: From Cells to Organs and Back. Cold Spring Harbor Perspectives in Biology, 4(10), a008243. doi:10.1101/cshperspect.a008243

65.) Arora, R., Metzger, R. J., & Papaioannou, V. E. (2012). Multiple Roles and Interactions of Tbx4 and Tbx5 in Development of the Respiratory System. PLoS Genetics, 8(8), e1002866. doi:10.1371/journal.pgen.1002866

66.) Volckaert, T., & De Langhe, S. (2014). Lung epithelial stem cells and their niches: Fgf10 takes center stage. Fibrogenesis & Tissue Repair, 7, 8. doi:10.1186/1755-1536-7-8

67.) El Agha, E., & Bellusci, S. (2014). Walking along the Fibroblast Growth Factor 10 Route: A Key Pathway to Understand the Control and Regulation of Epithelial and Mesenchymal Cell-Lineage Formation during Lung Development and Repair after Injury. Scientifica, 2014, 538379. doi:10.1155/2014/538379

68.) Volckaert, T., Campbell, A., Dill, E., Li, C., Minoo, P., & De Langhe, S. (2013). Localized Fgf10 expression is not required for lung branching morphogenesis but prevents differentiation of epithelial progenitors. Development (Cambridge, England), 140(18), 3731–3742. doi:10.1242/dev.096560

69.) Lazarus A, del Moral P-M, Ilovich O, Mishani E, Warburton D, Keshet E. 2011 A perfusion-independent role of blood vessels in determining branching stereotypy of lung airways. Development (Camb. Engl.) 138, 2359–2368. (doi:10.1242/dev.060723)

70.) Murray JD. 2003 Mathematical biology, 3rd edn, vol. 2. Mathematical biology: II. Spatial models and biomedical applications. New York, NY: Springer

71.) Gerlach, G., Wingert, R. 2013. Kidney organogenesis in the zebrafish: insights into vertebrate nephrogenesis and regeneration. *Wiley Interdiscip Rev Dev Biol*; 2(5): 559–585.

72.) Michos, O., Cebrian, C., Hyink, D., Grieshammer, U., Williams, L., D'Agati, V., … Costantini, F. (2010). Kidney Development in the Absence of Gdnf and Spry1 Requires Fgf10. PLoS Genetics, 6(1), e1000809. doi:10.1371/journal.pgen.1000809

73.) Sternlicht, M. 2006. The cues that regulate ductal branching morphogenesis. Breast Cancer Research. (BioMed Central Ltd) 8, 201 (doi:10.1186/bcr1368)

74.) Macias, H., & Hinck, L. (2012). Mammary Gland Development. Wiley Interdisciplinary Reviews. Developmental Biology, 1(4), 533–557. doi:10.1002/wdev.35

75.) Sakakura T, Nishizuka Y, Dawe CJ. Mesenchyme-dependent morphogenesis and epithelium-specific cyto differentiation in mouse mammary gland. Science. 1976;194:1439–1441

76.) Juppner H, Abou-Samra AB, Freeman M, Kong XF, Schipani E, Richards J, Kolakowski LF, Jr, Hock J, Potts JT, Jr, Kronenberg HM, et al. A G protein-linked receptor for parathyroid hormone and parathyroid hormone-related peptide. Science. 1991;254:1024–1026

77.) Cowin, P., & Wysolmerski, J. (2010). Molecular Mechanisms Guiding Embryonic Mammary Gland Development. Cold Spring Harbor Perspectives in Biology, 2(6), a003251. doi:10.1101/cshperspect.a003251

78.)Mailleux AA, Spencer-Dene B, Dillon C, Ndiaye D, Savona-Baron C, Itoh N, Kato S, Dickson C, Thiery JP, Bellusci S 2002. Role of FGF10/FGFR2b signaling during mammary gland development in the mouse embryo. Development 129:53–60

79.) Veltmaat JM, Relaix F, Le LT, Kratochwil K, Sala FG, van Veelen W, Rice R, Spencer-Dene B, Mailleux AA, Rice DP, et al. 2006. Gli3-mediated somitic Fgf10 expression gradients are required for the induction and patterning of mammary epithelium along the embryonic axes. Development133:2325–2335

80.) Aoto K, Nishimura T, Eto K, Motoyama J. Mouse GLI3 regulates Fgf8 expression and apoptosis in the developing neural tube, face, and limb bud. Dev Biol. 2002;251:320–332.

81.)Gajewska, M., Zielniok, K., Motyl, T. Autophagy in development and remodeling of mammary gland. Autophagy - A Double-Edged Sword - Cell Survival or Death?, Dr. Yannick Bailly (Ed.), ISBN: 978-953-51-1062-0, InTech, DOI: 10.5772/54558

82.) Zhou Y, Xu BC, Maheshwari HG, He L, Reed M, Lozykowski M, Okada S, Cataldo L, Coschigamo K, Wagner TE, et al. A mammalian model for Laron syndrome produced by targeted disruption of the mouse growth hormone receptor/binding protein gene (the Laron mouse) Proc Natl Acad Sci U S A.1997;94:13215–13220

83.) Krege JH, Hodgin JB, Couse JF, Enmark E, Warner M, Mahler JF, Sar M, Korach KS, Gustafsson JA, Smithies O. Generation and reproductive phenotypes of mice lacking estrogen receptor beta. Proc Natl Acad Sci U S A. 1998;95:15677–15682

84.) Lubahn DB, Moyer JS, Golding TS, Couse JF, Korach KS, Smithies O. Alteration of reproductive function but not prenatal sexual development after insertional disruption of the mouse estrogen receptor gene.Proc Natl Acad Sci U S A. 1993;90:11162–11166

85.) Silberstein GB, Van Horn K, Shyamala G, Daniel CW. Essential role of endogenous estrogen in directly stimulating mammary growth demonstrated by implants containing pure antiestrogens. Endocrinology.1994;134:84–90

86.) Luetteke NC, Qiu TH, Fenton SE, Troyer KL, Riedel RF, Chang A, Lee DC. Targeted inactivation of the EGF and amphiregulin genes reveals distinct roles for EGF receptor ligands in mouse mammary gland development. Development. 1999;126:2739–2750

87.) Ciarloni L, Mallepell S, Brisken C. Amphiregulin is an essential mediator of estrogen receptor alpha function in mammary gland development. Proc Natl Acad Sci U S A. 2007;104:5455–5460

88.) Coleman S, Silberstein GB, Daniel CW. Ductal morphogenesis in the mouse mammary gland: evidence supporting a role for epidermal growth factor. Dev Biol. 1988;127:304–315.

89.) Fata, J. E., Mori, H., Ewald, A. J., Zhang, H., Yao, E., Werb, Z., & Bissell, M. J. (2007). The MAPKERK-1,2 pathway integrates distinct and antagonistic signals from TGFα and FGF7 in morphogenesis of mouse mammary epithelium. Developmental Biology, 306(1), 193–207. doi:10.1016/j.ydbio.2007.03.013

90.) Srinivasan K, Strickland P, Valdes A, Shin GC, Hinck L. Netrin-1/neogenin interaction stabilizes multipotent progenitor cap cells during mammary gland morphogenesis. Dev Cell. 2003;4:371–382

91.) Strickland P, Shin GC, Plump A, Tessier-Lavigne M, Hinck L. Slit2 and netrin 1 act synergistically as adhesive cues to generate tubular bi-layers during ductal morphogenesis. Development. 2006;133:823–832

92.) Wua, J., Tzanakakisa, E. Deconstructing stem cell population heterogeneity: Single-cell analysis and modeling approaches. 2013. Biotechnol Adv;15; 31(7): 1047–1062. 10.1016/j.biotechadv.2013.09.001

93.) Takahashi, K., Yamanaka, S. 2006. Induction of Pluripotent Stem Cells from

Mouse Embryonic and Adult Fibroblast Cultures by Defined Factors. *Cell*; 126(4), p663–676. 10.1016/j.cell.2006.07.024

94.) Sims-Lucas S, Argyropoulos C, Kish K, McHugh K, Bertram JF, Quigley R, Bates CM. 2009 Three-dimensional imaging reveals ureteric and mesenchymal defects in Fgfr2-mutant kidneys. J. Am. Soc. Nephrol. 20, 2525–2533. (doi:10.1681/ASN.2009050532

95.) Boland, G.M., Perkins, G., Hall, D.J., Tuan, R.S. 2004. Wnt 3a promotes proliferation and suppresses osteogenic differentiation of adult human mesenchymal stem cell. *Journ. Cell. BioChem;* 93(6)1210-1230 10.1002/jcb.20284

96.) Lu BC et al. 2009. Etv4 and Etv5 are required downstream of GDNF and Ret for kidney branching morphogenesis. Nat. Genet. 41,1295 – 1302. doi:10.1038/ng.476

97.) Turner, N., Grose, R. Fibroblast growth factor signaling: from development to cancer. 2010 Nat Rev Canc. 10, 116-129.

98.) Itoh, N., & Ornitz, D. M. (2011). Fibroblast growth factors: from molecular evolution to roles in development, metabolism and disease. Journal of Biochemistry, 149(2), 121–130. doi:10.1093/jb/mvq121

99.) Ohta, H., Itoh, N. Roles of FGFs as adipokines in adipose tissue development, remodeling, and metabolism. 2014. Front. Endocrinol. 5, DOI:10.3389/fendo.2014.00018.

100.) Gospodarowicz D, Moran JS. Mitogenic effect of fibroblast growth factor on early passage cultures of human and murine fibroblasts. J. Cell Biol. 1975;66:451–457.

101.) Itoh N, Ornitz DM. Evolution of the Fgf and Fgfr gene families. 2004. Trends Genet20:563–569.

102.) Popovici C, Roubin R, Coulier F, Birnbaum D. An evolutionary history of the FGF superfamily. 2005. Bioessays 27: 849–857.

103.) Goetz, R., & Mohammadi, M. (2013). Exploring mechanisms of FGF signalling through the lens of structural biology. Nature Reviews. Molecular Cell Biology, 14(3), 166–180. doi:10.1038/nrm3528

104.) Mohammadi, M., Olsen, S., Ibrahimi, O. Structural basis for fibroblast growth factor receptor activation. 2005. Cytokine and Growth Factor Reviews 16(2), 107-137. doi:10.1016/j.cytogfr.2005.01.008

105.) Lin, X., Buff, E., Perrimon, N., Michelson, A.M. Heparan sulfate proteoglycans are essential for FGF receptor signaling during Drosophila embryonic development. 1999. Development 126, 3715-3723.

106.) H.P. Makarenkova, M.P. Hoffman, A. Beenken, A.V. Eliseenkova, R. Meech, C. Tsau, V.N. Patel, R.A. Lang, M. Mohammadi. Differential interactions of FGFs with heparan sulfate control gradient formation and branching morphogenesis. Sci. Signal., 2 (2009), p. ra55

107.) Johnson DE, Williams LT. Structural and functional diversity in the FGF receptor multigene family.1993. Adv Cancer Res 60: 1–41.

108.) Gong, G.S. Isoforms of Receptors of Fibroblast Growth Factors. 2014. J. Cell. Physiol. 229: 1887–1895.

109.) Kalinina J, Dutta K, Ilghari D, Beenken A, Goetz R, Eliseenkova AV, Cowburn D, Mohammadi M. The alternatively spliced acid box region plays a key role in FGF receptor autoinhibition. 2012. Structure. 20:77–88.

110.) Belov, A. A., & Mohammadi, M. (2013). Molecular Mechanisms of Fibroblast Growth Factor Signaling in Physiology and Pathology. Cold Spring Harbor Perspectives in Biology, 5(6), 10.1101/cshperspect.a015958 a015958. doi:10.1101/cshperspect.a015958

111.) Engel, J. 1996. Domain organizations of modular extracellular matrix proteins and their evolution. Matrix Biol. 15:295–299. doi:10.1016/S0945-053X(96)90130-4

112.) Patthy, L. 1999. Genome evolution and the evolution of exon-shuffling—a review. Gene.238:103 114. doi:10.1016/S0378-1119(99)00228-0

113.) Hynes, R. The evolution of the metazoan extracellular matrix. 2012. JBC. 196(6); 671-679

114.) Watt, F.M., Hodivala, K.J. Cell Adhesion: Fibronectin and integrin knockouts come unstuck (1994). Curr. Biol. Cell 4(3);270-272. 10.1016/S0960-9822(00)00063-4

115.) Liu, K., Cheng, L., Flesken-Nikitin, A., Huang, L., Nikitin, A. Y., & Pauli, B. U. (2010). Conditional knockout of fibronectin abrogates mouse mammary gland lobuloalveolar differentiation. Developmental Biology, 346(1), 11–24. doi:10.1016/j.ydbio.2010.07.001

116.) Sarras MP Jr, Zhang X, Huff JK, Accavitti MA, St John PL, Abrahamson DR. 1993. Extracellular matrix (mesoglea) of Hydra vulgaris: III. Formation and function during morphogenesis of hydra cell aggregates.Dev. Biol. 157(2):383–98

117.) Shimizu H, Zhang X, Zhang J, Leontovich A, Fei K, et al. 2002. Epithelial morphogenesis in hydra requires de novo expression of extracellular matrix components and matrix metalloproteinases. Development 129(6):1521–32

118.) Domogatskaya, A., Rodin, S., Tryggvason, K. 2012. Functional Diversity of Laminins. Annu. Rev. Cell Dev. Biol. 2012. 28:523–53. 10.1146/annurev-cellbio-101011-155750

119.) Hynes, R. 2002. Integrins: Bidirectional, allosteric signaling machines. Cell 110(6);673-687

120.) Kanchanawong, P., Shtengel, G., Pasapera, A., Ramko,E.,Davidson,M.W., Hess, H.F., Waterman,C.M. 2010. Nature 468, 580–58 doi:10.1038/nature09621

121.) Pradhan, S., Farach-Carson, M.C. 2010. Mining the extracellular matrix for tissue engineering applications. Regenerative Medicine, Vol. 5, No. 6 , Pages 961-970 doi: 10.2217/rme.10.61

122.) Lu, P., Takai, K., Weaver, V. M., & Werb, Z. (2011). Extracellular Matrix Degradation and Remodeling in Development and Disease. Cold Spring Harbor Perspectives in Biology, 3(12), a005058. doi:10.1101/cshperspect.a005058

123.) Khokha, R., & Werb, Z. (2011). Mammary Gland Reprogramming: Metalloproteinases Couple Form with Function. Cold Spring Harbor Perspectives in Biology, 3(4), a004333. doi:10.1101/cshperspect.a004333

124.) Kadoya, Y., Mochizuki, M., Sorokin, L., Yamashina, S. 2003. Role for laminin-alpha5 chain LG4 module in epithelial branching morphogenesis. Dev Biol. 263(1);153-164

125.) Suzuki, N., Ichikawa, N. Kasai, S., Yamada, M., Nishi, N., Morioka, H., Yamashita, H., Kitagawa, Y., Utani, A., Hoffman, M.P., Nomizu, M. 2003. Syndecan Binding Sites in the Laminin α1 Chain G Domain. Biochemistry 42 (43), 12625-12633

126.) Fukuda, Y., Masuda, Y., Kishi, J., Hashimoto, Y., Hayakawa, T.,Nogawa, H. and Nakanishi, Y. (1988)The role of interstitial collagens in cleft formation of mouse embryonic submandibular gland during initial branching. Development 103:259–267.

127.) Spooner, B.S. and Faubion, J.M. (1980) Collagen involvement in branching morphogenesis of embryonic lung and salivary gland. Dev Biol 77:84–102

128.) Epithelium-dependent extracellular matrix synthesis in transforming growth factor-beta 1-growth-inhibited mouse mammary gland. (1990). The Journal of Cell Biology, 110(6), 2209–2219.

129.) Kadoya, Y., Kadoya, K., Durbeej, M., Holmvall, K., Sorokin, L.and Ekblom, P. (1995) Antibodies against domain E3 of laminin-1 and integrin alpha 6 subunit perturb branching epithelial morphogenesis of submandibular gland, but by different modes.J Cell Biol 129:521–534

130.) Kadoya, Y. and Yamashina, S. (1993) Distribution of alpha 6 integrin subunit in developing mouse submandibular gland. J Histochem Cytochem 41:1707–1714.

131.) Menko AS, Kreidberg JA, Ryan TT, Van Bockstaele E, Kukuruzinska MA. Loss of alpha3beta1 integrin function results in an altered differentiation program in the mouse submandibular gland. Dev Dyn. 2001;220:337–49

132.) Gross, J. & Lapiere, C. M. 1962. Collagenolytic activity in amphibian tissues: a tissue culture assay. Proc. Natl Acad. Sci. USA 47, 1014–1022

133.) Brinckerhoff, C. E. & Matrisian, L. M. 2002. Matrix metalloproteinases: a tail of a frog that became a prince. Nature Rev. Mol. Cell Biol. 3, 207–214

134.) Page-McCaw, A., Ewald, A., Werb, Z. 2007. Matrix metalloproteinases and the regulation of tissue remodeling. Nature Reviews. 8;221-233.

135.) Sternlicht, M. D. & Werb, Z. How matrix metalloproteinases regulate cell behavior. Annu. Rev. Cell. Dev. Biol. 17, 463–516 (2001)

136.) Stocker, W. 1995. The metzincins--topological and sequential relations between the astacins, adamalysins, serralysins, and matrixins (collagenases) define a superfamily of zinc-peptidases. Protein Science 4, 823–840.

137.) Rebustini IT, Myers C, Lassiter KS, Surmak A, Szabova L, Holmbeck K, et al. 2009. MT2-MMP-dependent release of collagen IV NC1 domains regulates submandibular gland branching morphogenesis. Dev Cell. 17:482–93

138.) Wiseman BS. 2003. Site-specific inductive and inhibitory activities of MMP-2 and MMP-3 orchestrate mammary gland branching morphogenesis. J Cell Biol. 162:1123–1133.

139.) Steinberg Z, Myers C, Heim VM, Lathrop CA, Rebustini IT, Stewart JS, et al. FGFR2b signaling regulates ex vivo submandibular gland epithelial cell proliferation and branching morphogenesis. Development. 2005;132:1223–34

140.) Rebustini, I. T., Patel, V. N., Stewart, J. S., Layvey, A., Georges-Labouesse, E., Miner, J. H., & Hoffman, M. P. (2007). Laminin α5 is necessary for submandibular gland epithelial morphogenesis and influences FGFR expression through β1 integrin signaling. Developmental Biology, 308(1), 15–29. doi:10.1016/j.ydbio.2007.04.031

141.) Patel, V. N., Likar, K. M., Zisman-Rozen, S., Cowherd, S. N., Lassiter, K. S., Sher, I., … Hoffman, M. P. (2008). Specific Heparan Sulfate Structures Modulate FGF10-mediated Submandibular Gland Epithelial Morphogenesis and Differentiation. The Journal of Biological Chemistry, 283(14), 9308–9317. doi:10.1074/jbc.M709995200

142.) Patel N, Sharpe PT, Miletich I. Coordination of epithelial branching and salivary gland lumen formation by Wnt and FGF signals. Dev Biol. 2011;358:156–67.

143.) Melnick, M., Phair, R. D., Lapidot, S. A., & Jaskoll, T. (2009). Salivary gland branching morphogenesis: a quantitative systems analysis of the Eda/Edar/NFκB paradigm. BMC Developmental Biology, 9, 32. doi:10.1186/1471-213X-9-32

144.) Jaskoll T, Zhou YM, Trump G, Melnick M. Ectodysplasin receptor-mediated signaling is essential for embryonic submandibular salivary gland development. Anat Rec A Discov Mol Cell Evol Biol. 2003;271:322–31

145.) Haara O, Koivisto T, Miettinen PJ. EGF-receptor regulates salivary gland branching morphogenesis by supporting proliferation and maturation of epithelial cells and survival of mesenchymal cells. Differentiation. 2009;77:298–306

146.) Kadoya Y, Yamashina S. Cellular dynamics of epithelial clefting during branching morphogenesis of the mouse submandibular gland. Dev Dyn. 2010;239:1739–47.

147.) Daley WP, Gulfo KM, Sequeira SJ, Larsen M. Identification of a mechanochemical checkpoint and negative feedback loop regulating branching morphogenesis. Dev Biol. 2009;336:169–82

148.) Daley WP, Gervais EM, Centanni SW, Gulfo KM, Nelson DA, Larsen M. ROCK1-directed basement membrane positioning coordinates epithelial tissue polarity. Development. 2012;139:411–22.

149.) Sakai T, Larsen M, Yamada KM. Fibronectin requirement in branching morphogenesis. Nature. 2003;423:876–81.

150.) Onodera T, Sakai T, Hsu JC, Matsumoto K, Chiorini JA, Yamada KM. Btbd7 regulates epithelial cell dynamics and branching morphogenesis. Science. 2010;329:562–5

151.) Lombaert, I. M. A., & Hoffman, M. P. (2010). Epithelial Stem/Progenitor Cells in the Embryonic Mouse Submandibular Gland. Frontiers of Oral Biology, 14, 90–106. doi:10.1159/000313709

152.) Hudson DL, et al. J Histochem Cytochem. 2001 Feb;49:27

153.) Kent D., Copley M., Benz C., Dykstra B., Bowie M., Eaves C. Regulation of hematopoietic stem cells by the steel factor/KIT signaling pathway. Clin. Cancer Res. 2008;14:1926–1930.

154.) Lin, X. 2004. Functions of heparin sulfate proteoglycans in cell signaling during development. Development 131, 6009-6021 doi: 10.1242/dev.01522

155.) Häcker, U., Nybakken, K., Perrimon, N. 2005. Heparan sulphate proteoglycans: the sweet side of development. Nature Reviews Molecular Cell Biology 6, 530-541 doi:10.1038/nrm1681

156.) Umulis, D., Othmer, H. 2013. Mechanisms of scaling in pattern formation. Development. 140; 4830-4843. 10.1242/dev.100511

157.) Zhang, X., Martinex, D., Koledova, Z., Qiao, G., Streuli, C.H., Lu, P. 2014. FGF ligands of the postnatal mammary stroma regulate distinct aspects of epithelial morphogenesis. Development 141; 3352-3362

158.) Turing, A.M. 1952. The Chemical Basis of Morphogenesis. Philosophical Transactions of the Royal Society of London. Series B, Biological Sciences, 237(641); pp. 37-72

159.) Wolpert L.1969. Positional information and the spatial pattern of cellular differentiation. J. Theor. Biol. 25 (1): 1–47. doi:10.1016/S0022-5193(69)80016-0

160.) Wartlick, O., Kicheva, A., & González-Gaitán, M. (2009). Morphogen Gradient Formation. Cold Spring Harbor Perspectives in Biology, 1(3), a001255. doi:10.1101/cshperspect.a001255

161.) Driever, W., Nüsslein-Volhard, C. A gradient of bicoid protein in Drosophila embryos. 1988. Cell 54(1); 83-93. doi:10.1016/0092-8674(88)90182-1

162.) Müller, P., Rogers, K.W., Yu, S.R., Brand, M., Schier, A.F. 2013. Morphogen transport. Development 140, 1621-1638 doi:10.1242/dev.083519

163.) Gordon, P. V., Sample, C., Berezhkovskii, A. M., Muratov, C. B., & Shvartsman, S. Y. (2011). Local kinetics of morphogen gradients. Proceedings of the National Academy of Sciences of the United States of America, 108(15), 6157–6162. doi:10.1073/pnas.1019245108

164.) Kicheva, A., Pantazis, P., Bollenbach, T.,Kalaidzidis, Y., Bittig, T., Jülicher, F., González-Gaitán, M. 2007. Science. 315(5811);521-525.DOI: 10.1126/science.1135774

165.) Lander, A., Nei, Q., Wan, F. 2002. Do Morphogen Gradients Arise by Diffusion? Developmental Cell. 2(6); 785-796 doi:10.1016/S1534-5807(02)00179-X

166.) Nowak, M., Machate, A., Yu, S. R., Gupta, M. and Brand, M. (2011). Interpretation of the FGF8 morphogen gradient is regulated by endocytic trafficking. Nat. Cell Biol. 13, 153-158

167.) Sigurbjörnsdóttir,S., Renjith, M., Leptin, M. 2014. Molecular mechanisms of de novo lumen formation. Nature Reviews Molecular Cell Biology 15, 665–676 (2014) doi:10.1038/nrm3871

168.) Sacharidou, A., Stratman, A. N. & Davis, G. E. 2012. Molecular mechanisms controlling vascular lumen formation in three-dimensional extracellular matrices. Cells Tissues Organs 195, 122–143

Appendix A.

PERMISSIONS

Title:	Tissue remodelling through branching morphogenesis
Author:	Markus Affolter, Rolf Zeller and Emmanuel Caussinus
Publication:	Nature Reviews Molecular Cell Biology
Publisher:	Nature Publishing Group
Date:	Dec 1, 2009

Logged in as:

LOGOUT

Order Completed

Thank you very much for your order.

This is a License Agreement between Kevin Cannon ("You") and Nature Publishing Group ("Nature Publishing Group"). The license consists of your order details, the terms and conditions provided by Nature Publishing Group, and the payment terms and conditions.

Get the printable license.

License Number	3604260533258
License date	Apr 08, 2015
Licensed content publisher	Nature Publishing Group
Licensed content publication	Nature Reviews Molecular Cell Biology
Licensed content title	Tissue remodelling through branching morphogenesis
Licensed content author	Markus Affolter, Rolf Zeller and Emmanuel Caussinus
Licensed content date	Dec 1, 2009
Type of Use	reuse in a dissertation / thesis
Volume number	10
Issue number	12
Requestor type	academic/educational
Format	print
Portion	figures/tables/illustrations
Number of figures/tables/illustrations	2
High-res required	no
Figures	Figure 1 Figure 2
Author of this NPG article	no
Your reference number	None
Title of your thesis / dissertation	Inducing Epithelial Morphogenesis in Human Salivary Acinar-like Cells Cultured in Three-Dimensional Hyaluronic Acid:Extracellular Matrix-Modified Hydrogels.
Expected completion date	Apr 2015
Estimated size (number of pages)	100
Total	0.00 USD

Title:	Fibroblast growth factor signalling: from development to cancer
Author:	Nicholas Turner and Richard Grose
Publication:	Nature Reviews Cancer
Publisher:	Nature Publishing Group
Date:	Feb 1, 2010

Logged in as:

LOGOUT

Order Completed

Thank you very much for your order.

This is a License Agreement between Kevin Cannon ("You") and Nature Publishing Group ("Nature Publishing Group"). The license consists of your order details, the terms and conditions provided by Nature Publishing Group, and the payment terms and conditions.

Get the printable license.

License Number	3604260306401
License date	Apr 08, 2015
Licensed content publisher	Nature Publishing Group
Licensed content publication	Nature Reviews Cancer
Licensed content title	Fibroblast growth factor signalling: from development to cancer
Licensed content author	Nicholas Turner and Richard Grose
Licensed content date	Feb 1, 2010
Type of Use	reuse in a dissertation / thesis
Volume number	10
Issue number	2
Requestor type	non-commercial (non-profit)
Format	print
Portion	figures/tables/illustrations
Number of figures/tables/illustrations	2
High-res required	no
Figures	Figure 1 Figure 2
Author of this NPG article	no
Your reference number	None
Title of your thesis / dissertation	Inducing Epithelial Morphogenesis in Human Salivary Acinar-like Cells Cultured in Three-Dimensional Hyaluronic Acid:Extracellular Matrix-Modified Hydrogels.
Expected completion date	Apr 2015
Estimated size (number of pages)	100
Total	0.00 USD


Copyright Clearance Center
RightsLink
Home
Create Account
Help
Live Chat
SAGE
Title: Dynamics of Salivary Gland Morphogenesis:
Author: J. Harunaga, J.C. Hsu, K.M. Yamada
Publication: Journal of Dental Research
Publisher: SAGE Publications
Date: 09/01/2011
Copyright © 2011, International & American Associations for Dental Research
LOGIN
If you're a copyright.com user, you can login to RightsLink using your copyright.com credentials. Already a RightsLink user or want to learn more?
Gratis
Permission is granted at no cost for sole use in a Master's Thesis and/or Doctoral Dissertation. Additional permission is also granted for the selection to be included in the printing of said scholarly work as part of UMI's "Books on Demand" program. For any further usage or publication, please contact the publisher.
BACK
CLOSE WINDOW
Copyright © 2015 Copyright Clearance Center, Inc. All Rights Reserved. Privacy statement. Terms and Conditions.
Comments? We would like to hear from you. E-mail us at customercare@copyright.com

8 April 2015

Kevin Cannon

Re: Permission Requested for Thieme figures 4.1 and 3.2 both from Witt: Salivary Gland Diseases, © 2006, Thieme Medical Publishers, Inc

Dear Mr. Cannon,

Thank you for requesting permission to reproduce the above Thieme material. Permission is granted for your requested use in your thesis.

There is no cost for these figures.

This permission is valid and is subject to the following conditions:

1) A credit line will be prominently placed and include: for books – the author(s), title of book, editor, copyright holder, year of publication (reprinted with permission); for journals – the author(s), title of article, title of journal, volume number, issue number and page range (reprinted by permission).

2) The requestor warrants that the material shall not be used in any manner which may be considered derogatory to the title, content, or authors of the material or to Thieme.

3) For journals, permission is granted for print and online in perpetuity. For books, CD-Roms, or DVDs, permission is granted for one time use only in print, CD or DVD for the life of the edition, and online for five years from the date of this permission. Rights herein do not apply to future reproductions, editions, revisions, or other derivative works.

4) Permission granted is non-exclusive, and is valid throughout the world.

5) Thieme cannot supply the requestor with the original artwork or a "clean copy".

6) Permission is valid if the borrowed material is valid to a Thieme imprint (Thieme Medical Publishers Inc., Georg Thieme Verlag Stuttgart).

7) If you opt not to use the material requested above, please notify Thieme within ninety days.

Thank you again for your request.

Sincerely,

Timothy Y. Hiscock
Executive Editor

Permission to re-use a figure from the book Autophagy - A Double-Edged Sword - Cell Survival or Death?" Inbox

Kevin Cannon Wed, Apr 8, 2015 at 11:10 AM

Sasa Marcan<permissions@intechopen.com> Thu, Apr 9, 2015 at 9:28 AM

To: Kevin Cannon <kcannon@udel.edu>

Reply | Reply to all | Forward | Print | Delete | Show original

Hi Kevin,

Thank you for your message.

You may freely reproduce the specified figure in your thesis as long as you reference its source chapter and include the following notice in the figure caption:

© 2013 Gajewska M, Zielniok K, Motyl T. Originally published in [short citation] under CC BY 3.0 license. Available from: http://dx.doi.org/10.5772/54558

Please feel free to contact me if you have any additional questions or concerns regarding this matter.

Kind regards,
Sasa

--
Sasa Marcan
Library and Information Service Coordinator

_____
InTech - open science | open minds
Email: marcan@intechopen.com
Website: http://www.intechopen.com
Phone: +385 51 688 994
Fax: +385 51 686 166

Journal Department
Janeza Trdine 9
51000 Rijeka, Croatia

Appendix B.

IRB PROTOCOL FOR TISSUE PROCUREMENT

CHRISTIANA CARE
Institutional Review Board
FWA00006557

Helen F. Graham Cancer Center & Research Institute
West Pavilion - Suite 2350
4701 Ogletown Stanton Road
Newark, DE 19713

302-623-4983 phone
302-623-4989 phone
302-623-6863 fax

MEMORANDUM

DATE: April 8, 2015

TO: Robert Witt, MD
Oncology Research
Christiana Hospital

FROM: Wendy Bassett WB

RE: *CCC# 26131* - Acquisition and Experimental Use of Head and Neck Tissue for Tissue Engineering and Biomarker Discovery: (DDD# 504560)

This is to officially inform you that the Continuing Review to your protocol which was received on 04/07/2015 was reviewed by Expedited Review and approved by Jerry Castellano, Pharm.D, CIP, Corporate Director of the Christiana Care Health System Institutional Review Board, on 04/07/2015.

Approval was extended for a period of one year, through 04/06/2016.

Our records indicate this study is OPEN.

If you have any questions or concerns, please contact the IRB Office. Thank you.

This approval verifies that the IRB operates in Accordance with applicable ICH, federal, local and institutional regulations, and with all GCP Guidelines that govern institutional IRB operation.

Informed Consent
CHRISTIANA CARE HEALTH SERVICES,
HELEN F. GRAHAM CANCER CENTER

STUDY TITLE: Acquisition and Experimental Use of Head and Neck Tissue for Tissue Engineering and Biomarkers Discovery

Christiana Care Health Services Helen F. Graham Cancer Center and Research Institute is conducting research in regeneration (regrowing) of diseased salivary glands, thyroid glands, parathyroid tissue, and vocal folds, preservation of tissue (cryopreservation), along with finding biomarkers (looking for differences in how cells are constructed) of different forms of cancer. To make this research possible, we are collecting tissue samples from many individuals. We will make these specimens available to researchers who want to study causes of cancer. We are asking you to take part in this cancer research. In addition we will link scientific data to your clinical information as part of research proposals.

You should understand why we are asking you to join this tissue collection program and whether there are any risks or benefits. This allows you to decide whether or not you want to join. This form provides information about this program. By signing this form, you give us your informed consent. Informed consent means this: You have the information you need to choose whether or not you want to be in this study.

VOLUNTARY PARTICIPATION: You can choose not to take part in this research. Your decision will not affect your medical care at Christiana Care Health Services Helen F. Graham Cancer Center and Research Institute.

We will give you a copy of this consent form to keep. After you read this form, and after we discuss it with you, you may still have questions. If you have questions now or in the future, please ask us.

THE GOAL OF CANCER RESEARCH: The goal of cancer research is ultimately to regenerate salivary gland tissue, thyroid tissue, parathyroid tissue, and vocal fold tissue, to preserve tissue (cryopreservation), and find biomarkers that provide information to develop new and better ways to prevent, detect and treat cancer. This material will be provided to research scientists.